Available online at www.sciencedirect.com
SCIENCE DIRECT®
Progress in Materials Science 50 (2005) 181–292
Progress in Materials Science
www.elsevier.com/locate/pmatsci

# On the crystallography of precipitation ☆

W.-Z. Zhang [a,*], G.C. Weatherly [b]

[a] Department of Materials Science and Engineering, Tsinghua University, Beijing 100084, China
[b] Department of Materials Science and Engineering, McMaster University, Hamilton, Canada L8S 4M1

Dedicated to J.W. Christian

**Abstract**

A general approach for investigating the crystallography of precipitation is developed from a systematic analysis of interfacial structures. The central hypothesis in this approach is that a habit plane or major facet developed in a precipitation reaction is the physical realization of a singular interface. The common characteristics in the structures of any singular interfaces are periodicity and singularity. Similar to the division between small and large angle grain boundaries, the distinction between the 3D primary and 2D secondary preferred state has been specially emphasized for correct descriptions of the interfacial defects. Twelve types of singular interfaces have been classified according to their characteristic features. The relationship between this microstructural description and the macroscopic parameters used to characterize discrete singular interfaces is established in the framework of the model lattices, i.e. the O-lattice/CSL/DSCL. The macroscopic parameters can be identified in reciprocal space according to three $\Delta\mathbf{g}$ parallelism rules, where $\Delta\mathbf{g}$ is a difference vector linking correlated reciprocal lattice vectors in the two lattices. These rules can consistently account for the crystallography of precipitation, with either rational or irrational orientation relationship and habit planes, observed in a broad variety of systems. Other major models in the literature have been reviewed and their connections with the present approach have been discussed.


☆ Wenzheng Zhang also wishes to dedicate this paper to late Professor Weatherly, in memory of his contribution to the better understanding of interfaces.

* Corresponding author. Fax: +86-10-62771160.
*E-mail address:* zhangwz@tsinghua.edu.cn (W.-Z. Zhang).

0079-6425/$ - see front matter © 2004 Elsevier Ltd. All rights reserved.
doi:10.1016/j.pmatsci.2004.04.002

**Contents**

## 1. Introduction

Control of the microstructure that results from a precipitation reaction during the heat treatment of engineering materials is one of the ultimate goals of materials science. The factors that control precipitation crystallography, e.g. the shape, orientation, distribution, and interface stability of precipitates, are of obvious importance in this context. However, in contrast to well-developed theories that underpin the thermodynamics and kinetics of precipitation reactions, our understanding of the factors that determine the crystallography of precipitation is still rudimentary. Moreover, any theoretical study of the thermodynamics and kinetics of phase transformations must remain qualitative in nature without a full understanding of the role of crystallography. The importance of a quantitative description of precipitation crystallography in the design and control of precipitation reactions, to obtain certain desired properties, will become more prominent as ''trial and error'' approaches are supplanted by more scientific methods. Many structure-sensitive microstructural features depend strongly on the orientation relationship (OR) and habit plane (i.e. the predominant facet plane) or other facets of the boundary between a precipitate and matrix. Although precipitates often adopt a variety of shapes, the OR and orientation of the habit plane in many precipitation systems are frequently reproducible and are often uniquely defined. The subject matter of this paper, ''The Crystallography of Precipitation'', addresses the question—''How can we rationalize the OR and the habit plane, for systems having a broad range of misfits?''

A common observation in many systems is that precipitates are fully coherent with the matrix phase. In these systems, the crystal structure of the precipitates is usually similar to or identical with that of the matrix, and the lattice misfit is small. Then, the OR can often be determined a priori, e.g. symmetry elements common to both crystals are normally parallel to one another. Strain energy is the key factor affecting the development of the morphology of these precipitates [1–4]. However, in many important phase transformations, the Bravais lattice and lattice constants of the two phases are quite different. Usually, the precipitates in these systems are not

**Nomenclature**

*Symbols and abbreviations*

1 (2, 3, 5)D one (two, three, five) dimensional or dimension(s)

$\mathbf{A}$, $\mathbf{A}^{\mathrm{II}}$ transformation strain or misfit strain matrices (superscript 'II' denotes a secondary, while default implies a primary transformation matrix)

$A_{\mathrm{I}}$, $A_{\mathrm{II}}(B_{\mathrm{I}}, B_{\mathrm{II}}, \ldots)$ singular interfaces classified by the structures in Table 1

$a_{\alpha 1}$, $a_{\beta 1}$, $a_{\alpha 2}$, $a_{\beta}$, $a'_{\alpha 2}$, $a'_{\beta 2}$ lattice constants

$\alpha$, $\beta$, $\alpha_1$, $\beta_1$, $\alpha_2$, $\beta_2$ lattices or phases

BGP boundary geometrical phase

$\mathbf{b}^{\mathrm{L}}$, $\mathbf{b}_i^{\mathrm{L}}$, $\mathbf{b}^{\mathrm{II}}$, $\mathbf{b}_i^{\mathrm{II}}$, $\mathbf{b}_s^{\mathrm{II}}$ Burgers vectors (subscript '$s$' indicates step)

$b_a$, $b_b$ Burgers vectors in scalar form for 1D misfit

$\mathbf{b}_i^*$, $\mathbf{b}_i^{\mathrm{II}*}$, $\mathbf{b}_s^{\mathrm{II}*}$ reciprocal Burgers vectors

CSL coincidence site lattice

CCSL, $\mathrm{CCSL}_{\alpha}$, $\mathrm{CCSL}_{\beta}$ constrained CSL, with one crystal lattice being constrained (subscript indicates the unconstrained lattice)

CDSCL, $\mathrm{CDSCL}_{\alpha}$, $\mathrm{CDSCL}_{\beta}$ constrained DSCL, with one crystal lattice being constrained (The subscript indicates the unconstrained lattice)

$\mathbf{c}_i^{\mathrm{O}}$, $\mathbf{c}_i^{\mathrm{O\text{-}II}}$ reciprocal vectors for the O-cell walls

DSCL complete pattern shift lattice

$\mathbf{d}$ relative displacement

$\mathbf{d}_{\mathrm{O}}$ terrace vector

$d^{\mathrm{O}}$ spacing between O-planes

$\Delta d$ difference of the interplanar spacing of the conjugate planes

$\langle d \rangle$ interplanar spacing

$d_{\mathrm{CCSL}}$ spacing of planes in the CCSL

$d_{i\text{-dis}}$, $d_{i\text{-dis}}^{\mathrm{II}}$, $D$ dislocation spacing

$\Delta\mathbf{g}$, $\Delta\mathbf{g}_{\parallel}$, $\Delta\mathbf{g}_i$ difference vector between $\mathbf{g}_{\alpha}$ and $\mathbf{g}_{\beta}$ ('$\parallel$' denotes parallel)

$\{\Delta\mathbf{g}_{\mathrm{I}}, \Delta\mathbf{g}_{\mathrm{P\text{-}I}}, \Delta\mathbf{g}_{\mathrm{P\text{-}I}i}, \Delta\mathbf{g}_{\mathrm{II}}, \Delta\mathbf{g}_{\mathrm{P\text{-}II}}, \Delta\mathbf{g}_{\mathrm{P\text{-}CSL}}, \Delta\mathbf{g}_{\mathrm{P\text{-}CCSL}}\}$ reciprocal vectors of the O-lattice, CSL, or CCSL (where '$P$' denotes principal)

$E_{\mathrm{c}}$, $E_{\mathrm{s}}$, $E$ chemical, structural component, and total interfacial energy

$\{\mathbf{g}, \mathbf{g}_{\alpha}, \mathbf{g}_{\beta}, \mathbf{g}_a, \mathbf{g}_{\mathrm{b}}, \mathbf{g}_{\mathrm{P\text{-}}\alpha}, \mathbf{g}_{\mathrm{P\text{-}}\beta}, \mathbf{g}_{\mathrm{P\text{-}}\alpha i}, \mathbf{g}_{\mathrm{P\text{-}}\beta i}, \mathbf{g}_{\mathrm{P\text{-}}\alpha\mathrm{CSL}}, \mathbf{g}_{\mathrm{P\text{-}}\beta\mathrm{CSL}}, \mathbf{g}_{\mathrm{P\text{-}}\alpha\mathrm{CCSL}}, \mathbf{g}_{\mathrm{P\text{-}}\beta\mathrm{CCSL}}, \mathbf{g}_{\alpha\mathrm{CDSCL}}, \mathbf{g}_{\mathrm{P\text{-}}\alpha\mathrm{CDSCL}}, \mathbf{g}_{\mathrm{P\text{-}}\beta\mathrm{CDSCL}}, \mathbf{g}_{\mathrm{step}}\}$ reciprocal vectors of crystal lattices (measurable vectors), and those that also define planes in the CSL, CCSL or CDSCL (where 'P' denotes principal)

$h$ step height

$i$ (as subscript) identifies different vectors

IO interface orientation

I (II) (as superscript or subscript) indicates primary (secondary) preferred state

$\mathbf{I}$ unit matrix

$\mathbf{l}$ vector lying over a terrace plane

$\Delta\mathbf{l}$ displacement associated with $\mathbf{l}$

| | |
|---|---|
| $\mathbf{n}$ | unit vector for an interface normal |
| {O-cell, O-element, O-lattice, O-line, O-plane} | periodic features of fit/misfit formed from superimposing lattices $\alpha$ and $\beta$, as described in Bollmann's O-lattice theory |
| OR | orientation relationship |
| PTMC | phenomenological theory of martensitic crystallography |
| $P$ and $R$ | geometric parameters representing interfacial energy |
| $\mathbf{r}$ | general unit reciprocal vector |
| $r$ | parameter for 1D misfit strain |
| $\mathbf{T}$, $\mathbf{T}^{\mathrm{II}}$ | displacement matrices |
| TEM | transmission electron microscopy |
| $\mathbf{v}$ | step vector |
| $\Delta\mathbf{v}$ | displacement associated with a step |
| $\Delta\mathbf{v}_{\mathrm{c}}$ | displacement associated with a step defined in a CCSL |
| $\mathbf{x}_i$ | vectors satisfying the O-cell wall equation |
| $\{\mathbf{x}_\alpha, \mathbf{x}_\beta, \mathbf{x}_i^{\mathrm{O}}, \mathbf{x}_i^{\text{O-II}}, \mathbf{x}_\alpha^{\mathrm{CCSL}}, \mathbf{x}_\beta^{\mathrm{CCSL}}, \mathbf{x}_\alpha^{\mathrm{CDSCL}}, \mathbf{x}_\beta^{\mathrm{CDSCL}}\}$ | vectors defined in various lattices (in direct space) |
| $\mathbf{y}$ | general vector (in direct space) |
| $\theta$ | angle between a stepped interface and the terrace plane |
| $\xi$, $\xi_i^{\mathrm{II}}$ | vectors for describing dislocation geometry |
| $\Sigma$ | reciprocal density of the CSL points relative to a crystal lattice |

fully coherent. Moreover, in some precipitation systems neither the OR nor the habit plane is rational. [1]

The reduction of the energy barrier to precipitate nucleation by the formation of faceted low energy interfaces has been considered as the primary cause for the development of a preferred OR, although a subsequent modification of the precipitation crystallography may occur during growth [5,6]. It would be desirable to determine the interfacial energy as a function of both the OR and the interface orientation (IO) such that local energy minima could be identified. For fully relaxed interfaces in a simple system, e.g. grain boundaries in a pure metal [7–9], or coherent precipitates whose misfit strain is isotropic and negligibly small [10], the interfacial energy can be determined from atomistic calculations. Nevertheless, for more general boundaries the calculation of interfacial energy to reasonable precision represents a major challenge for any current theory. Moreover, it appears to be a formidable task to obtain experimental evidence for a quantitative association between the interfacial energy and a macroscopic description of the interface. Simplified treatments have been proposed whereby the interfacial energy of an

[1] The crystallography is rational when an accurate OR or faceted interfaces can be expressed using a low index $\{hkl\}\langle uvw\rangle$ representation in either crystal base; otherwise it is irrational.

interphase boundary is separated into two components: a chemical and a structural component [11,12]. The important role of interfacial structure in determining the energy of an interface is then made clear. However it is often difficult to separate these components and an alternative. Perhaps more realistic approach to explain the observations of the habit planes is to study their interfacial structures experimentally. In this context, our knowledge of the structure of the habit plane and other parts of the interface has made rapid progress as the techniques of electron microscopy have developed [13–15].

In practice, our understanding of precipitation crystallography has, to date, largely depended on simple geometric models. These models can provide a quantitative interpretation of the experimental observations based on an evaluation of the interfacial lattice misfit. However, despite sharing a common geometric approach, the constraints and particular emphases placed on the study of crystallography in the different models vary from one author to the next. For example certain models concentrate on one aspect of precipitation crystallography, e.g. the OR, while others concentrate on trying to explain the habit plane. In the former category, the existence of an invariant line (a line of zero misfit) has been suggested by Dahmen as a criterion to explain the OR developed from precipitation reactions [16]. This implies that the habit plane must contain the invariant line. However, to fix the selection of both the invariant line and the habit plane orientation, other constraint(s) must be invoked. The invariant line hypothesis has been tested against experimental observations in many systems, with good agreement being found between the theory and observations [17–25]. More recently, a criterion based on the near-coincidence of reciprocal lattice vectors has also been suggested [26]. This approach has been used to explain the OR, or lattice correspondence.

Other models focus on interpretation of the structure of the habit plane, while the OR is usually taken to be fixed. The structural ledge model, developed by Aaronson and colleagues [27–29], is one example of this approach. This model evaluates the interface in terms of the density of ''patches'' of good-fit, and provides a reasonable explanation for the irrational habit plane found in various systems. Other approaches for rationalizing the habit plane for a given OR also interpret the habit plane in terms of the areas of good matching of the interfacial structure [30–32]. Recently, computer modeling of the structural ledges has been extended in a near-coincidence site model [33]. In this method both the areal density of near-coincident sites (similar to the good fit ''patches'') and the individual area of near-coincidence sites have been used as criteria for selecting the OR and habit plane.

The most comprehensive consideration of misfit should take both OR and IO into account. Various parameters, to be discussed below, based on interfacial dislocation models have been proposed to represent the interfacial energy. The magnitude of these parameters varies with the OR and the IO, so that the OR and the IO (presumably corresponding to a local minimum of interfacial energy) can be identified. A simple method, first suggested by Knowles and Smith [34], evaluates the interfacial misfit in terms of the Burgers-vector content of the interface. While this approach gives a straightforward picture of the distribution of interfacial misfit, the model is essentially continuum in nature, since it disregards the discrete character of any

dislocation structure in a crystalline interface. Alternative approaches include the use of the geometric parameters $P$ and $R$, defined as simple functions of the interface dislocation spacing and Burgers vectors, as proposed by Bollmann and Nissen [35] and extended by Ecob and Ralph [36]. However, the dislocation structures used for the calculation of $P$ and $R$ are based on the assumption of a structure that always contains three sets of dislocations, determined from a simplified O-lattice calculation [37].

While major geometric models evaluated the lattice misfit, the development of the CSL/DSCL model (CSL stands for coincidence site lattice, while DSCL is a term standing for the complete pattern shift lattice [2] [37]) allows the degree of misfit to be analyzed as the deviation from a CSL state. Though this model was originally proposed for high angle grain boundaries [37,38], it has been extended for analysis of interphase boundaries when a set of "good matching" points (CSL points) can be identified [39,40]. The CSL/DSCL approach is usually applied when the lattice misfit is so large that only fractional lattice point matching rather than maintenance of coherency in individual areas is possible [41–45].

A different approach, without taking any misfit into account, was proposed by Cahn and Kalonji [46]. By analyzing the point symmetry elements common to both crystalline phases, they were able to identify the local energy extrema. According to their model, the OR corresponding to a set of interface facets is associated with a symmetry-dictated energy minimum. While this elegant approach has been applied to explain the precipitate morphology in several systems [47,48], it is in conflict with observations of irrational ORs and irrationally oriented habit planes in many systems. Again this suggests that the role of misfit is often so important that it cannot be neglected.

Despite the limitation of geometric models, remarkably good agreement has been obtained between the models and a large body of experimental data. In fact, all published geometric models have found some supports from experimental observations. The same set of experimental data can often be explained by different models. More frequently, however, a model that has achieved success in one system may fail to explain the observations in another. There is no general consensus on the validity of a particular geometrical model, since it is not clear how a geometric parameter is related to the interfacial energy [49]. While much effort has been made to develop models that agree with particular sets of experimental observations, less attention has been paid to explore the conditions where a model might be valid, and to establish the links between different models. On the other hand, while a large body of experimental data is available, little systematic work has been done to classify the precipitation crystallography or to identify the principles that govern the

[2] Here we have followed the original definition given by Bollmann [37], but DSCL has often been considered to stand for displacement shift complete lattice in literature. More completely, it should stand for a lattice in which any translation vector is a displacement that can cause a complete CSL pattern shift.

development of precipitation crystallography. The principles controlling precipitation crystallography may vary with the conditions under which the boundaries are formed, so that in a particular system one type of habit plane may be preferred over others. It is important to recognize where any principle of a particular type might be valid. Once this is recognized, a geometric approach can serve as a useful tool for understanding the observations of precipitation crystallography.

The present study has made a comprehensive examination of the experimental data for a broad range of materials and an extensive survey of the major models for precipitation crystallography in the literature. The purpose of this paper is to provide readers with a simple approach applicable to the understanding of precipitation crystallography in the most general systems; i.e. we seek an integrated model that will explain observations in systems of both small and large lattice misfit, and where the two crystals may have different Bravais lattices. We will demonstrate that the use of concepts derived from reciprocal space rather than direct space provides a key method to resolving the observations from many systems.

The habit plane is assumed to be a singular interface associated with a local energy minimum. It will be explained how a singular interface can be recognized by their characteristic structures. The structure of a singular interface is then described in the framework of one or two model lattices. The application of a set of simple rules, quantitatively described in terms of a group of correlated reciprocal vectors, provides an experimental link between the singular interfaces and the model lattice descriptions. These rules are directly compared with observations of the precipitation crystallography in a wide variety of systems. The paper also discussed other major models in the literature and their links with the present approach.

## 2. Descriptions of habit planes in terms of singular interfaces

### *2.1. Singular interfaces*

The classification made by Balluffi and Sutton [50,51] has proved to be particularly useful in describing interfaces. According to their definition, interfaces consist of three types: singular, vicinal and general. A singular interface is ''an interface, the free energy of which is at a local minimum with respect to at least one macroscopic geometrical degree of freedom''; a vicinal interface is ''an interface, the free energy of which is near a local minimum with respect to at least one of the macroscopic geometrical degrees of freedom''; a general interface is ''an interface, the free energy of which is at, or near, a local maximum with respect to one or more macroscopic geometrical degrees of freedom''. Here, the term ''macroscopic geometrical degree of freedom'' is a degree of freedom in a five dimensional boundary geometrical phase space (5D BGP space). (This term was coined to emphasize that five variables are required to define an interface: these are the three variables describing the OR, and

two variables specifying the IO [3]) [50]. Balluffi and Sutton's classification emphasizes the association of a particular interface with respect to a singularity in the energy rather than the absolute value of the energy per se.

### 2.2. Habit plane hypothesis

The fact that a habit or a facet plane has a unique IO at a fixed OR, suggests that a change of its coordinates in the 5D BGP space of a point is most likely associated with a rise in interfacial energy. This suggestion is restated in the following hypothesis: *The habit plane* (*or major facet*) *associated with a precipitation reaction is the physical realization of a singular interface whose interfacial energy corresponds to a local minimum in the 5D BGP space*. This hypothesis provides a physical basis on which the crystallography of precipitation is analyzed throughout this paper. Both the OR and the habit plane normal are such as to allow a minimum energy state to be realized. Understanding precipitation crystallography is thus equivalent to rationalizing the habit plane as a singular interface, the free energy of which is a local minimum with respect to all macroscopic geometrical degrees of freedom, if a fixed OR and IO are observed for the habit plane. However, as will be explained later, in certain systems one degree of freedom may be left unfixed locally. In such systems a small degree of scattering in the OR or habit plane orientation may be found.

The limitations of the approach adopted in this work should be appreciated. The effects of temperature, particularly the contribution of the entropic term to the free energy of the interface, have been ignored. Below some critical temperature, entropy will influence only the depth and sharpness of the energy cusps, not its position in the 5D BGP space. Though the facets may become less distinct as temperature increases [10,12], their coordinates in 5D BGP could be explained without considering the temperature effect. Kinetic effects and volume strain energy might also be important to the development of the shape of a precipitate. Although these factors should not be overlooked, they are considered only to determine whether a particular one or a set of singular interfaces can be realized in a given condition of precipitation. A habit plane, if observed, should be always among the candidates of singular interfaces. Therefore, identifying plausible singular interfaces is an essential step for rationalizing the habit plane.

## 3. Characterization of singular interfaces by their structures

### 3.1. Association of singularities in interfacial energy and in interfacial structures

The connection between the crystallography of a phase transformation and the choice of a habit plane based on the minimization of energy is not immediately

[3] Strictly speaking one should define eight variables, with the additional three needed to define a rigid body translation at the interface, but we will assume that the two lattices coincide at a common origin, located at the interface.

obvious. Although efforts have been made to develop an approximate relationship between the structural characteristics and interfacial energy (Section 6.2), precise data to show the association of interfacial energy and interfacial structures for heterophase interfaces are very limited. On the other hand, the interfacial energy has been determined from more physically rigorous models for grain boundaries [7–9,12]. The association of the interfacial structure with minima in energy of simple interface can provide useful information [50].

According to a study of the relationship between grain boundary structure by Goodhew [52], the structures of many boundaries contain a fine-scale periodic arrangement of atoms, plus one or more sets of line defects. Consider first high angle grain boundaries. Energy cusps have been associated with coincidence type boundaries, especially with low $\Sigma$ values that reflect the reciprocal density of the CSL points [7,12,52–55]. However, the $\Sigma$ value only restricts the OR but not the facet plane. As noted by Randle [54], a low $\Sigma$ CSL is a necessary but not a sufficient criterion for special properties of grain boundaries, and a low $\Sigma$ boundary that contains the highest density of the CSL points will almost certainly exhibit special properties. The size of different facets in a $\Sigma 11$ boundary in gold can be rationalized based on the planar density of the CSL [56], which is consistent with the results obtained from atomistic calculations [57]. Though a quantitative relationship can not be built between the $\Sigma$ values and the interfacial energy, short wavelength periodicity in the interfacial structure, usually associated with a small $\Sigma$ value, is an important characteristic of singular large angle grain boundaries, as pointed out by Bollmann [58]. Prominent singular high angle grain boundaries are often associated with identical structural units that repeat periodically along the facets [9], and the existence of structural units of short period is ensured by dense planar CSL points in the interfaces. In the low misorientation regime, typical small grain boundaries always contain dislocations. For a pure tilt small angle grain boundary, the energy cusps have been found to be associated with interfaces with a single set of dislocations, i.e. a symmetrical tilt grain boundary, as demonstrated by the $\gamma$-plot [59] for a small angle boundary determined using the Read–Shockley formula [60], or by other parameters related to the dislocation structure [61].

Although the details of the structure of singular grain boundaries vary from one example to the next, both experimental and theoretical results from both low and high angle singular grain boundaries indicate a strong connection between the periodic characteristics of the interfacial structures and the singularity in the energy. The periodicity can be described in terms of either structural units or dislocations, or both. It can be expected, as often implied in various experimental or theoretical studies, that the characteristic feature of a singular interface should be independent of the size of the facet or the location in the facet. In this context, the interfacial structure must be periodic so that the low energy characteristic feature in the interface can repeat ad infinitum. However, not all periodic structures define singular interfaces. To emphasize the singular nature of the structure in a singular interface,

we must focus only on a particular type of periodic characteristic, denoted as a singular periodic structure, which can only be realized in discrete interfaces at energy cusps, but not at vicinal orientations.

The results from single-phase systems can be extended to multi-component heterophase systems, which also often exhibit characteristic periodic structures in the habit planes [19,21,44,62–69]. In addition, the condition of a singular periodicity is also in accord with models for heterophase interfaces, based either on the CSL concept or periodic atomic structural units [8,52,70]. However the variation of interfacial energy in the BGP space is much more complicated in a heterophase system than in a homophase system due to the chemical component of the interfacial energy. Nevertheless, a local minimum in the structural component of the interfacial energy in a heterophase system is often a priori the cause for the observation of a preferred OR, which would not be necessary without the effect of the structural component. In some cases, e.g. metal–ceramic systems, the chemical component may be the determining factor in deciding which of several possible precipitation crystallographies is favored. Taking this factor into consideration wherever necessary, we will proceed with the hypothesis that *the observed habit plane is among the candidates of singular interfaces associated with a local minimum of the structural component of the interfacial energy*. Since the structural aspects of homophase and heterophase systems should be similar, a singular periodicity in the interfacial structure can be considered as a necessary characteristic that any singular heterophase interface must maintain over a significant area.

### *3.2. Preferred states between dislocations*

An interfacial structure reflects how the lattice misfit is distributed within the interface region. The formation of dislocations implies the presence of a preferred structure between the dislocation lines, which have automatically relaxed to a low energy configuration. For a simple interface of small misfit, a fully coherent state is usually expected between the dislocation lines. For a more general interface, the structure between the dislocations will vary from one system to another.

The description of the structure between the dislocations can be greatly simplified by adopting the classification of the preferred reference state, as suggested by Bollmann [58]. A preferred state specifies an idealized, periodic structure, whereby the real structure between the dislocations can be developed through a local relaxation, leading to elastically forced structure bearing a close resemblance to the ideal one. Such a relaxation, though its details may vary from one location to another and hence are difficult to specify, does not alter the overall dislocation periodicity, and also does not affect the coordinates of the singular interfaces in the BGP space. Bollmann has classified the preferred states into primary and secondary types [58]. The identification of the preferred state is a critical step for describing the interfacial structure, since the Burgers vectors and the configuration of the dislocations can be

specified only when the preferred state is defined or implied. Unlike the situation in homophase systems, where different models pertain for small and high angle grain boundaries, the importance of the preferred state to the description of interfacial structure is not broadly appreciated in studies of heterophase systems. For this reason, the two types of preferred states and the possible candidates for Burgers vectors of interface defects are explained below.

*3.2.1. Primary preferred state*

This state refers to a coherent or full coincidence state. The lattice of either crystal phase (matrix or precipitate) can be taken as the reference for the ideal state. This state is defined by the periodic structure of the reference lattice in three dimensions (3D). An interface favoring a primary preferred state occurs when the lattice misfit is sufficiently small (typically less than 15%). The lattice misfit is in general assessed in terms of the relative deviation between the correlated small vectors (the magnitude of displacement compared with that of either correlated vector), whose correlation relationship is defined on a basis of a *one-to-one* lattice point (or atom) correspondence. Fig. 1a is a schematic plot of a relaxed interphase boundary exhibiting a one dimensional (1D) misfit, where the interface adopts a primary preferred state so that local coherency is conserved between the dislocations. Because of the loss of coherency at the cores of the primary dislocations, such a boundary is also known as a semi-coherent boundary. In an interface in the primary preferred state, the interfacial misfit strain, i.e. the primary misfit strain, is equivalent to the lattice misfit strain for a given OR.

The misfit dislocations, corresponding to the primary preferred state in their separated areas, are also termed primary dislocations. However, the term "primary" is often omitted, since the Burgers vectors of the primary dislocations are often identical to the Burgers vectors of dislocations within either crystal. When two patches, separated by a dislocation, conserve a coherent structure, the displacement associated with the dislocation must be a lattice translation vector of either crystal to ensure the repetition of the coherent structure, and it must be a vector connecting the nearest lattice points because the border between the adjacent coherent patches must be associated with a unit shift of the nearest neighbor relationship. Energy considerations also dictate that the Burgers vectors are among the small lattice translation vectors for crystal dislocations. Therefore, only a limited set of misfit dislocations, specified by the crystal Burgers vectors, can be present in an interface in the primary preferred state. For the simple 1D example in Fig. 1a, the Burgers vector of the dislocations is either $a_{\alpha 1}$ or $a_{\beta 1}$, referred to lattice $\alpha_1$ or $\beta_1$, respectively. The interface in Fig. 1b is between rigid lattices, whose lattice constants are identical to that in Fig. 1a. The possible misfit dislocations in the un-relaxed interface are identified, locating at the worst matching positions. As can be seen from a comparison of Fig. 1a and b, the relaxation does not change the average periodicity of the dislocations. Since periodicity is a crucial signature of singular interfaces, we can identify possible singular interfaces according to the calculated dislocation periodicity in the un-relaxed state.

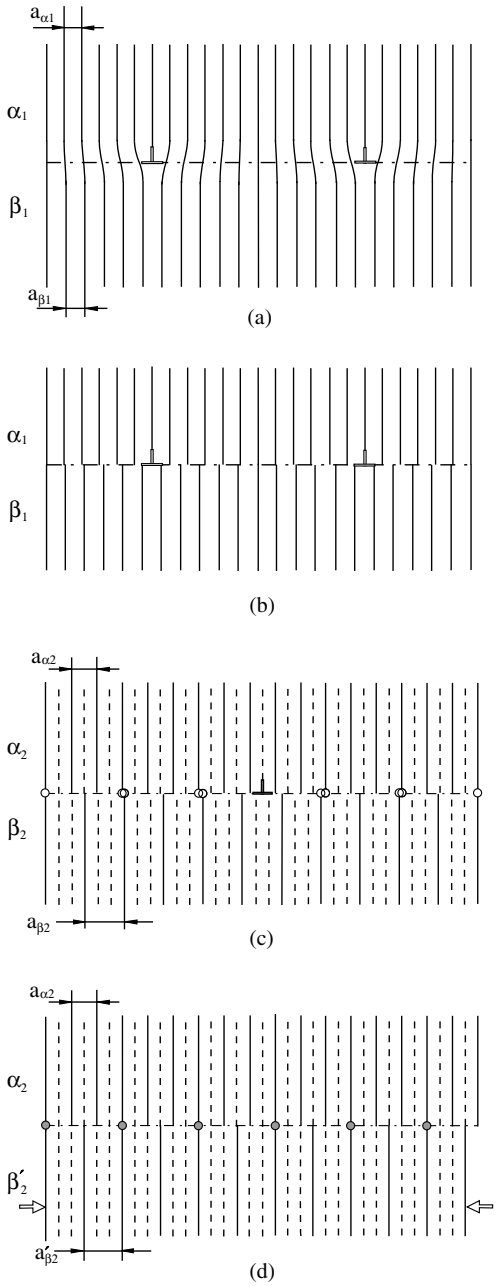


Fig. 1. An illustration of the preferred states in a 1D model: (a) relaxed and (b) non-relaxed interfaces in a primary preferred state; (c) a non-relaxed interface in a secondary preferred state and (d) the CCSL used as a reference lattice for the relaxation of the interface in (c). The solid lines are lattice planes and the dashed lines define CDSCLs; the open and gray circles in (c) and (d) represent CCSL points.

*3.2.2. Secondary preferred state*

Secondary preferred states consist of various "fractional coincidence states" [58]. They occur when short periodic atomic structural units, different from those of either crystal structure, [4] are preferred in major local areas (terraces) of the interface. Without knowing a priori the specific atomic structure between the dislocations, this state can be conveniently described in terms of a fractional coincidence state, or as a 2D CSL preferred state, since periodic 2D CSL (in an un-relaxed state) is the necessary condition for the periodic atomic structural units. The application of the CSL model to heterophase system is different from that to the homophase systems. The CSL model often applies to special large angle grain boundaries, such as a $\Sigma 3$ twin boundary in fcc crystals, in which a fully coherent structure can be realized. An interfacial structure consisting of fully coherent patches is not regarded to be in a secondary preferred state, no matter whether a 3D CSL of a small unit can be constructed or not. [5]

A secondary preferred state usually occurs in an interface when the lattice misfit in the major areas of the interface is large. While the lattice misfit is assessed on a one-to-one lattice point basis, the interfacial misfit strain in an interface in a secondary preferred state is the secondary misfit strain, describing the deviation of the matching condition between real lattices from the secondary preferred state. Clearly, the interfacial misfit for this case is different from the lattice misfit. The patches where the secondary preferred state sustains locally are separated by the secondary dislocations. As suggested by Bollmann [37,58], any translation that leads to a conservation of the CSL pattern must be a lattice vector of the DSCL. As for the case of the primary dislocations, the Burgers vector of the secondary dislocation between the adjacent patches in the preferred state is usually a vector connecting the nearest points in the DSCL.

Fig. 1c illustrates an interface, with 1D secondary misfit strain, in which a secondary preferred state is obtained after relaxation. The corresponding reference for the preferred state is given in Fig. 1d, where the constrained CSL (CCSL) points in the interface are represented by gray circles. The constrained DSCL (CDSCL) used to define the Burgers vector is identified by the dashed lines in Fig. 1d. The subscript $\alpha$ in $\mathrm{CCSL}_\alpha$ and $\mathrm{CDSCL}_\alpha$ is used to denote the specially constrained state in which lattice $\alpha_2$ is undeformed. The large arrows indicate that lattice $\beta_2$ has been compressed, so that the new lattice constant $a'_{\beta 2}$ exactly equals $3a_{\alpha 2}/2$. Alternatively, one can define $\mathrm{CCSL}_\beta$ and $\mathrm{CDSCL}_\beta$, commensurate with lattice $\beta_2$, by extending lattice $\alpha_2$. In Fig. 1c, the points of $\mathrm{CCSL}_\alpha$ and $\mathrm{CCSL}_\beta$ in local interface are indicated by open circles, with the lattice constant of the $\mathrm{CCSL}_\alpha$ being $3a_{\alpha 2}$ or $2a'_{\beta 2}$, while that of the $\mathrm{CCSL}_\beta$ is $2a_{\beta 2}$ or $3a'_{\alpha 2}$. Correspondingly, two sets of CDSCLs, $\mathrm{CDSCL}_\alpha$ and $\mathrm{CDSCL}_\beta$, can be obtained, as indicated by the dashed lines in Fig. 1c. Either of these

[4] The structure between primary dislocations can be considered to contain atomic structural units of either crystal.

[5] It is possible that different parts of an interface around a precipitate are in different preferred states. Each part of the interface can then be differently modeled.

small lattices can be taken as the basis for defining the Burgers vector of the secondary dislocations [58]. These dislocations can be determined from the mismatch between the $CDSCL_\alpha$ and $CDSCL_\beta$ (not between the $CCSL_\alpha$ and $CCSL_\beta$!), in the same way as the primary dislocations are defined for lattices $\alpha_1$ and $\beta_1$ in Fig. 1a or b. Note that the planes in the different CCSLs are discontinuous, at any secondary dislocation, upon a translation of the shortest vector in the CDSCL. In other words, elastically constrained CSL points can only be preserved locally between the secondary dislocations. Either $CCSL_\alpha$ or $CCSL_\beta$ can serve as the reference state for the preferred state.

In more general case, when studying a stepped interface or different facets surrounding a particle, the interfacial structure is intimately linked with the construction of a 3D CSL. Since the CSL pattern that represents the preferred state in the interface is a 2D structure, any step will cause discontinuity of the 2D CSL pattern. This is an important distinction of a secondary preferred state from the primary preferred state, which extends in 3D. The atomic steps in an irrational interface in the primary preferred state do not necessarily cause local loss of coherency (refer Fig. 6), and hence the areas where the preferred state is continuously preserved are separated only by the misfit dislocations. In contrast, the areas where the secondary preferred state is continuously preserved can be separated by either misfit dislocations or steps (either associated with misfit dislocations or not). Thus, special attention must be paid to the steps in studies of interfacial structure in a secondary preferred state.

The choice of primary preferred state is obvious when the lattice misfit strain is small. However, the border separating different preferred states is not always distinct. One may always draw various CCSL for a given system, but any preferred state must be tested by experimental observations. A secondary preferred state is adopted only if the primary preferred state is invalid. A convenient parameter to check the validity of a selection of primary preferred state is the dislocation spacing. If the calculated spacing of the primary dislocations is significantly larger than the Burgers vectors, the coherent patches between misfit dislocations will be so large that the dislocation description is physically meaningful and a primary preferred state should be realized. Otherwise, a secondary preferred state would be favored. A secondary preferred state is more complicated than a primary one, because its structure for a given system varies with the OR and IO. The particular choice of CSL to be taken as a reference state remains a challenging problem, as in the case of high angle (vicinal) grain boundaries. A high planar density of coincident sites has been recognized important for grain boundaries [53,54], providing useful insights for the heterophase interfaces. The construction of a CCSL in the heterophase systems has been guided mainly by experimental observations [41,42,45]. The ambiguity in the selection of the preferred state is greatly reduced when the construction of a 2D CCSL is guided by the observed habit plane.

In the following analysis, the structure in any singular interface is presumed to sustain a preferred state. Periodic structures in the singular interfaces containing dislocations will be assessed mainly in terms of misfit dislocations. Because of the restriction of the Burgers vectors, interfaces that contain periodic (in average

spacing) dislocations are limited. The major concern in the next section is to define the interface containing periodic misfit dislocations. The singular interfaces free from any dislocations are more special and their identification can be included as special cases in the subsequent modeling.

### 3.3. Singular periodic dislocation structures

A dislocation structure is considered periodic, if each dislocation free area plus the surrounding dislocations of one, two or three sets characterized by the Burgers vectors (the dislocation cell) can be repeated side by side over an unlimited area of an interface of a unique orientation. The distances between the adjacent dislocations may not be precisely identical everywhere, but they are all close to an average value. Only when the lattice constants are specially related can the dislocation spacing be precisely identical everywhere. This can be seen from Fig. 1.

In the examples in Fig. 1, the long-range misfit strain in the interface is accommodated completely by the misfit dislocations. In practice, this condition may not be truly satisfied. However, to characterize a general interface that contains a singular periodic structure, we must assume that the interface is free of long-range strain. Otherwise, any interface might contain a singular periodic structure, leaving some part of the misfit strain to be accommodated elastically. This assumption is reasonable for precipitates whose sizes are significantly larger than the dislocation spacing. We will proceed with this assumption in the following analysis, leaving the possible residual long-range strain to be discussed in Section 5.4.

With this assumption, periodic dislocation structures can only exist in interfaces of certain orientations. A tilt grain boundary is taken to illustrate this point. In Fig. 2 two lattices have been rotated with respect to each other and superimposed, with the positions of edge-on interfaces being represented by lines *a–a* and *b–b*. [6] In this simple case, there is no misfit along the rotation axis, and the overall misfit strain lies in the plane of the figure. A maximum of three Burgers vectors, lying in the plane normal to the rotation axis, is allowed at any interface in this system. Any edge-on interface (normal to the plane of paper) will contain one, two or even three sets of parallel dislocations. For an interface to contain one set of periodic dislocations, it must contain a special vector along which the relative displacement between the two lattices must lie exactly parallel to a Burgers vector. This vector has a specific orientation, such as the one parallel to interface *a–a* (forming a symmetric tilt grain boundary) in Fig. 2.

Consider next an interface deviated from the above condition, for example the interface indicated by *b–b* (forming an asymmetric tilt grain boundary) in Fig. 2. Though the misfit in interface *b–b* is still a 1D strain, the relative displacement along the vector parallel to the interface *b–b* is not in the direction of an amenable Burgers vector. While the same set of dislocations as in interface *a–a* might be the only misfit

[6] The O-lattice structure in this figure will be explained in Section 3.1. Once the interface is defined, only one lattice remains in each different side of the boundary.

dislocations present in a certain area, a second set of dislocations of another Burgers vector must be present in order for interface *b–b* to be free of any long-range strain. The elastic strain in interface *b–b* will extend over a distance defined by the spacing of the dislocations in the second set. This medium-range strain may produce a significant contribution to the increase of the structural component of the interfacial energy, as calculated for the simple case of a small angle boundary in a cubic lattice with a rotation axis around [0 0 1] given in [59,61]. Due to the energy gradient, vicinal interface *b–b* is subject to a torque (as indicated by the pair of arrows) which tends to rotate the local interface to orientation of the singular interface *a–a*, resulting in a stepped boundary consisting of facets parallel to *a–a*.

The above analysis can be extended to heterophase systems, in either a primary or secondary preferred state. A general heterophase system usually exhibits 3D misfit, i.e. the vectors of misfit displacement must be expressed in 3D. [7] Then, the interfacial misfit is in 2D, and at least two sets of dislocations will be present in any interface. For an interface to contain such a periodic dislocation structure, at least two independent special vectors, (the principal O-lattice vectors, as will be explained later), must be available. The relative displacement along each of these vectors should be completely accommodated by a single set of dislocations. Since the selection of the Burgers vectors of the dislocations is finite and discrete, an interface can fulfill the above condition only when it has a particular and discrete orientation.

One must recognize that only in a system of 3D misfit, periodicity of the dislocations is the necessary and sufficient condition for an interface to be singular with respect to the IO. If the misfit strain field is 1D or 2D, periodicity of the dislocations is a necessary but not a sufficient condition. In the example of 2D misfit in Fig. 2, while a singular interface contains a single set of parallel dislocations, the periodic characteristic will be maintained as the interface alters its orientation as long as the interface is inclined to the rotation axis (Such an interface contains a network of three sets of dislocations). Whether a periodic dislocation structure is singular with respect to the orientation of the interface can be distinguished according to the misfit strain field: a structure consisting of a network of periodic dislocations is singular only when the misfit strain field is 3D; a structure consisting of one set of periodic dislocations is singular only when the misfit strain field is 2D; a structure of fully coherent (zero set of dislocations) is singular (and only occurs) when the misfit strain field is 1D. While the dislocation structure varies with dimensions of the misfit strain field, a singular periodicity is often possible for an arbitrary OR. The above condition is general for interfaces in either primary or secondary preferred state. However, some periodic structures may become singular with respect to the IO when the atomic structures in the interfaces are also taken into consideration.

[7] In contrast to 3D misfit, 2D misfit means that the displacement vectors are coplanar, which occurs when the misfit strain is an invariant line strain; 1D misfit means that all displacement vectors lie in one direction, which occurs when the misfit strain is an invariant plane strain.

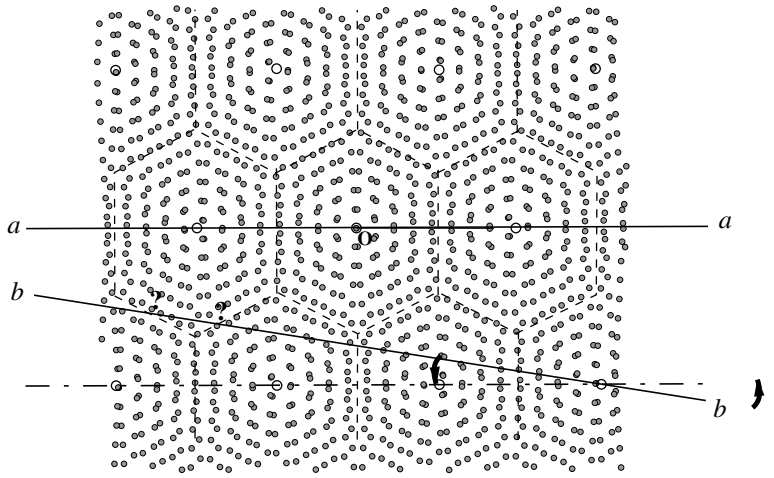


Fig. 2. An illustration of the distribution of lattice misfit in two edge-on interfaces, indicated by *a–a* and *b–b*. In the superimposed pattern of the rotated two lattices, the periodic positions of best matching define a 2D O-point lattice. See text for the detail.

### *3.4. Singularities described by optimum conditions for interfacial structures*

To restrict the OR, at least one other constraint must be applied in addition to the condition of a singular periodic dislocation structure. Such a constraint imposes a condition that can be fulfilled in a discrete interface only when the two lattices are related by a specially defined OR. Thus, the interfacial structure is also singular with respect to the variation of the OR. A well-known example is the fully coherent $\{1\,0\,0\}$ habit plane between $\theta''$ and the matrix in an Al–Cu alloy, which is generally regarded to have a very low interfacial energy, as documented in many textbooks (e.g. [11]). Any deviation from either the particular OR or IO will destroy the defect-free singular structure. However, a defect-free structure is possible only when the lattice constants of the related phases are restricted to discrete values. It is also possible in a homophase system, where a vicinal interface, according to the notation of Balluffi and Sutton, "consists of the singular interface at the local minimum with a superimposed array of discrete line defects, which may be dislocations or pure steps" [50]. The message from the special systems suggests that a singular interface should be characterized by elimination of linear defects. In a general heterophase system, complete elimination of linear defects is in conflict with the condition of no long-range strain. However, the evidence from a broad range of precipitation systems suggests that elimination of certain set(s) of linear defects is possible at discrete ORs, and should represent singularity with respect to the OR.

Guided by experimental observations, we have summarized three optimum conditions for the OR, covering either rational or irrational interfaces of small or large misfit. The linear defects considered in the conditions include misfit dislocations and steps. A misfit dislocation is characterized by a discontinuity of one lattice (crystal

lattice or CSL/DSCL) with respect to the correlated lattice across the interface by a well-defined primary or secondary Burgers vector associated with the core of the defect (Fig. 1). Hirth et al. [71] used the term of "disconnection" to describe steps with dislocation characteristic. In the present description an interfacial step, either associated with a local displacement (or effective Burgers vector) or not, is identified by its topographic discontinuity (discontinuity of flat areas or terraces) of the interface at the atomic scale. When a singular interface contains steps, as the intrinsic linear defects, it is macroscopically flat with a unique orientation. [8]

The first optimum condition requires the complete elimination of interfacial steps, with respect to planes containing dense lattice points. This condition is analogous to a criterion requiring the minimization of broken bonds in a surface of low energy, i.e. it requires the minimization of bonds crossing the interface. The important role of low index crystal planes in the development of singular interfaces has been noted in previous studies [8,49,50,52,54]. Singular interfaces in different systems have been found to be those with the largest $\langle d \rangle$ value (or equivalently with densest lattice points), where $\langle d \rangle$ is the interplanar spacing of the planes parallel to the boundary [8,50]. As frequently noted in experimental studies, close-packed crystal planes often serve as the habit plane, particularly when the chemical component of the interfacial energy has a strong influence (also see Table 5). Interfacial steps in crystalline interfaces are usually associated with localized distortions [55]. In a system consisting of crystal(s) with covalent or ionic bonds, steps may also introduce bonds of high energy, e.g. due to wrong atom pairs, as often occurs when a ceramic phase is involved. Whether this condition is satisfied or not can often be determined simply from parallelism of the interface plane with respect to low index planes of the bounding crystals, or to planes of low surface energy of the crystal(s).

The first optimum condition should readily be extended to systems in a secondary preferred state. This condition should be particularly favored, because the steps are typical linear defects in the case of a secondary preferred state. However, these systems are more complicated for the following reasons. First, the planar interface should be identified with respect to the plane containing a dense array of CCSL points, rather than simply to planes containing dense lattice points in either crystal. This plane may be parallel to a rational crystal plane containing dense regular atomic steps, but these atomic steps may become part of periodic atomic structural units and lose their identity with respect to the crystal lattice. Second, if the interface plane contains secondary misfit strain, the application of the above condition is subject to the requirement of periodic dislocation structure. In the primary preferred state, a dislocation structure with the amenable Burgers vectors can often be realized when the interface contains no interfacial steps, because in this case the low index interface plane usually contains the Burgers vectors that define the dislocations necessary for

[8] Distinction should be made between these intrinsic steps within a singular interface and the steps connecting the singular interfaces, either containing intrinsic steps or not, as the terrace planes. In the latter case, the step spacing is irregular and the step height is usually large compared with the atomic distance.

accommodating the misfit. However, this may not be the situation for a system in a secondary preferred state, as planes containing dense CCSL points may not be parallel to the planes containing the small CDSCL vectors that serve as Burgers vectors. Then, a stepped structure described by the third optimum condition may prevail, provided that the broken bonds associated with the step risers do not cause a significant rise of the chemical component of the interfacial energy.

The second optimum condition requires the complete elimination of the dislocations in one direction, i.e. the spacing of a set of dislocations should reach infinity. The misfit strain field is characterized by an invariant line. This condition is possible in a limited number of systems when the two phases corresponding to this condition are related by special ORs. The invariant line strain has been used as a criterion for understanding ORs by many researchers [16,17,23,72–74]. In fcc/bcc systems the cusps in the curves representing the variation of the interfacial energy are associated with an invariant line condition [75]. The success of the invariant line criterion is found in systems in the primary preferred state. It is implicitly assumed that the energy of the misfit dislocations provides a major contribution to the structural component of the interfacial energy for an interface in the primary preferred state.

However, caution must be exercised if one is to apply this optimum condition to systems in secondary preferred states. It has been concluded by Goodhew [52] that "the energy of the special (e.g., CSL) boundary is generally a larger component of the total than that contained in the secondary dislocation arrays". This conclusion from homophase systems may be extended to heterophase systems. The change of the OR and IO to meet the invariant line strain criterion may alter the atomic structure in subtle ways in the regions between the dislocations. Formation of an invariant line is often at the expense of increasing atomic steps. While the atomic steps do not usually affect conservation of the primary preferred state in the region between the dislocations, they will cause discontinuity of secondary preferred state. Hence, a secondary invariant line crossing steps may not be preferred, as noticed in recent investigation of cementite/austenite system [45]. On the other hand, as explained later, the distinction between the steps crossed by a secondary invariant line and steps associated with secondary dislocations specified in the following condition is not substantial.

The third optimum condition requires a one-to-one coincidence of steps and secondary misfit dislocations, instead of eliminating the steps or dislocations. For the convenience of discussion, such a dislocation and step pair is denoted as a d-step. Interfacial steps carrying dislocation characteristic have been studied in detail for grain boundaries associated with the CSL/DSCL model [39,76,77]. If the step height ($h$) is not equal to the spacing of the (C)CSL planes ($d_{\mathrm{CCSL}}$), the step must be associated with a displacement. The displacement must be in units of a lattice vector in the (C)DSCL in order for the structure in the plane of the (C)CSL to be fully maintained in different terrace planes [39,76]. The role of such a d-step is twofold: to preserve repetition of a 2D CCSL pattern in the terraces and to accommodate the misfit in the interface with the amenable secondary Burgers vector. It is useful to recollect at this point the energetic argument proposed by van der Merwe et al. in favor of the structural ledges [78,79]. Though their argument was developed for the

systems in the primary preferred state, it is likely that preference of a d-step structure could be explained by the same reason, because cancellation of the misfit in the terrace planes by the d-steps is similar to the cancellation of the misfit by the "pattern advance" associated with the structural ledges. However, because the structure in an interface in a secondary preferred state is more complicated, validation of this hypothesis would require quantitative justification.

The following argument for preference of d-steps is given on the basis of misfit analysis. While secondary misfit dislocations are often the necessary defects in a long-range strain free interface as an ideal 2D CSL is not allowed by the lattice constants, the steps are not the necessary defects since an interface is free to lie parallel to low index planes. Stepped interfaces are preferred when the small CDSCL vectors, as theoretical candidates for the Burgers vectors of the secondary dislocations, are not available in the terrace plane containing dense CCSL points. If the interface is parallel to such a CCSL plane, the secondary misfit in the plane would be accommodated by the dislocations with rather large Burgers vector(s), limited by the inplane CDSCL vectors. In this case, a structure consisting of terraces parallel to the plane of dense CCSL points and steps associated with a smaller Burgers vector may be favored, because the decrease of the Burgers vector by a discrete value may result in an abrupt reduction of the maximum secondary misfit distortion in the interface. This effect is illustrated by an example in Appendix A, showing that the degree of overall interfacial matching is improved significantly in the stepped interface compared with the step free interface (refer Fig. 15d). A d-step structure may occur when the CCSL/CDSCL structure carries the following two types of features. In the first type, the plane containing dense CCSL points is not parallel to the plane containing small CDSCL vectors (refer Fig. 8a). In the second type, the plane containing small CDSCL vectors is parallel to the plane containing dense points in the CCSL, but the parallel planes do not lie in the same position (refer Fig. 15a). A displacement of such a small vector in this case will not yield a complete pattern shift in the plane of the CCSL, but it will shift the CCSL pattern to a sequent plane.

While the first two optimization conditions have been extensively tested against experimental data, the third condition has not, due to the demanding precision in either experimental studies or modeling of interfacial structure at the level of interfacial steps. However, the terrace planes of the habit planes from several systems have been found to exhibit a coincidence of steps with dislocations [66,80,81]. Periodic steps observed from the habit plane between ferrite and cementite in steels are probably d-steps because of large lattice misfit between the related phases, but they were regarded as structural ledges accommodating the interfacial misfit [82]. An interesting case is that the periodic d-steps were introduced to avoid stacking faults in flat interfaces between ordered phases [81]. An interface that obeys the second optimum condition may also contain steps. Unlike the model that incorporated interfacial steps with dislocations for estimating the interfacial energy [36], the optimum conditions suggested above have emphasized the singularity of the defects. Usually, a singular interface should either contain no step or contain steps that they themselves can accommodate completely the interfacial misfit along a particular direction, along

Table 1
Interfacial structures for different combination of the optimum conditions

| Dislocation structures | First condition: step free interfaces | | Stepped interfaces | | |
|---|---|---|---|---|---|
| | Primary state | Secondary state | Primary state | Secondary state | |
| | | | | $h = d_{CCSL}$ | Third condition |
| Second condition | | | | | |
| 0 set | $A_I$ | $A_{II}$ | $B_I$ | $B_{II}$ | |
| 1 set | $C_I$ | $C_{II}$ | $D_I$ | $D_{II}$ | $F_{II}$ |
| Network | $E_I$ | $E_{II}$ | | | $G_{II}$ |

an invariant line [9] or a quasi-invariant line crossing the d-steps. In terms of the dislocations, the singularity simply corresponds to the dislocation spacing of infinite.

Each optimum condition imposes a constraint on the OR since the condition can be realized only when the two lattices are oriented in a unique way. Any interface that is singular with respect to both the IO and OR must satisfy at least one of the three optimum conditions. Such a singular interface can either be rational or irrational in its orientation, depending on which optimum condition is active. For those systems in the appropriate preferred state, each optimum condition might be independently realized. When allowed by the lattice constants, two or more conditions can be satisfied in a single interface. The possible combinations of the optimum conditions in addition to the single optimum condition cases lead to a finite set of singular structures, which are listed in Table 1. In this table, each type of singular interfacial structure, denoted by an alphabetical letter, satisfies at least one optimum condition, plus the condition of dislocation periodicity. To distinguish the structures in the different preferred states, primary and secondary preferred states are denoted by subscripts I and II, respectively. Note that the second optimum condition can be applied twice, in different directions, leading to a dislocation free interface. For example, an interface identified by $A_I$, or simply an $A_I$ interface, meets the first and second (in more than one direction) optimum conditions. It contains neither dislocations nor steps. So far, there is no evidence to show that the third optimum condition is satisfied in different directions. Thus, this choice is not included in the table. The optimum structures are illustrated schematically in Fig. 3, in which fine solid lines and thick dashed lines represent dislocations and interfacial steps, respectively. The superposition of solid and dashed lines indicates coincidence of the cores of the dislocations and the step risers in the structures. [10]

[9] If the invariant line is parallel to a low index direction, though it is a rare case, the singular interface that obeys the secondary optimum condition may contain steps so that the interface can contain periodic dislocations.

[10] The difference between $B_{II}$ and $F_{II}$ or between $D_{II}$ and $G_{II}$ interfaces may not be substantial, since, as discussed in Appendix A, the 2D CCSL representing the preferred state will be discontinuous at any steps, and the displacement associated with the steps will cancel the secondary misfit in the terrace planes, whether the steps are described to be associated with secondary dislocations or not.

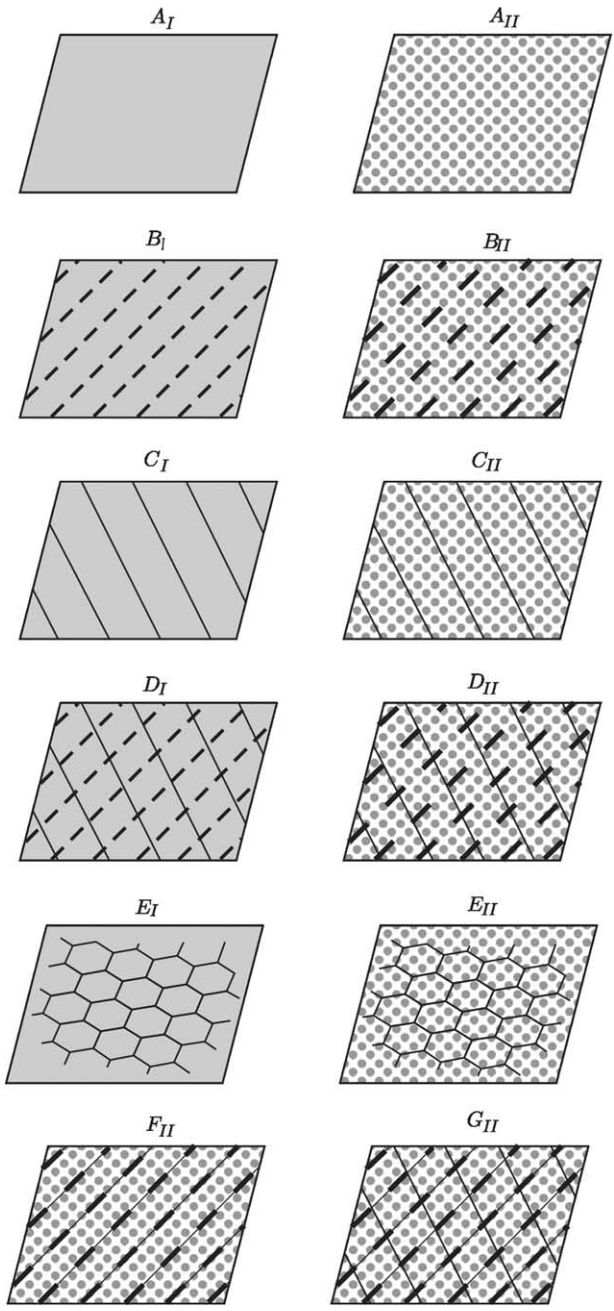


Fig. 3. Characteristic structures in the singular interfaces, whose notations are listed in Table 1. The primary and secondary preferred states are shown by an even and gray background and by a background of gray dots respectively. Misfit dislocations and interfacial steps are represented respectively by solid and dashed lines.

The singular interfacial structures listed in Table 1 are general, in the sense that these structures may be present in any crystalline material, though the completeness of this set of structures requires further testing. The interfacial structures in systems containing complicated crystal phases may be developed through a dislocation reaction or by decomposition from one of the structures in Table 1, but such a reaction will not alter the crystallography of the singular interfaces. Satisfaction of one optimum condition alone does not impose a full constraint on the OR, but it restricts two degrees of freedom in the OR (This will be explained in Section 5.2). Five out of 12 structures in the table (i.e. $E_{\mathrm{I}}$, $E_{\mathrm{II}}$, $D_{\mathrm{I}}$, $D_{\mathrm{II}}$, $G_{\mathrm{II}}$) satisfy one optimum condition only once. They leave one undefined degree of freedom in the OR. The remaining structures are singular to any variation in the 5D BGP space. These structures, in addition to those consisting of no steps, or d-steps must be singular with respect to the IO, as they can form only in interfaces of discrete orientations. The remaining structures, $D_{\mathrm{I}}$ and $D_{\mathrm{II}}$, are not singular only if they are in a system of an invariant plane strain. The invariant plane strain is rare, and once the strain is realized, any ambiguity about the singular structure is unlikely to be encountered since the dislocation free habit plane would be the dominant face of the precipitate. Therefore, if the structure $D_{\mathrm{I}}$ or $D_{\mathrm{II}}$ is observed in a broad interface, this structure must be singular with respect to the IO.

## 4. Determination of singular interfaces in framework of model lattices

Given a general precipitation system, what interfaces in the 5D BGP space will contain singular structures? This question addresses the intimate connection between the microscopic and macroscopic descriptions of an interface. An important clue to the answer to this general question can be deduced from the common characteristic of all singular interfaces, i.e. their singular periodicity. Various model lattices, including the O-lattices, the CSL and DSCL (with or without constraint), have proven particularly helpful to the investigation of periodicity of fit/misfit between two lattices of crystalline phases [37]. Detailed descriptions of these model lattices can be found from the well-known books by Bollmann [37,58]. The following review focuses on the use of the model lattices for identifying interfaces with singular periodic structures. In addition to the expression of the model lattices in direct space, their expression in reciprocal space will be emphasized. This approach helps to bridge the descriptions of singular interfaces in different scales. In contrast to common applications, which usually input the macroscopic description of an interface (i.e. the OR and IO) and obtain an output of the microscopic description (e.g. the interfacial structure) from a calculation with a model lattice, an inverse route has been employed here, i.e. the output of the analysis is the characteristic OR and IO that permit a structure with singular periodicity to be realized.

For a valid description of an interfacial structure, it is important to specify the structural element considered to define the periodicity. The singular structures in Table 1 may be described by three types of periodic elements: primary dislocations, atomic structural units, or secondary dislocations. Periodicity of dislocations can be

most conveniently described in the framework of a primary or secondary O-lattice [37,58]. If the periodicity is described in terms of atomic structural units, the CSL, instead of the O-lattice, must be adopted. In the following sections we will describe different singular interfaces separately with appropriate model lattices.

### 4.1. Primary O-lattice and planes containing periodic dislocation structures

The primary O-lattice is the model lattice for the description of the primary dislocations, but the prefix "primary" is often omitted, as the Burgers vectors of the dislocations are simply those for the allowed dislocations in either phase. The primary O-lattice applies to a system in which the primary preferred (fully coherent) state is maintained between the dislocations. The lattice misfit in this system must be small, so that the spacing of the primary dislocations is large enough to permit validity of the model.

Let us consider a system of two lattices ($\alpha$ and $\beta$) related by an arbitrary OR. As proposed by Bollmann [37], an O-lattice is constructed by letting lattices $\alpha$ and $\beta$ to interpenetrate according to the given OR. The pattern in Fig. 2 is a simple example of a 2D O-lattice formed by superimposing a pair of identical lattices that are rotated relatively to one another. The periodicity of this fit/misfit pattern is described by the O-lattice, with O-points, indicated by open circles, located at the centers of good fit. The regions of poor lattice match form a cell structure, with O-cell walls located at the positions where the lattice match is the poorest, as indicated by the dashed lines in Fig. 2. In 3D, the O-lattice element can be a point, a line or a plane. Each element defines the center of O-cell, a volume in which the lattice fit varies continuously from good at the center to poor at the borders between the adjacent cells. These borders are called O-cell walls. Regardless of the nature of the O-lattice elements, the O-cell walls are always periodic planes defining the locations of poor lattice match. According to the suggestion by Bollmann, the lines where O-cell walls are intercepted by an interface represent the configurations of the possible misfit dislocations after relaxation to a long-range strain free state [37].

However, it should be emphasized that the representation of the dislocations by the intersections between an interface and the O-cell walls is valid only if the area enclosed by the intersection lines becomes a coherent region upon relaxation. Take the simple case shown in Fig. 2 as an example. In this figure, there is an O-point between each pair of adjacent intersection points in interface *a–a*. Upon relaxation, one would expect that these O-points become the centers of the coherent patches where the primary preferred state is maintained. The relaxation will result in the formation of a periodic array of dislocations (perpendicular to the plane of the paper) at the locations where the patches of coherent regions meet. Consequently, the cores of the dislocation lines will most likely be located near the mathematical intersections of the O-cell walls and the interface *a–a*, as described by the well-accepted model for a small angle symmetric tilt grain boundary. In contrast, not all mathematical intersection points between the O-cell walls with an interface can become dislocations. For example, it is questionable whether those intersections denoted by "?" in interface *b–b* will become dislocations, as the regions between the

dislocations may not become fully coherent upon relaxation. However, regardless of its precise relaxed structure, interface *b–b* must contain more than one set of dislocations, described by different Burgers vectors.

Our present concern is the interfaces containing simple periodic structure, as favored by nature. For an interface to contain regular patches of good matching separated by periodic dislocations, the interface must intersect a set of parallel O-cell walls and pass all O-elements between walls. Formally, the interface must contain the vector connecting the O-elements separated by a single O-cell wall. Such a vector, referred to *the principal O-lattice vector*, can be readily identified in a graphical presentation of an O-lattice, as identified by open circles in Fig. 2. The intimate relationship between a principal O-lattice vector and the Burgers vector of the dislocation is that "*the relative displacement between lattices α and β connected by a principal O-lattice vector is a Burgers vector*." This important relationship lays the basis for numerical expression of the O-lattice.

For generality and mathematical simplicity, let us first consider a system with a 3D misfit strain field. The locations of all points from lattices $\alpha$ and $\beta$ are conveniently described by vectors, $\mathbf{x}_\alpha$ and $\mathbf{x}_\beta$, in lattices $\alpha$ and $\beta$ respectively, with a point from each lattice located at the origin. The vectors are related by a matrix operation, **A**, conventionally called a transformation strain, i.e. [11] [37,58]

$$\mathbf{x}_\beta = \mathbf{A}\mathbf{x}_\alpha. \tag{1}$$

Since the strain is defined with respect to the primary preferred state, **A** is also referred to as the primary misfit strain, in contrast to the secondary misfit strain discussed later. The primary misfit strain is determined according to the nearest neighbor principle applied to the shortest lattice vectors (or other pairs within the central O-cell) [37]. The displacement field of the phase transformation is defined by matrix **T**, given by

$$\mathbf{T} = \mathbf{I} - \mathbf{A}^{-1}, \tag{2}$$

where **I** is a unit matrix. The operation of the displacement matrix **T** on any vector from lattice $\beta$ yields the displacement with respect to its associated vector in lattice $\alpha$. The rank of the matrix **T**, rank(**T**), defines the dimension of the misfit strain field (also in reciprocal space). Given a 3D misfit strain, rank(**T**) = 3 and the O-lattice is an O-point lattice. A principal O-lattice vector, $\mathbf{x}_i^{\mathrm{O}}$, is defined by [37]

$$\mathbf{T}\mathbf{x}_i^{\mathrm{O}} = \mathbf{b}_i^{\mathrm{L}}, \tag{3}$$

where $\mathbf{b}_i^{\mathrm{L}}$ is a Burgers vector defined in lattice $\alpha$, which is conventionally called the reference lattice. The subscript '*i*' is used to specify the correspondence: the relative displacement associated with $\mathbf{x}_i^{\mathrm{O}}$ (in lattice $\beta$) is $\mathbf{b}_i^{\mathrm{L}}$. This relationship is illustrated in Fig. 4, where three inplane $\mathbf{b}_i^{\mathrm{L}}$'s and the related $\mathbf{x}_i^{\mathrm{O}}$'s are specified. A 3D O-lattice

[11] Lower-case letters in bold face type are used to represent column vectors, while upper-case letters in bold face type are used to represent 3×3 matrixes. All vectors in the matrix calculations are defined in orthogonal coordinates.

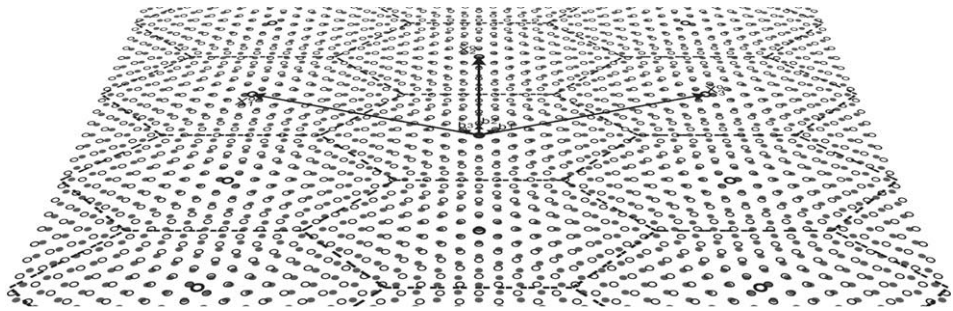

Fig. 4. A principal primary O-lattice plane (formed by superimposing an fcc {1 1 1} plane with a bcc {1 1 0} plane according to the N–W OR) in which the three basis O-lattice vectors are specified as vectors connecting the O-points at the centres of adjacent O-cells; possible locations of the periodic dislocations are indicated by dashed lines, as defined by the intersection of the O-cell walls with the interface plane.

point lattice is completely defined by translations of three non-coplanar $\mathbf{x}_i^{\mathrm{O}}$ vectors, associated with non-coplanar $\mathbf{b}_i^{\mathrm{L}}$'s. While the relative displacement is a linear function of the point position with respect to the origin, the lattice misfit varies periodically from one O-cell to the next. Any O-point always defines the position where the misfit displacement is the smallest.

The O-cell wall (as well as the dislocations inherited from the O-cell walls) dividing the $\mathbf{x}_i^{\mathrm{O}}$ vector is associated with the same Burgers vector. The set of O-cell walls can be represented by a reciprocal vector defined by [83]

$$\mathbf{c}_i^{\mathrm{O}} = \mathbf{T}'\mathbf{b}_i^*, \tag{4a}$$

where

$$\mathbf{b}_i^* = \mathbf{b}_i^{\mathrm{L}}/|\mathbf{b}_i^{\mathrm{L}}|^2 \tag{4b}$$

defines a reciprocal Burgers vector, which represents a set of faces (normal to $\mathbf{b}_i^{\mathrm{L}}$) of the Wigner–Seitz cells of the reference lattice. The symbol prime "′" denotes a transpose operation on the associated matrix or vector. Usually, $\mathbf{c}_i^{\mathrm{O}}$ is not parallel to $\mathbf{x}_i^{\mathrm{O}}$. A simple way to examine whether a set of periodic dislocations will be present in a particular interface is to examine whether this interface contains the $\mathbf{x}_i^{\mathrm{O}}$ vector corresponding to $\mathbf{b}_i^{\mathrm{L}}$. Given the normal, $\mathbf{n}$ (a unit vector), of an interface containing $\mathbf{x}_i^{\mathrm{O}}$, the direction of the periodic dislocations is given by [83]

$$\boldsymbol{\xi}_i = \mathbf{c}_i^{\mathrm{O}} \times \mathbf{n} \tag{5a}$$

and the dislocation spacing is

$$d_{i\text{-dis}} = 1/|\boldsymbol{\xi}_i|. \tag{5b}$$

For rank($\mathbf{T}$) = 3, a singular interface must contain two or three $\mathbf{x}_i^{\mathrm{O}}$'s corresponding to different $\mathbf{b}_i^{\mathrm{L}}$'s. This interface will contain a network (two or three sets) of periodic

dislocations defined by these Burgers vectors, e.g. $E_I$ in Table 1. The 2D O-lattice in Fig. 4 can be regarded as an example of such an interface. [12] The dashed lines in Fig. 4, defined by the intersections of the O-cell walls with the interface plane, indicate possible locations of the periodic dislocations. Such a special O-lattice plane, containing at least two $\mathbf{x}_i^O$ has been defined as a primary O-lattice plane [83]. To avoid confusion between the general planes of the primary O-lattice and the primary O-lattice planes defined above, we re-define this special group of O-lattice planes as principal primary (or principal) O-lattice planes and extend the definitions for the other types of the O-lattice elements as follows.

When $\text{rank}(\mathbf{T}) < 3$, the definitions in Eqs. (1)–(5) remain valid, but the existence of an O-lattice depends on the solution of Eq. (3). A strictly periodic distribution of the O-elements in 3D (3D O-lattice) in this case is limited by the lattice constants, and is seldom fulfilled in reality. On the other hand, a plane of O-lines or a single O-plane is often possible. Since a fit/misfit pattern normal to a singular interface does not affect the description of the interface, for practical applications it is convenient to emphasize the plane of the O-element(s) rather than the 3D O-lattice. While the principal primary O-lattice plane for $\text{rank}(\mathbf{T}) = 3$ is the plane containing the periodic O-points, the principal primary O-lattice plane for $\text{rank}(\mathbf{T}) = 2$ is one containing the periodic O-lines (or a single set of periodic dislocations, i.e. $C_I$ or $D_I$). In case of $\text{rank}(\mathbf{T}) = 1$, we define the principal primary O-lattice plane to be parallel to the O-plane element. A single O-plane element, or the invariant plane in general, is sufficient to define a dislocation-free singular interface (i.e. $A_I$ or $B_I$). While the singular interface in this special case can be determined from different methods without reference to the O-lattice concept, it is included here for completeness.

*In this context, all candidates for the singular interfaces in primary preferred state, containing either periodic or no dislocations, should be chosen from the principal primary O-lattice planes*. An interface so defined is always singular with respect to the IO, because any principal primary O-lattice plane is always a discrete plane. The periodic structure in a principal primary O-lattice plane is guaranteed by the inplane periodic O-elements alternating with the intersected O-cell walls, which may be inherited as the dislocations. Whether the calculated dislocation structure can be realized in an interface parallel to a principal O-lattice plane, containing the appropriate O-elements, depends on whether the regions centered at the O-lattice elements can become coherent after relaxation.

### 4.2. Principal primary $\Delta\boldsymbol{g}$ vectors ($\Delta\boldsymbol{g}_{\text{P-I}}$)

Based on the O-lattice in direct space considered above, a quantitative description of a singular interface containing two sets of dislocations can be obtained by the cross product of the two $\mathbf{x}_i^O$'s corresponding to different $\mathbf{b}_i^L$'s. The plane containing

[12] The 2D O-lattice and O-cell structure in Fig. 4 has been plotted from a program, written by Min Zhang according to Eqs. (3)–(5) available from http://www.mse.tsinghua.edu.cn/faculty/zhangwzh/english/index.htm.

one set of parallel dislocations (or O-lines) can also be determined by two $\mathbf{x}_i^{\mathrm{O}}$'s (or equivalently one $\mathbf{x}_i^{\mathrm{O}}$ plus the invariant line, since all $\mathbf{x}_i^{\mathrm{O}}$'s must be coplanar with the invariant line). In contrast to the O-point lattice, both $\mathbf{x}_i^{\mathrm{O}}$'s are solved corresponding to the same $\mathbf{b}_i^{\mathrm{L}}$ (since multiple solutions exist for Eq. (3) in this case). However, as for other periodic structures, it is much simpler to define the principal O-lattice planes through a formulation in reciprocal space [83]. Moreover, the reciprocal vectors for the O-lattices are readily measured using conventional transmission electron microscopy (TEM). This allows one to identify candidates for singular interfaces in reciprocal space, where the experimental measurement of the macroscopic parameters of interfaces or the precipitation crystallography is conventionally recorded.

In reciprocal space, vectors in different lattices, $\mathbf{g}_\alpha$ and $\mathbf{g}_\beta$, are related by the same transformation strain in a different way [84]:

$$\mathbf{g}_\beta = (\mathbf{A}^{-1})'\mathbf{g}_\alpha. \tag{6}$$

The displacement between a pair of correlated reciprocal vectors is

$$\Delta\mathbf{g}'_{\mathbf{I}} = \mathbf{g}'_\alpha(\mathbf{I} - \mathbf{A}^{-1}) = \mathbf{g}'_\alpha\mathbf{T}, \tag{7a}$$

where the subscript '**I**' is used to distinguish a primary $\Delta\mathbf{g}$ that only connects $\mathbf{g}_\alpha$ and $\mathbf{g}_\beta$ related by a primary misfit strain from any $\Delta\mathbf{g}$ that is otherwise related. Provided that $\mathrm{rank}(\mathbf{T}) = 3$, hence $\mathbf{T}$ is invertible and the O-lattice is a point lattice. Rewriting Eq. (7a) as

$$(\mathbf{T}^{-1})'\Delta\mathbf{g}_{\mathbf{I}} = \mathbf{g}_\alpha, \tag{7b}$$

one immediately sees that Eq. (7b) defines an O-lattice transformation in reciprocal space corresponding to Eq. (3) in direct space. Therefore, the displacement vector $\Delta\mathbf{g}_{\mathbf{I}}$ defined by Eq. (7a) is a reciprocal vector of the primary O-lattice [83].

A set of periodic principal primary O-lattice planes is defined by a principal primary $\Delta\mathbf{g}$ vector, denoted by $\Delta\mathbf{g}_{\text{P-I}}$, which is associated with $\mathbf{g}_{\text{P-}\alpha}$ by

$$\Delta\mathbf{g}_{\text{P-I}} = \mathbf{T}'\mathbf{g}_{\text{P-}\alpha} = \mathbf{g}_{\text{P-}\alpha} - \mathbf{g}_{\text{P-}\beta} \tag{8}$$

with $\mathbf{g}_{\text{P-}\alpha}$ representing a set of principal planes containing at least two Burgers vectors in lattice $\alpha$, while $\mathbf{g}_{\text{P-}\beta}$ is the vector in lattice $\beta$, correlated to $\mathbf{g}_{\text{P-}\alpha}$ by Eq. (6). The vector of $\Delta\mathbf{g}_{\text{P-I}}$ is measurable, since $\mathbf{g}_{\text{P-}\alpha}$ and $\mathbf{g}_{\text{P-}\beta}$ can often be easily recognized from low index spots in an appropriate superimposed diffraction pattern.

A unique character of the interface normal to $\Delta\mathbf{g}_{\text{P-I}}$ is that the planes $\mathbf{g}_{\text{P-}\alpha}$ and $\mathbf{g}_{\text{P-}\beta}$ should be in perfect registry at the interface. This property can be seen from the construction of Moiré fringes formed by interference of the planes defined by $\mathbf{g}_{\text{P-}\alpha}$ and $\mathbf{g}_{\text{P-}\beta}$ in Fig. 5a. The Moiré planes in this figure are normal to the vector $\Delta\mathbf{g}_{\text{P-I}}$, and their positions are defined by the locations where the two sets of planes intersect, [13] as indicated by the dashed and dotted lines in the figure. Based on this definition, the

[13] In an earlier publication [58], positions of the Moiré planes were defined at the regions of the worst matching, identical to the dark Moiré fringes. For the convenience of applications, we redefine them, and this new definition is consistent with the definition by Bollmann [58].

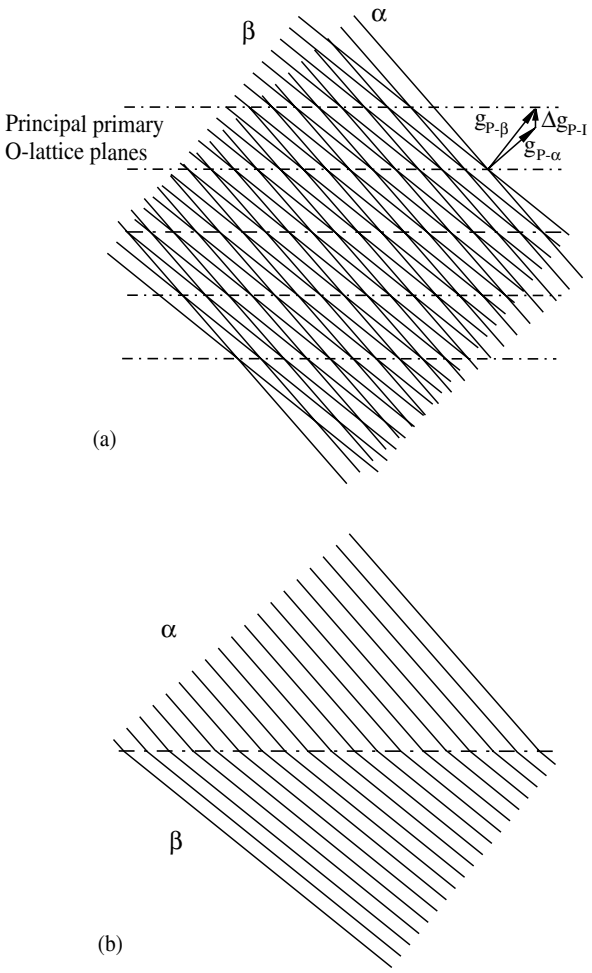


Fig. 5. (a) Relationship between Moiré fringes, principal primary O-lattice planes, and a $\Delta\mathbf{g}_{P\text{-}I}$ vector and (b) registry of planes $\mathbf{g}_{P\text{-}\alpha}$ and $\mathbf{g}_{P\text{-}\beta}$ at the interface lying along a principal primary O-lattice plane normal to $\Delta\mathbf{g}_{P\text{-}I}$.

related planes should meet edge-to-edge in each Moiré plane. This above property of the Moiré planes is completely general, without referring to the concept of the O-lattice. For a Moiré plane to be parallel to an O-lattice plane, the $\Delta\mathbf{g}$ vector normal to the Moiré plane must connect two $\mathbf{g}$'s that are related by Eq. (6), in which a one-to-one correspondence is implied. The Moiré planes formed from intersection of two sets of principal (usually low index) planes of crystal lattices, $\mathbf{g}_{P\text{-}\alpha}$ and $\mathbf{g}_{P\text{-}\beta}$, are often the most important in the study of interfaces. We further define these Moiré planes as principal Moiré plane, but, for general applications, we do not require the corresponding $\mathbf{g}_{P\text{-}\alpha}$ and $\mathbf{g}_{P\text{-}\beta}$ to be related by any particular strain. In systems where the

lattice misfit is larger, the principal Moiré planes may be formed by planes $m\mathbf{g}_{\text{P-}\alpha}$ and $n\mathbf{g}_{\text{P-}\beta}$ (where $m$ and $n$ are integers). Thus, though the difference between $\mathbf{g}_{\text{P-}\alpha}$ and $\mathbf{g}_{\text{P-}\beta}$ may be large, $\Delta\mathbf{g}(m\mathbf{g}_{\text{P-}\alpha} - n\mathbf{g}_{\text{P-}\beta})$ to define the principal Moiré planes may be small and easy to be recognized in a diffraction pattern. Then, one finds fractional, rather than one-to-one, matching between the planes $\mathbf{g}_{\text{P-}\alpha}$ and $\mathbf{g}_{\text{P-}\beta}$ in the principal Moiré planes. On the other hand, when the lattice misfit is small, the principal primary O-lattice planes normal to $\Delta\mathbf{g}_{\text{P-I}}$ must be identical to the principal Moiré planes formed by the related planes $\mathbf{g}_{\text{P-}\alpha}$ and $\mathbf{g}_{\text{P-}\beta}$. After the removal of the different sets of planes from either side of an interface lying along a principal O-lattice plane, the two sets of related planes are in exact registry, as seen in Fig. 5b. Since Moiré fringes are frequently visible from TEM image, the association of $\Delta\mathbf{g}$'s with habit planes or facets can be tested by the TEM studies, as already done in several investigations [21,23,85,86]. The geometric phase technique recently developed by Hytch et al. [87] is particularly helpful for this purpose.

The displacement associated with a point located in one or more principal Moiré planes can be elucidated by the following equations. In case of an O-point lattice, all $\mathbf{x}_i^{\text{O}}$'s in the plane normal to $\Delta\mathbf{g}_{\text{P-I}}$ must be associated with the $\mathbf{b}_i^{\text{L}}$'s lying in the plane normal to $\mathbf{g}_{\text{P-}\alpha}$. This result can be seen from the following relationship that combines Eqs. (3) and (8) [88]

$$\Delta\mathbf{g}'_{\text{P-I}}\mathbf{x}_i^{\text{O}} = \mathbf{g}'_{\text{P-}\alpha}\mathbf{T}\mathbf{x}_i^{\text{O}} = \mathbf{g}'_{\text{P-}\alpha}\mathbf{b}_i^{\text{L}} = 0. \tag{9a}$$

If we replace $\mathbf{x}_i^{\text{O}}$ in Eq. (9a) by a general vector, $\mathbf{y}$, lying in the interface, and replace $\mathbf{b}_i^{\text{L}}$ by the relative displacement $\mathbf{d}(=\mathbf{T}\mathbf{y})$, then the above equation becomes

$$\Delta\mathbf{g}'_{\text{I}}\mathbf{y} = \mathbf{g}'_{\alpha}\mathbf{T}\mathbf{y} = \mathbf{g}'_{\alpha}\mathbf{d} = 0. \tag{9b}$$

Eq. (9b) is completely general, and it indicates that the relative displacement associated with any vector in the interface normal to $\mathbf{g}_{\text{I}}$ must lie in the plane of the related $\mathbf{g}_{\alpha}$. In deriving the Eq. (9) it is implied that any set of planes from either crystal lattice must contain one plane that passes through the origin (since a lattice point is located at the origin), so that any set of Moiré planes will also contain one that passes through the origin.

Matching of one pair of planes only ensures elimination of the misfit in 1D, i.e. in the direction normal to the correlated planes. To eliminate the misfit in 3D, any good matching point must be located at place where at least three pairs of correlated planes cross one another. The geometry of an O-element meets the above requirement, because it is located at the intersection of at least three sets of principal O-lattice planes, in the condition that the $\Delta\mathbf{g}_{\text{P-I}}$ vectors defining O-lattice planes are associated with no-coplanar $\mathbf{g}_{\text{P-}\alpha}$'s or $\mathbf{g}_{\text{P-}\beta}$'s. It is convenient to elucidate the shape and distribution of the O-lattice elements in terms of the orientations of these three $\Delta\mathbf{g}_{\text{P-I}}$'s. If these $\Delta\mathbf{g}_{\text{P-I}}$'s are non-coplanar, which occurs when $\text{rank}(\mathbf{T}) = 3$, one finds an O-point element wherever the planes defined by the $\Delta\mathbf{g}_{\text{P-I}}$'s meet. If the $\Delta\mathbf{g}_{\text{P-I}}$'s are coplanar, which occurs when $\text{rank}(\mathbf{T}) = 2$ [73], all principal O-lattice planes must meet at least at one line (an invariant line) passing through the origin. This line defines a single O-line element. If, in addition, two of the $\Delta\mathbf{g}_{\text{P-I}}$'s are parallel, the parallel Moiré planes passing through the origin must overlap. Then, one finds

periodic O-line elements at the periodic positions wherever the third set of Moiré planes intersect in the common Moiré plane. The Burgers vector of the O-lines must be contained in both planes that are related to the parallel $\Delta\mathbf{g}_{\text{P-I}}$'s. It can be shown that various sets of other inclined principal Moiré planes will intersect the interface at the same periodic positions [89]. In more special cases, if the parallel $\Delta\mathbf{g}_{\text{P-I}}$'s are identical, then the overlapped principal Moiré planes will become strictly periodic. The plane containing the parallel O-lines will repeat with the common spacing of the principal Moiré planes, resulting in a 3D O-line lattice. Meanwhile, one may also find one or two more pairs of identical $\Delta\mathbf{g}_{\text{P-I}}$'s normal to different planes containing the periodic O-lines. A more general condition for the existence of the 3D O-line lattice is that a $\Delta\mathbf{g}_{\text{P-I}}$ should be zero vector, i.e. its related $\mathbf{g}_{\text{P-}\alpha}$ or $\mathbf{g}_{\text{P-}\beta}$ defines the invariant line in reciprocal space [73]. This condition ensures that the planes related by this zero $\Delta\mathbf{g}_{\text{P-I}}$ vector constantly match with each other, when they are parallel. Consequently, 3D distributed O-line elements can be defined by the locations where two sets of the principal Moiré planes intersect. Each $\Delta\mathbf{g}_{\text{P-I}}$ defines a plane containing the O-lines, and this $\Delta\mathbf{g}_{\text{P-I}}$ can be regarded to be parallel to another $\Delta\mathbf{g}_{\text{P-I}}$ with infinite spacing. While the above condition is special, overlap of two principal Moiré planes may still be possible in a longer range, with a "high order" periodicity determined by a "high order" Moiré pattern formed between these parallel Moiré planes. Finally, if all $\Delta\mathbf{g}_{\text{P-I}}$'s are parallel, which occurs when $\text{rank}(\mathbf{T}) = 1$ [90], all principal Moiré planes at least share a common plane (an invariant plane) passing through the origin, as a single O-plane element. The plane normal to all $\Delta\mathbf{g}_{\text{I}}$'s must contain no dislocations, as it is impossible to define any non-zero vector lying in all $\mathbf{g}_{\text{P-}\alpha}$ planes required by Eq. (9b). Again, the existence of a periodic O-plane lattice requires the parallel $\Delta\mathbf{g}_{\text{P-I}}$'s be identical.

An example of a $D_{\text{I}}$ interface from an fcc/bcc system is given in Fig. 6b, to show the matching condition in an interface lying in the position of two principal Moiré planes. (Third parallel principal Moiré plane in the figure is linearly dependent of the

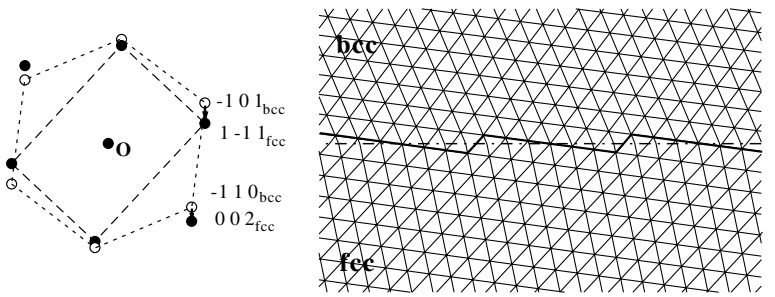


Fig. 6. (a) Superimposed planes of reciprocal points from the parallel zone axes, $[1\,1\,0]_{\text{f}}$ and $[1\,1\,1]_{\text{b}}$. The OR is uniquely defined by a set of parallel $\Delta\mathbf{g}_{\text{P-I}}$'s (identified by the arrows), connecting adjacent low index reciprocal points from the two lattices and (b) matching of correlated low index planes in the interface normal to the parallel $\Delta\mathbf{g}_{\text{P-I}}$'s.

other two.) A superimposed diffraction pattern from the zone axes of $[1\,1\,0]_f$ and $[1\,1\,1]_b$ has been plotted in Fig. 6a, in which the lattice constants have been selected to exaggerate each $\Delta\mathbf{g}_{P\text{-}I}$. (A real diffraction pattern similar to this example can be found in Fig. 12.) The two phases are related by an OR that meets the O-line condition, so that three $\Delta\mathbf{g}_{P\text{-}I}$'s are parallel with one another. These are $\Delta\mathbf{g}_{P\text{-}I1} = (1\,-1\,1)_f - (-1\,0\,1)_b$, $\Delta\mathbf{g}_{P\text{-}I2} = (0\,0\,2)_f - (-1\,1\,0)_b$, $\Delta\mathbf{g}_{P\text{-}I3} = (-1\,1\,1)_f - (0\,1\,-1)_b$. According to the relationship in Fig. 5, all planes (from different lattices) related by the parallel $\Delta\mathbf{g}_I$'s should be in registry at the interface. In Fig. 6b, three sets of low index planes from different lattices fit perfectly at the mathematic interface, indicated by a dashed and dotted line, normal to the parallel $\Delta\mathbf{g}_{P\text{-}I}$'s in Fig. 6a. The term of "mathematic" was used because the actual interface should consist of terraces and steps, as indicated by the thick solid line. The relative displacement in the interface, i.e. the Burgers vector of the interfacial dislocations, lies in the direction of the parallel zone axes, $[1\,1\,0]_f/[1\,1\,1]_b$, normal to the plane of the diffraction pattern. This type of interface has been observed repeatedly using high resolution TEM from Ni–Cr alloys [91,92].

Unlike the principal O-lattice vectors, which may not be solvable using Eq. (3) for some Burgers vectors when the rank($\mathbf{T}$) < 3, all $\Delta\mathbf{g}_{P\text{-}I}$'s can always be calculated from Eq. (8). It is convenient in practice to identify the principal O-lattice planes with $\Delta\mathbf{g}_{P\text{-}I}$'s, since a principal O-lattice plane can always be identified from the $\Delta\mathbf{g}_{P\text{-}I}$'s, no matter what form (point, line or plane) an O-element takes, whether or not this plane periodically repeats in its normal direction. Consequently, *any singular interface in the primary state, being parallel to a principal O-lattice plane, will be normal to at least one* $\Delta\mathbf{g}_{P\text{-}I}$. However, whether a single $\Delta\mathbf{g}_{P\text{-}I}$ will define a singular interface depends on rank($\mathbf{T}$). When rank($\mathbf{T}$) = 3, a one-to-one relationship can be established between a principal O-lattice plane and a $\mathbf{g}_{P\text{-}I}$ vector. Hence, different singular interfaces can be defined, each of which is normal to a $\Delta\mathbf{g}_{P\text{-}I}$. When rank($\mathbf{T}$) = 1, all $\Delta\mathbf{g}_{P\text{-}I}$'s are in one direction normal to the invariant plane, and hence any $\Delta\mathbf{g}_{P\text{-}I}$ defines the singular interface. In the case of rank($\mathbf{T}$) = 2, the singular interface containing the O-lines will be normal to two (or three) $\Delta\mathbf{g}_{P\text{-}I}$'s. In this case, an interface normal to a single $\Delta\mathbf{g}_{P\text{-}I}$ cannot contain a dislocation structure with simple periodicity, given that the interface is free from a long-range strain. On the other hand, an interface inclined to an invariant element (line or plane), which is not singular with respect to the IO in terms of the dislocation structure, will not be normal to any $\Delta\mathbf{g}_I$, though a periodic dislocation structure may be present in the interface if a 3D O-lattice is available.

Table 2 summarizes the relationships between the O-lattice, $\Delta\mathbf{g}_{P\text{-}I}$'s and the singular interfaces, as defined by the principal O-lattice planes, plus the dislocation structure in the singular interfaces. The $\Delta\mathbf{g}_{P\text{-}I}$'s vectors representing the singular interfaces are readily measured from their associated low index $\mathbf{g}_{P\text{-}\alpha}$'s using conventional TEM (e.g. Figs. 6a and 12). Since the plane $\mathbf{g}_{P\text{-}\alpha}$ containing at least two Burgers vectors is limited, the total number of $\Delta\mathbf{g}_{P\text{-}I}$'s is usually small (e.g. <8). Therefore, using $\Delta\mathbf{g}_{P\text{-}I}$'s to identify singular interfaces can be straightforward and simple to apply, provided that the interface is in the primary preferred state. However, if the system is not in the primary preferred state, the singular

Table 2
Descriptions of singular interfaces in the primary preferred state in terms of the primary O-elements and $\Delta\mathbf{g}_{\text{P-I}}$ vectors

| Rank(**T**) | Solution for Eq. (3) | | No. of singular interface | Dislocation set in the interface | No. of $\Delta\mathbf{g}_{\text{P-I}} \perp$ a singular interface |
|---|---|---|---|---|---|
| | No. of $\mathbf{b}_i^{\text{L}}$ | O-element | | | |
| 3 | All | Periodic points in 3D | All $\Delta\mathbf{g}_{\text{P-I}}$'s | 2 or 3 ($E_{\text{I}}$) | 1 |
| 2 | 0 | One line | | 0 | |
| | 1 | Periodic lines in 2D | 1 | 1($C_{\text{I}}/D_{\text{I}}$) | 2 or 3 |
| | 2 or 3 | Periodic lines in 3D | 2 or 3 | | |
| 1 | 0 | One plane | 1 | 0 ($A_{\text{I}}/B_{\text{I}}$) | All |
| | 1 | Periodic planes in 3D | | | |

interfaces can still be characterized by a group of $\Delta\mathbf{g}$'s, but the useful $\Delta\mathbf{g}$'s in this case might be more complicated to identify. This will be considered in the following sections.

### 4.3. CSL/CCSL and their reciprocal vectors

Useful $\Delta\mathbf{g}$'s for identifying singular interfaces in a secondary preferred state are often but not always associated with low index $\mathbf{g}_\alpha$'s. An important step in the association of useful $\Delta\mathbf{g}$'s with the interfacial structures is to classify the $\Delta\mathbf{g}$'s in terms of their representation as the principal planes in the different model lattices. [14] We consider first a simple system in which an ideal CSL can be defined. In contrast to the O-lattice, the calculation of the CSL is independent of the selection of the lattice correspondence [58]. A $\Delta\mathbf{g}$ vector, defined by the difference between any pair of $\mathbf{g}_\alpha$ and $\mathbf{g}_\beta$, is a lattice vector of the DSCL in reciprocal space [56]. According to the reciprocity theorem of the CSL and DSCL due to Grimmer [93], any $\Delta\mathbf{g}$ is a reciprocal vector of the CSL (in direct space). The most important $\Delta\mathbf{g}$'s are those that, as reciprocal vectors, represent the planes containing relatively high density of CSL points, since these planes are plausible candidates for singular interfaces, as discussed in Section 3.1.

Given a CSL, which can be determined either by a graphical method or by calculation [58], a systematic way to identify the dense planes is to construct the Wigner–Seitz cell in the CSL. As is the case for the Burgers vectors in crystals, the

[14] The reciprocity theorem of Grimmer [93] shows that the reciprocal vector of a CSL in direct space is a vector of DSCL in reciprocal space, and vice versa. To identify the representation of a reciprocal vector, we adopt the direct space convention, and designate a reciprocal vector by its representation in direct space.

vectors bisected by the faces of the Wigner–Seitz cell should comprises the smallest vectors. A plane that contains at least two vectors from this set will contain a relatively high density of CSL points. Such a plane is termed a principal CSL plane, and the corresponding reciprocal vector is a principal reciprocal vector of the CSL, designated as $\Delta\mathbf{g}_{\text{P-CSL}}$. Any $\Delta\mathbf{g}_{\text{P-CSL}}$ is a small vector of the DSCL in reciprocal space [93]. The group of smallest $\mathbf{g}_{\text{P-CSL}}$'s usually defines the most plausible choice for the singular interfaces, because of the high CSL point density in the interfaces. It should be noted that there exist identical $\Delta\mathbf{g}_{\text{P-CSL}}$'s connecting different pairs of $\mathbf{g}_\alpha$ and $\mathbf{g}_\beta$, because they are lattice vectors in the DSCL and will repeat periodically, together with the unit cell of the CSL in reciprocal space [56]. Therefore, in the case of a 3D CSL, a dense CSL plane is always normal to a group of differently connected but identical $\Delta\mathbf{g}_{\text{P-CSL}}$'s. Because the CSL must be commensurate with the crystal lattices [58], one can always find a pair of $\mathbf{g}_{\text{P-}\alpha\text{CSL}}$ and $\mathbf{g}_{\text{P-}\beta\text{CSL}}$ parallel to a $\Delta\mathbf{g}_{\text{P-CSL}}$. In practice a CSL plane is usually identified by these crystal planes. The linear relationship between such a crystal vector and different $\Delta\mathbf{g}_{\text{P-CSL}}$'s for the same CSL plane will yield numerous parallel $\Delta\mathbf{g}$'s of various lengths, which can be identical to or even larger than the $\mathbf{g}$ vectors of either crystal lattice. Therefore, a CSL plane should be parallel to various Moiré planes defined by these parallel $\Delta\mathbf{g}$'s normal to the CSL plane. When the general property of Moiré planes is applied (Fig. 5), the planes defined by a pair of $\mathbf{g}$'s connected by one of the parallel $\Delta\mathbf{g}$'s must match with each other at the interface normal to the CSL plane. In addition, all planes whose reciprocal vectors are in coincidence (i.e. their $\mathbf{g}$'s define a CSL point in reciprocal space) must continuously cross any interface. In terms of these continuous planes or matching planes, an interface parallel to a principal CSL plane is a plane of good matching. Numerous planes meet their counterpart at rows of CSL points in the interface.

Unfortunately, such an ideal CSL is rare for heterophase systems. The lattice constants in real systems do not often permit an ideal CSL plane to be formed. However, an appropriate CCSL may be constructed for suggesting a principal CCSL plane as the reference for the secondary preferred state in a singular interface (refer Fig. 1d). Vectors related to the CCSL are denoted by the appropriate subscript, e.g. $\Delta\mathbf{g}_{\text{P-CCSL}}$. A construction of the CCSL is essential for identifying $\Delta\mathbf{g}_{\text{P-CCSL}}$. It is convenient to construct the CCSL in reciprocal space, not only because it is straightforward to determine $\Delta\mathbf{g}_{\text{P-CCSL}}$ but also because the crystallographic data are usually recorded in reciprocal space. In general, a pair of $\mathbf{g}_\alpha$ and $\mathbf{g}_\beta$ in close vicinity to each other can be constrained to become a CCSL point in reciprocal space, so that the secondary strain is reasonably small. An example of the construction of a CCSL in reciprocal space for the cementite/austenite system near the T–H OR is given in Fig. 7. The diffraction pattern in Fig. 7a has been plotted based on the measured data [94]. However, the reciprocal lattice of cementite in Fig. 7b has been constrained, so that a set of nearby reciprocal points in Fig. 7a become coincident, as indicated by a circle around a solid spot. In this hypothetical diffraction pattern, the smallest $\Delta\mathbf{g}$'s are $\pm(-101)_{\text{C}}/2$ or $\pm(-1\,-13)_{\text{A}}/7$, where the subscripts 'C' and 'A' denote the basis of the cementite and austenite lattices respectively. A further analysis suggested that the smallest $\Delta\mathbf{g}_{\text{P-CCSL}}$ in 3D is defined by $\pm(-101)_{\text{C}}/4$ [45]. The 2D CCSL in the

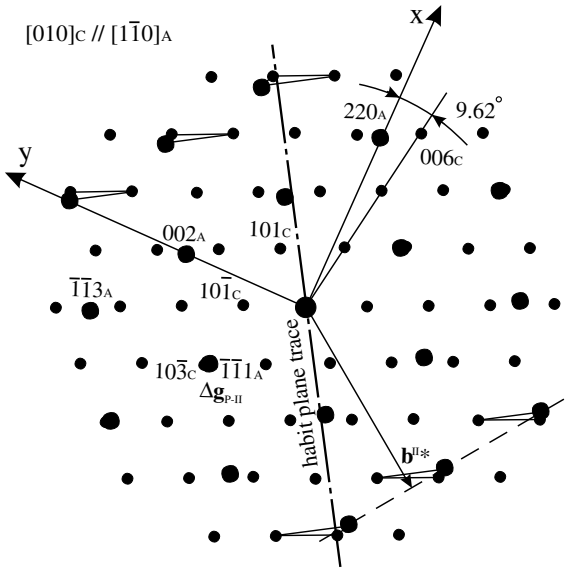


(a)

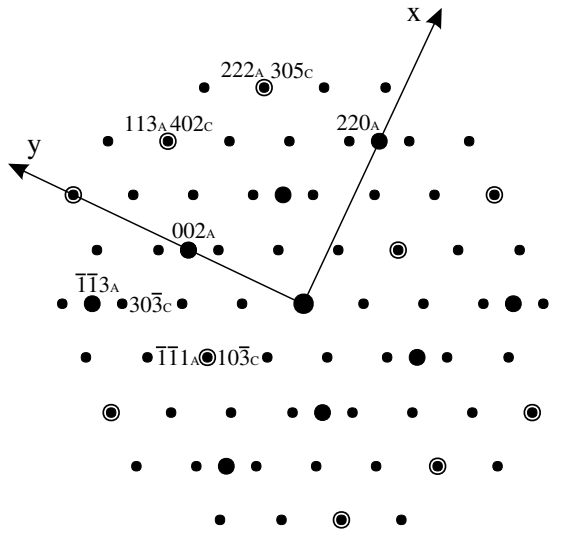


(b)

Fig. 7. Superimposed patterns of reciprocal points in the zone axes of cementite $[0\,1\,0]_C$ (small dots) and austenite $[1\,-1\,0]_A$ (large dots) using real lattice constant for the T–H OR in (a); using constrained lattice parameters for cementite in (b), so that a $CCSL_A$ can be constructed near the T–H OR. These figures have been slightly modified from Figs. 1 and 2 in [45].

plane normal to this vector was adopted as the reference of the secondary preferred state.

While $\Delta\mathbf{g}_{\text{P-CCSL}}$'s are important for defining the useful CCSL plane, the vectors are not measurable in electron diffraction patterns (where the artificial constraint does not exist), unlike the measurable $\mathbf{g}_{\text{P-CSL}}$'s for the ideal case of CSL. The set of $\Delta\mathbf{g}$'s that would be identical to a $\Delta\mathbf{g}_{\text{P-CCSL}}$ in the constrained state will usually be restored to vectors having slightly different directions and lengths compared to the original $\Delta\mathbf{g}_{\text{P-CCSL}}$, as can be seen from a comparison of $\Delta\mathbf{g}$'s in Fig. 7a and b. Though these restored $\Delta\mathbf{g}_{\text{P-CCSL}}$'s can still be identified by their associated $\mathbf{g}$'s (defined in a crystal basis so that the indexing is independent of constraint), the CCSL plane is practically identified by $\mathbf{g}_{\text{P-}\alpha\text{CCSL}}$ or $\mathbf{g}_{\text{P-}\beta\text{CCSL}}$ vector (in their own crystal basis), which is parallel to the $\Delta\mathbf{g}_{\text{P-CCSL}}$ in the constrained state. For example, one can identify from Fig. 7b that the $\mathbf{g}_{\text{P-}\alpha\text{CCSL}}$ or $\mathbf{g}_{\text{P-}\beta\text{CCSL}}$ parallel to the selected $\Delta\mathbf{g}_{\text{P-CCSL}}$ is $(-1\,-1\,3)_{\text{A}}$ or $(1\,0\,-1)_{\text{C}}$.

The vector $\mathbf{g}_{\text{P-}\alpha\text{CCSL}}$ may or may not be parallel to $\mathbf{g}_{\text{P-}\beta\text{CCSL}}$, which depends on whether the singular interface contains steps. When the singular interface does not contain steps, $\mathbf{g}_{\text{P-}\alpha\text{CCSL}}$ should be parallel to $\mathbf{g}_{\text{P-}\beta\text{CCSL}}$, both normal to the interface. A small angular deviation between these vectors usually occurs when the corresponding plane of the CCSL serves as the terrace plane of a stepped singular interface. It results from the difference of the step heights defined in the different lattices. The angular deviation between them is usually small, arising from the secondary strain. In the following analysis we assume that at least one plane of the CCSL can be defined as the preferred state in the majority of the interface area. This plane normal is defined by either $\mathbf{g}_{\text{P-}\alpha\text{CCSL}}$ or $\mathbf{g}_{\text{P-}\beta\text{CCSL}}$.

### 4.4. Secondary O-lattice and principal secondary $\Delta\boldsymbol{g}$ vectors ($\Delta\boldsymbol{g}_{\text{P-II}}$)

When the system (lattice parameters) does not permit the formation of a plane of dense CSL points as the singular interface ($A_{\text{II}}$ in Fig. 3), steps or secondary dislocations may be introduced to accommodate the deviation from the secondary preferred state. Then, a singular interface will consist of periodic steps ($B_{\text{II}}$ in Fig. 3) and/or secondary dislocations ($C_{\text{II}} \sim G_{\text{II}}$ in Fig. 3) in addition to the elastically strained structure of the secondary preferred state. While the determination of the structure of the steps in an interface of a fixed orientation is simple geometry when the terrace plane (defined by either $\mathbf{g}_{\text{P-}\alpha\text{CCSL}}$ or $\mathbf{g}_{\text{P-}\beta\text{CCSL}}$) and step height are known, the determination of the structure of the secondary dislocations is more complicated and will be analyzed below. The O-lattice models can be extended for analysis of the distribution of the secondary misfit strain [37,58]. The formulas in Sections 4.1 and 4.2 remain applicable, only with the replacement of $\mathbf{A}$ and $\mathbf{b}^{\text{L}}$ for the primary dislocations with the secondary misfit strain $\mathbf{A}^{\text{II}}$ and secondary Burgers vectors $\mathbf{b}^{\text{II}}$, respectively. The vectors in the $\text{CCSL}_\alpha$ and $\text{CCSL}_\beta$ and those in the $\text{CDSCL}_\alpha$ and $\text{CDSCL}_\beta$ (as illustrated in Fig. 1c) should be related by the same secondary misfit strain $\mathbf{A}^{\text{II}}$, i.e.

$$\mathbf{x}_\beta^{\text{CCSL}} = \mathbf{A}^{\text{II}}\mathbf{x}_\alpha^{\text{CCSL}} \tag{10a}$$

and

$$\mathbf{x}_{\beta}^{\mathrm{CDSCL}} = \mathbf{A}^{\mathrm{II}}\mathbf{x}_{\alpha}^{\mathrm{CDSCL}}, \tag{10b}$$

where $\mathbf{x}_{\alpha}^{\mathrm{CCSL}}$, $\mathbf{x}_{\beta}^{\mathrm{CCSL}}$, $\mathbf{x}_{\alpha}^{\mathrm{CDSCL}}$ and $\mathbf{x}_{\beta}^{\mathrm{CDSCL}}$ define vectors in the $\mathrm{CCSL}_{\alpha}$, $\mathrm{CCSL}_{\beta}$, $\mathrm{CDSCL}_{\alpha}$ and $\mathrm{CDSCL}_{\beta}$ respectively (refer Section 3.2). It is more convenient to determine $\mathbf{A}^{\mathrm{II}}$ according to the relative positions of the points in $\mathrm{CCSL}_{\alpha}$ and $\mathrm{CCSL}_{\beta}$, either in direct or reciprocal space [45]. If one lattice, e.g. $\alpha$, is fixed in formation of the CCSL (Fig. 1d), $\mathbf{A}^{\mathrm{II}}$ is equivalent to the constraint which brings a set of points in $\beta$ into coincidence with the corresponding points in $\alpha$. An example of determining $\mathbf{A}^{\mathrm{II}}$ can be found in a recent calculation of the secondary dislocation structure for the cementite/austenite system [45]. According to Bollmann [37,58], the Burgers vectors of the secondary dislocations, $\mathbf{b}^{\mathrm{II}}$, should be selected from the lattice vectors of the DSCL. The candidates for $\mathbf{b}^{\mathrm{II}}$ can be determined as the vectors bisected by the faces of the Wigner–Seitz cell of the reference $\mathrm{CDSCL}_{\alpha}$, as these vectors should include the smallest vectors in the DSCL.

Once $\mathbf{b}_i^{\mathrm{II}}$ and $\mathbf{A}^{\mathrm{II}}$ have been determined, the secondary O-lattice, the secondary O-cell, etc. can be determined in the same way as for the primary preferred state. A principal vector of the secondary O-lattice, $\mathbf{x}_i^{\mathrm{O\text{-}II}}$, is defined by [95]

$$\mathbf{T}^{\mathrm{II}}\mathbf{x}_i^{\mathrm{O\text{-}II}} = \mathbf{b}_i^{\mathrm{II}}, \tag{11}$$

where $\mathbf{T}^{\mathrm{II}} = \mathbf{I} - \mathbf{A}^{\mathrm{II}}$ describes the secondary displacement matrix. The secondary O-cell walls are defined by

$$\mathbf{c}_i^{\mathrm{O\text{-}II}} = (\mathbf{T}^{\mathrm{II}})'\mathbf{b}_i^{\mathrm{II}*}, \tag{12}$$

where $\mathbf{b}_i^{\mathrm{II}*} = \mathbf{b}_i^{\mathrm{II}}/|\mathbf{b}_i^{\mathrm{II}}|^2$ is a secondary reciprocal Burgers vector. Given an interface normal $\mathbf{n}$ (a unit vector), the direction of the secondary dislocations is

$$\boldsymbol{\xi}_i^{\mathrm{II}} = \mathbf{c}_i^{\mathrm{O\text{-}II}} \times \mathbf{n}, \tag{13a}$$

and the dislocation spacing is

$$d_{i-\mathrm{dis}}^{\mathrm{II}} = 1/|\boldsymbol{\xi}_i^{\mathrm{II}}|. \tag{13b}$$

A general reciprocal vector of the secondary O-lattice is given by

$$\Delta\mathbf{g}_{\mathrm{II}} = (\mathbf{T}^{\mathrm{II}})'\mathbf{g}_{\alpha\mathrm{CDSCL}}, \tag{14}$$

where $\mathbf{g}_{\alpha\mathrm{CDSCL}}$ is a reciprocal vector representing a set of parallel planes in the $\mathrm{CDSCL}_{\alpha}$.

Following the approach used to define the principal primary O-lattice plane, an interface containing a periodic secondary dislocation network must be parallel to a principal secondary O-lattice plane, which must contain at least two $\mathbf{x}_i^{\mathrm{O\text{-}II}}$'s. This secondary O-lattice plane is transformed from a principal $\mathrm{CDSCL}_{\alpha}$ plane containing at least two $\mathbf{b}_i^{\mathrm{II}}$'s. If $\mathbf{g}_{\mathrm{P\text{-}}\alpha\mathrm{CDSCL}}$ is designated as the reciprocal vector that represents a set of (parallel) principal $\mathrm{CDSCL}_{\alpha}$ planes, the related principal secondary O-lattice plane is defined by

$$\Delta\mathbf{g}_{\mathrm{P\text{-}II}} = (\mathbf{T}^{\mathrm{II}})'\mathbf{g}_{\mathrm{P\text{-}}\alpha\mathrm{CDSCL}} \tag{15}$$

or

$$\Delta\mathbf{g}_{\text{P-II}} = \mathbf{g}_{\text{P-}\alpha\text{CDSCL}} - \mathbf{g}_{\text{P-}\beta\text{CDSCL}},$$

where $\mathbf{g}_{\text{P-}\beta\text{CDSCL}}$ is a reciprocal vector for $\text{CDSCL}_\beta$, related to $\mathbf{g}_{\text{P-}\alpha\text{CDSCL}}$ by the secondary strain. In common with the principal primary O-lattice planes, a principal secondary O-lattice plane is always normal to at least one $\Delta\mathbf{g}_{\text{P-II}}$ irrespective the shape of the O-elements. The secondary O-lattice determined from the above formulas is derived mainly according to the misfit between the $\text{CDSCL}_\alpha$ and $\text{CDSCL}_\beta$, rather than the misfit between the $\text{CCSL}_\alpha$ and $\text{CCSL}_\beta$. However, if the calculated dislocation structure can be realized in an interface parallel to a principal secondary O-lattice plane depends on whether the O-lattice elements in the plane really define good matching between $\text{CCSL}_\alpha$ and $\text{CCSL}_\beta$. Since good matching between $\text{CDSCL}_\alpha$ and $\text{CDSCL}_\beta$ is a necessary condition for good matching between $\text{CCSL}_\alpha$ and $\text{CCSL}_\beta$, the secondary O-elements must comprise the good matching regions between $\text{CCSL}_\alpha$ and $\text{CCSL}_\beta$. The principal secondary O-lattice planes, containing a single one (in secondary invariant plane strain) or periodic O-elements, should serve as candidates for the singular interfaces, which may contain either no or periodic secondary dislocations.

Accordingly, any singular interface must lie normal to at least one $\Delta\mathbf{g}_{\text{P-II}}$. If the $\Delta\mathbf{g}_{\text{P-II}}$('s) is parallel to $\mathbf{g}_{\text{P-}\alpha\text{CCSL}}$ and $\mathbf{g}_{\text{P-}\beta\text{CCSL}}$, which define the CCSL plane for the preferred state, then the interface normal to $\Delta\mathbf{g}_{\text{P-II}}$('s) will not contain steps. In a special case when a secondary O-plane element can be defined, the interface normal to all $\Delta\mathbf{g}_{\text{P-II}}$'s, $\mathbf{g}_{\text{P-}\alpha\text{CCSL}}$ and $\mathbf{g}_{\text{P-}\beta\text{CCSL}}$ will contain neither secondary dislocations nor steps. Then, all restored $\Delta\mathbf{g}_{\text{P-CCSL}}$'s for the particular CCSL plane remain the same orientation parallel to $\mathbf{g}_{\text{P-}\alpha\text{CCSL}}$ and $\mathbf{g}_{\text{P-}\beta\text{CCSL}}$ once the constraint is removed, and an ideal plane of dense CSL points (or with negligible strain) truly exists ($A_{\text{II}}$). If the parallel $\Delta\mathbf{g}_{\text{P-II}}$'s are not parallel to the $\mathbf{g}_{\text{P-}\alpha\text{CCSL}}$ and $\mathbf{g}_{\text{P-}\beta\text{CCSL}}$, the dislocation free interface normal to all $\Delta\mathbf{g}_{\text{P-II}}$'s must contain steps ($B_{\text{II}}$). Similarly, an interface containing periodic dislocations may or may not contain steps, depending on relative orientations between the $\Delta\mathbf{g}_{\text{P-II}}$('s) defining the interface and $\mathbf{g}_{\text{P-}\alpha\text{CCSL}}$ or $\mathbf{g}_{\text{P-}\beta\text{CCSL}}$.

Unlike $\Delta\mathbf{g}_{\text{P-CCSL}}$, $\Delta\mathbf{g}_{\text{P-II}}$'s can be directly measured from a diffraction pattern. Moreover, like the $\Delta\mathbf{g}_{\text{P-I}}$'s, the total number in the set of $\Delta\mathbf{g}_{\text{P-II}}$'s is limited. It is easy to recognize $\Delta\mathbf{g}_{\text{P-II}}$'s once the CCSL in reciprocal space is determined. According to the reciprocity theorem [93], a set of planes in the CDSCL in direct space is represented by a point of the CCSL in reciprocal space. In other words, when a constraint is applied to form a CCSL, the points defined by $\mathbf{g}_{\text{P-}\alpha\text{CDSCL}}$ and $\mathbf{g}_{\text{P-}\beta\text{CDSCL}}$ should be in coincidence, defining a point of either $\text{CCSL}_\alpha$ or $\text{CCSL}_\beta$ in reciprocal space. Without the constraint, $\Delta\mathbf{g}_{\text{P-II}}$ is the vector connecting the points defined by $\mathbf{g}_{\text{P-}\alpha\text{CDSCL}}$ and $\mathbf{g}_{\text{P-}\beta\text{CDSCL}}$ (identified in their own crystal basis). Since the principal $\text{CDSCL}_\alpha$ plane is among the planes containing the densest lattice points, $\mathbf{g}_{\text{P-}\alpha\text{CDSCL}}$ should be among the small vectors of $\text{CCSL}_\alpha$ in reciprocal space. Thus, a $\Delta\mathbf{g}_{\text{P-II}}$ can easily be identified from a diffraction pattern, as its associated points should be close to the origin and be nearly in coincidence. Although, in contrast to a $\Delta\mathbf{g}_{\text{P-I}}$, a $\Delta\mathbf{g}_{\text{P-II}}$ is not necessarily associated with a low index $\mathbf{g}_\alpha$ or $\mathbf{g}_\beta$, it is often so defined because it is associated with a small $\mathbf{g}_\alpha$ or $\mathbf{g}_\beta$. For example of the CCSL in Fig. 7a, the set of $\Delta\mathbf{g}_{\text{II}}$'s include

$(-1\,-11)_A - (10-3)_C$, $(222)_A - (305)_C$ and $(113)_A - (402)_C$, as can be seen by a comparison of Fig. 7a and b. The particular $\Delta\mathbf{g}_{P\text{-}II}$ normal to the habit plane is defined by $(-1\,-11)_A - (10-3)_C$. The orientation of this $\Delta\mathbf{g}_{P\text{-}II}$ is close but not parallel to $(-1\,-13)_A$ or $(10-1)_C$, which are the $\mathbf{g}_{P\text{-}\alpha CCSL}$ and $\mathbf{g}_{P\text{-}\beta CCSL}$ vectors that define the terrace plane in the stepped habit plane.

### 4.5. Steps in singular interfaces in a secondary preferred state

A singular interface will contain steps when it is inclined to the plane of 2D CCSL representing the preferred state. For the interfacial steps to be coincident with the periodic secondary dislocations that completely accommodate the secondary misfit in the habit plane, i.e. as described by the third optimum condition for the d-steps, the OR and IO of the habit plane must be special. Based on the derivation given in Appendix B, the geometrical condition that permits the d-step structure can be examined according to a series of characteristic triangles in reciprocal space. The edges of a characteristic triangle are defined by three measurable reciprocal vectors: $\mathbf{g}_{step}$, $\Delta\mathbf{g}_{\parallel}$, and $\Delta\mathbf{g}_{II}$ (see also Fig. 16). The $\mathbf{g}_{step}$ vector is parallel to the smaller vector of $\mathbf{g}_{P\text{-}\alpha CCSL}$ and $\mathbf{g}_{P\text{-}\beta CCSL}$ that defines the terrace planes of the stepped interface, and $1/|\mathbf{g}_{step}|$, as an interplanar spacing, serving as the unit for step height. The $\Delta\mathbf{g}_{II}$ vector is a secondary $\Delta\mathbf{g}$ vector, whose related $\mathbf{g}_{\alpha CDSCL}$ must satisfy the condition $\mathbf{g}'_{\alpha CCSL}\mathbf{b}_s^{II} = i$, where $i$ is a non-zero integer number and $\mathbf{b}_s^{II}$ is the Burgers vector of the secondary dislocation associated with the d-step. The $\Delta\mathbf{g}_{\parallel}$ vector is a vector parallel to the particular $\Delta\mathbf{g}_{P\text{-}II}$ normal to the singular interface. While the relationship between $\mathbf{g}_{step}$ and $\Delta\mathbf{g}_{\parallel}$ determines the spacing of the steps, the relationship between $\mathbf{g}_{II}$ and $\Delta\mathbf{g}_{\parallel}$ is associated with the dislocation spacing. It is shown in Appendix B that formation of a characteristic triangle by these three vectors ensures the identity of step spacing and dislocation spacing. The condition for the characteristic triangle can only be realized at special ORs, and thus restricts the OR for the singular interface containing the d-steps. The geometry of the characteristic triangles also guarantees that fractional planes from different phases, saying $n/|\mathbf{g}_{P\text{-}\alpha CCSL}|$ vs. $m/|\mathbf{g}_{P\text{-}\beta CCSL}|$ (with $n$ and $m$ being integers), will meet edge-to-edge constantly at every step, as explained in Appendix B. Because of the linear relationship among the vectors in the same zone axis, one finds a group of parallel $\Delta\mathbf{g}_{\parallel}$'s in a set of characteristic triangles. In addition, many other $\Delta\mathbf{g}$'s (including restored $\Delta\mathbf{g}_{P\text{-}CCSL}$'s) may also lie in the same direction due to the linear relationship.

In addition to the d-steps, a singular interface in a secondary preferred state may contain steps when it contains a secondary invariant line. As explained for the case of primary invariant line strain, this stepped interface must be normal to a group of parallel $\Delta\mathbf{g}_{II}$'s, whose related $\mathbf{g}$'s must lie in the zone axis of the Burgers vector for the secondary O-lines. The parallel $\Delta\mathbf{g}$'s are classified differently from that for the interface containing a d-step structure. The parallel $\Delta\mathbf{g}_{\parallel}$'s in the characteristic triangles do not belong to $\Delta\mathbf{g}_{II}$'s, and $\Delta\mathbf{g}_{II}$'s in the triangles are not parallel to one another. The interpretation of the parallel $\Delta\mathbf{g}$'s depends on the construction of the 3D CCSL, which often involves a certain degree of ambiguity. However, because a 2D CCSL structure will be discontinuous at any step, a step in an interface in a

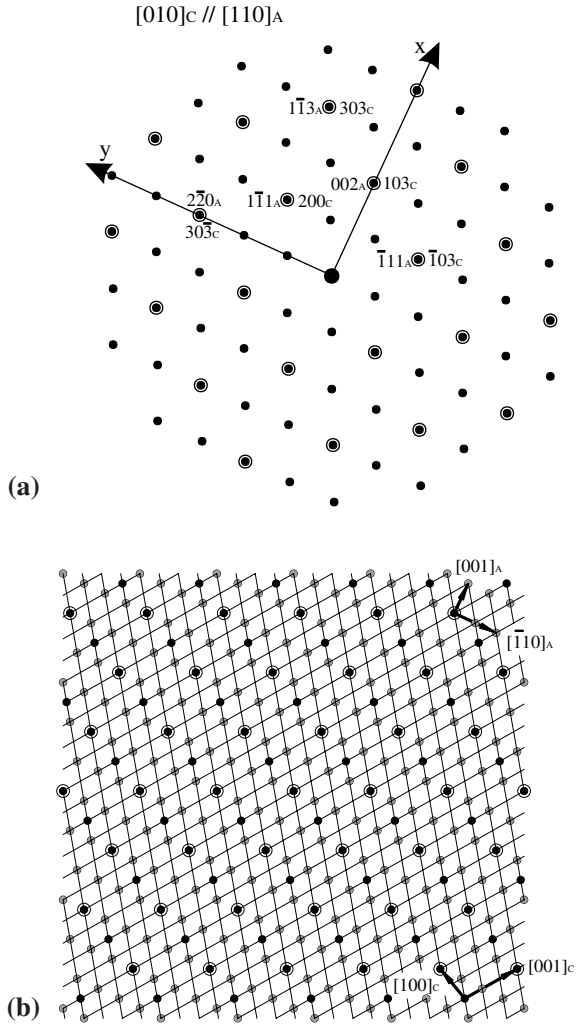


Fig. 8. Different singular interfaces between a cementite (black dots)/austenite (grey dots) phases near the Pitsch OR and corresponding reciprocal lattices (the same symbols as in Fig. 7 were used): (a) and (b) are the $CCSL_A$'s (circles around dots) in the reciprocal and direct space respectively; planes of CDSCL are shown with line grids; (c) and (f) are interfaces containing d-steps and secondary invariant line respectively; CDSCL are shown to indicate their continuity across the interface; (g) and (h) are the same interfaces as in the (c) and (f), with the repeated structural units in the terrace planes being highlighted and (d) and (e) are the reciprocal lattices in the ORs corresponding to the interfaces in (c) and (f), respectively. Note that the singular interfaces are normal to the parallel $\Delta\mathbf{g}$'s in both cases ((a)–(d) and (f) were adopted from [45], with minor modifications).

secondary preferred state should be treated as a linear defect, no matter whether or not the step is associated with a dislocation according to a model lattice. As long as the 2D CCSLs as the reference for the preferred state are identical, the difference in

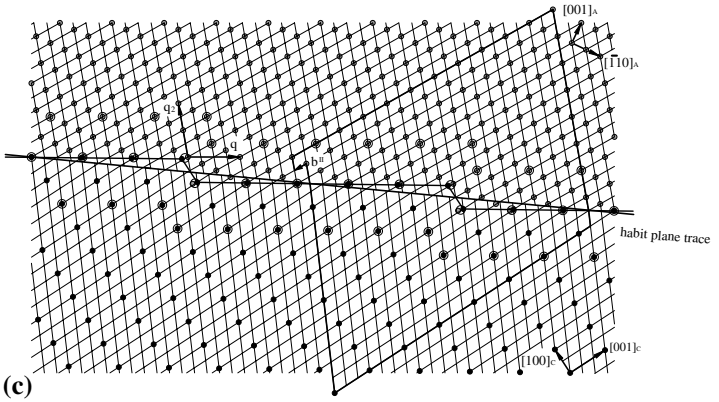


(c)

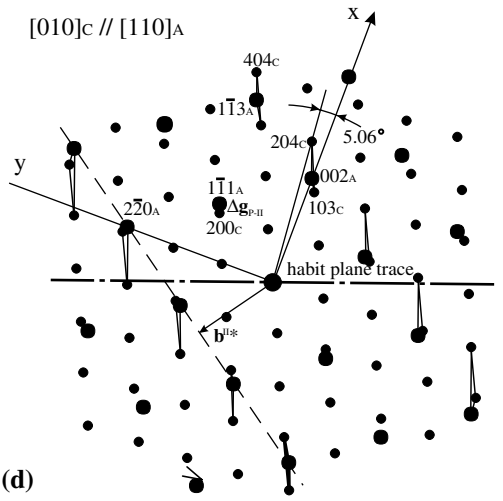


(d)

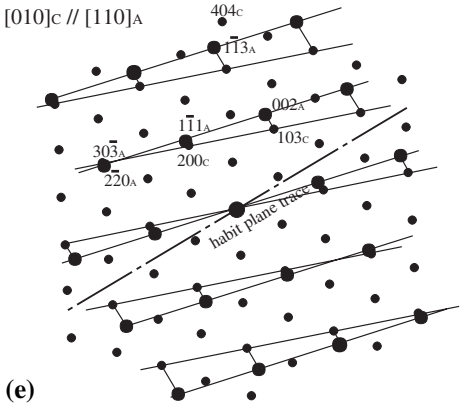


(e)

Fig. 8 (*continued*)

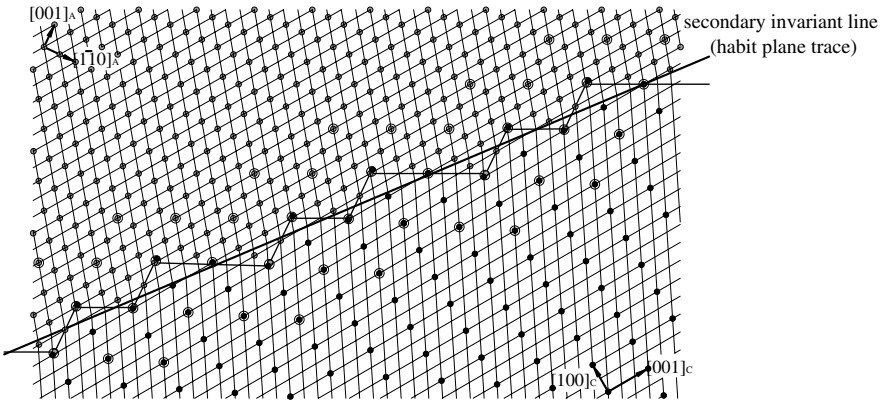


**(f)**

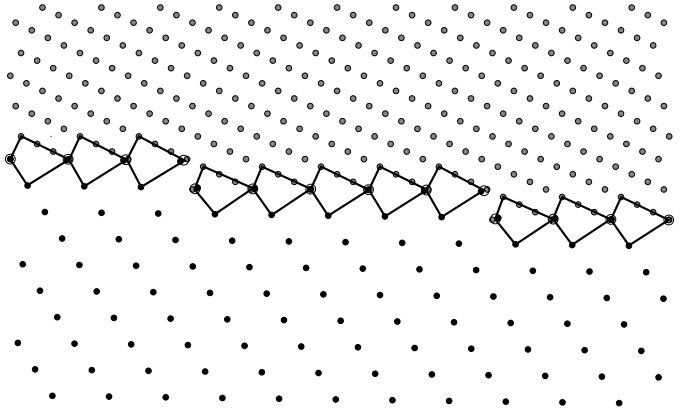

**(g)**

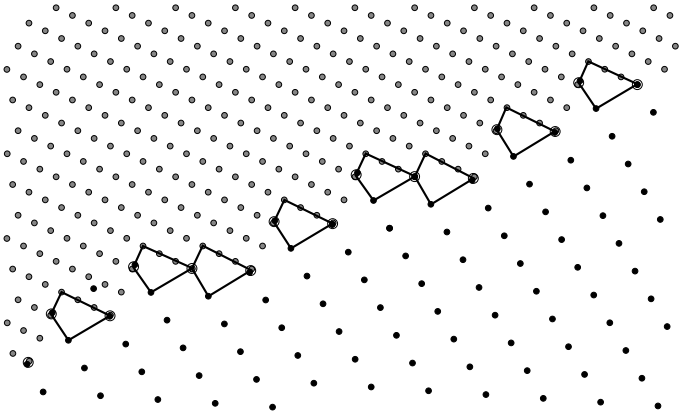

**(h)**

Fig. 8 (*continued*)

the results from different models is not substantial, as demonstrated in the following example. Note that the above conclusion is a special property of the interfaces in a secondary preferred state. It is in contrast to an interface in the primary referred state, in which the steps at the atomic scale do not usually cause discontinuity of coherency, i.e. the primary preferred state. Only the dislocations, associated with discontinuity of coherency, are the prominent structural defects in the interface.

According to the observed diffraction pattern at the Pitsch OR in a cementite/austenite system (refer Fig. 13a), a $CCSL_A$ (cementite lattice in constraint) in reciprocal space has been constructed in Fig. 8a based on a principle of small secondary misfit and small unit CCSL cell [45]. Unlike the case of the T–H OR in Fig. 7, all $\Delta\mathbf{g}$'s in this pattern are identical to the small $\mathbf{g}$ vectors of cementite lattice. The corresponding $CCSL_A$ in direct space has been determined based on a 3D analysis [45], as given in Fig. 8b. Since the selected 2D $CCSL_A$ for the preferred state in the plane normal to $\mathbf{g}_{\text{P-}\alpha\text{CCSL}}$ $(= (1\,{-}1\,3)_A)$ or $\mathbf{g}_{\text{P-}\beta\text{CCSL}}$ $(= (1\,0\,1)_C)$, does not consist of the small $CDSCL_A$ vectors as the amenable Burgers vector, an interface containing the d-steps has been suggested (Fig. 8c), with the OR in the condition of parallel $\Delta\mathbf{g}$'s in Fig. 8d [45]. This OR is consistent with the observation (refer Fig. 13a) [66]. On the other hand, it is possible to determine another OR (Fig. 8e) in about 3° from that in Fig. 8d, in which all $\Delta\mathbf{g}_{\text{P-II}}$'s are parallel as required for a secondary invariant line strain. The matching condition of the hypothetic interface normal to parallel $\Delta\mathbf{g}_{\text{P-II}}$'s is illustrated in Fig. 8f [45]. The interfaces normal to the parallel $\Delta\mathbf{g}$'s in both cases contain steps, because in no case can the parallel $\Delta\mathbf{g}$'s be parallel to any $\mathbf{g}_{\text{P-}\alpha\text{CCSL}}$ and $\mathbf{g}_{\text{P-}\beta\text{CCSL}}$. The planes of 2D $CCSL_A$ representing the preferred state, i.e., $\mathbf{g}_{\text{P-}\alpha\text{CCSL}} = (1\,{-}1\,3)_A$ and $\mathbf{g}_{\text{P-}\beta\text{CCSL}} = (1\,0\,1)_C$, are the same for both interfaces. Both interfaces are normal to $\Delta\mathbf{g}_{\text{P-II}}$ $(= (1\,{-}1\,1)_A - (2\,0\,0)_C)$. The interface in Fig. 8c is normal to the $\Delta\mathbf{g}_{\parallel}$ connecting $(0\,0\,2)_A$ with $(2\,0\,4)_C$) (Fig. 8d), while the interface in Fig. 8f is normal to the $\Delta\mathbf{g}_{\text{P-II}}$ connecting $(0\,0\,2)_A$ with $(1\,0\,3)_C$. As can be expected, the planes of the CDSCLs defined in the different lattices (fine lines), and the CCSLs defined in the different lattices (indicated by circles around the lattice points in the different phases near the boundary), discontinue at the steps in Fig. 8c. In contrast, the planes of the CDSCLs together with the CCSLs from different lattices fully match at the interface along the secondary invariant line in Fig. 8f, similar to the case of an interface containing a primary invariant line (Fig. 6).

However, unlike the interface in the primary preferred system, the secondary invariant line is not favored by nature. After the lines representing the planes of the CDSCL were removed, as shown in Fig. 8g and h corresponding to Fig. 8c and f, respectively, the common aspects of the interfaces become clear: the repeat structural units (carrying a slight distortion) in the terrace planes are identical in both interfaces. Though the CDSCL or 3D CCSL continues at steps in interface containing the secondary invariant line, the 2D CCSL or the pattern of the structural units disrupts at the steps, as the intrinsic linear defects, no matter whether or not the steps are associated with secondary dislocation. As stated earlier, it is the 2D CCSL that represents the preferred state. In this consideration, the discontinuity of 3D CCSL or CDSCL probably has less physical significance compared with the discontinuity of the 2D CCSL. To preserve the 2D CCSL as far as possible, the density of the steps

should be minimized. For the reduction of the steps, the orientation of the parallel $\Delta\mathbf{g}$'s to define the singular interface should be close to both $\mathbf{g}_{\text{P-}\alpha\text{CCSL}}$ and $\mathbf{g}_{\text{P-}\beta\text{CCSL}}$ as far as possible. This may be the reason why the interface containing the secondary dislocations is preferred (as it was observed [66]) to the interface containing the secondary invariant line that crosses denser steps, since the average spacing between the steps in the latter interface is smaller (i.e.1.67 vs. 4.57 nm [45]). [15]

While the interpretation of the steps in terms of dislocations should not make substantial difference in the selection of the singular interface, it is possible to interpret the same stepped interface either in terms of d-steps or an invariant line strain. Though $\Delta\mathbf{g}_{\text{II}}$'s are usually much smaller than $\Delta\mathbf{g}_{\|}$'s, one may determine a "misfit strain" so that it relates all parallel $\Delta\mathbf{g}$'s. In this strain, a "quasi-invariant" could be defined along the direction of "zero misfit" [96]. If the strain generating the "quasi-invariant" line is interpreted as a secondary strain, then any interface containing d-steps could also be regarded as a plane containing a secondary invariant line. As can be seen from Fig. 8c and f, any step in these interfaces is associated with a displacement. The essential role of the steps is to cancel the secondary misfit in the terrace plane, or to allow for repetition of a region of good matching in every terrace plane. In a secondary invariant line model, the secondary misfit along the projection of the invariant line in the terrace plane is cancelled by the secondary misfit associated with the step vector. The step height must be commensurate with the interplanar spacing of the CCSL planes normal to $\mathbf{g}_{\text{P-}\alpha\text{CCSL}}$ and $\mathbf{g}_{\text{P-}\beta\text{CCSL}}$ (Fig. 8f). In the d-step model, the secondary misfit along a particular direction, over a distance of the step spacing, must be cancelled by the dislocation associated with a d-step. The Burgers vector of the dislocation, as a CDSCL vector, is specified by the displacement vector (between the lattice points) associated with the step vector in the constrained state (refer Appendix A). The step height must be commensurate with the interplanar spacing of the planes defined by $\mathbf{g}_{\text{P-}\alpha\text{CCSL}}$ and by $\mathbf{g}_{\text{P-}\beta\text{CCSL}}$ (Fig. 8c).

Different definitions of the secondary misfit strain are based on different CCSL. While the interface in Fig. 8c could be interpreted by an invariant line model, the secondary strain may appear too large to be considered reasonable. However, as long as the 2D CCSL for a given singular interface is unique, the OR, IO and periodicity of the steps can be determined solely from the parallelism condition of the $\Delta\mathbf{g}$'s, independent of the construction of the CCSL. To avoid confusion in the description of the steps, it is convenient to characterize the steps by their intrinsic characteristics of the steps, including the spacing and height of the steps and the displacement associated with a step vector (i.e. $\Delta\mathbf{v}$ in Fig. 15c). These features only depend on the OR and IO, and they are invariant with the model of the 3D CCSL. On the other hand, though the intrinsic characteristics of the steps are clearly shown in Fig. 8g and h, it is not obvious whether the interfacial misfit is balanced by the steps. Complete cancellation only occurs in the singular interfaces, which are defined

[15] The step spacing would be large if the terrace plane is defined by $(1\,{-}1\,1)_{\text{A}}$ which is near parallel to $(2\,0\,0)_{\text{C}}$. Nature does not favor this pair of low index planes, implying the role density of the CCSL prevails over the effect of the density of the crystal lattice points.

by discrete ORs and IOs. The CCSL model is still a useful tool, despite some uncertainty in the construction of the 3D CCSL. Modeling with a CCSL helps one to identify the ORs and IOs of the singular interfaces, as well as the 2D CCSL for the preferred state. The descriptions of the intrinsic characteristics of the periodic steps should be identical whether the interface is described in terms of secondary invariant line or d-steps by the CCSL model.

From the experimental viewpoint, steps as linear defects in an interface in a secondary preferred state are likely visible due to their associated local strain. Possible observations of the steps crossed by a secondary invariant line by diffraction contrast may appear in conflict with the conventional experience (mainly from study of interfaces in the primary preferred state). Dislocations in an interface containing a primary invariant line should lie along, rather than crossed by the invariant line. In this context, it is often convenient to analyze the visible steps (using diffraction contrast) in a system in a secondary preferred state in terms of d-steps. While the displacement associated with a step vector is variable with the OR, the secondary Burgers vector is a rational fraction of a lattice translation vector of either crystal lattice and is independent of the OR. For a proper interpretation of the diffraction contrast associated with the steps, the CCSL should be constructed so that the Burgers vector of the d-step should be close to $\Delta\mathbf{v}$, which is the cause of the strain contrast. It is worth clarifying that an effective Burgers vector associated with a step is not always unique, because there might be multiple choices of the step vector and misfit along the step riser causes the difference. [16] However, the secondary Burgers vector associated with a d-step must be unique, and the misfit along the step riser, if exists, should be accommodated by another set of dislocations. On the other hand, one can always draw a CCLS for any heterophase system, and define a Burgers vector associated with a step in terms of a CDSCL vector. However, if the system is in the primary preferred state, the CCSL and CDSCL are meaningless. The atomic steps or structural ledges in an interface in the primary preferred state are not associated with discontinuity of the preferred state, and they are not usually treated as linear defects.

An extra plane associated with a d-step may be observed from a high resolution image (Fig. 13c) [66]. Caution must be exercised in applying the result of the extra plane for deducing the secondary Burgers vector. As discussed in detail in Appendix A, whether there is an extra plane associated with a step depends solely on the orientation of the Moiré plane formed by the related planes with respect to the interface plane. The related planes may or may not be linked by the secondary misfit strain. This is in contrast to the systems in the primary preferred state, in which the related low index planes are usually associated by the primary $\Delta\mathbf{g}$'s connecting the reciprocal spots in the nearest neighbor. Only when the $\Delta\mathbf{g}$'s are associated by the

[16] Attributing a unique effective Burgers vector to structural ledge is a common mistake. It has not been broadly recognized that a structural ledge is different from a twinning dislocation associated with a step, which is fully coherent along the step riser.

Table 3
Descriptions of singular interfaces in primary preferred states in terms of the CCSL, secondary O-lattice and various $\Delta\mathbf{g}$ vectors

| Model lattice | Identification of principal planes | | | Reciprocal vectors for singular interfaces | | | | | | |
|---|---|---|---|---|---|---|---|---|---|---|
| | Crystal basis | $\Delta\mathbf{g}$ | Related $\mathbf{g}_{\alpha}$ | $A_{\mathrm{II}}$ | $B_{\mathrm{II}}$ | $C_{\mathrm{II}}$ | $D_{\mathrm{II}}$ | $F_{\mathrm{II}}$ | $E_{\mathrm{II}}$ | $G_{\mathrm{II}}$ |
| Ideal CSL | $\mathbf{g}_{\text{P-}\alpha\text{CSL}}$'s $\mathbf{g}_{\text{P-}\beta\text{CSL}}$ | $\Delta\mathbf{g}_{\text{P-CSL}}$'s (measurable) | Any | $\Delta\mathbf{g}_{\text{P-CSL}}$'s | | | | | | |
| CCSL | $\mathbf{g}_{\text{P-}\alpha\text{CCSL}}$ $\mathbf{g}_{\text{P-}\beta\text{CCSL}}$ | $\Delta\mathbf{g}_{\text{P-CCSL}}$'s (unmeasurable) | Any | Restored $\Delta\mathbf{g}_{\text{P-CCSL}}$'s In $m$-ZX | | Restored $\Delta\mathbf{g}_{\text{P-CCSL}}$'s In 1-ZX | | | One restored $\Delta\mathbf{g}_{\text{P-CCSL}}$ | |
| Crystal | $\mathbf{g}_{\text{P-}\alpha}$ $\mathbf{g}_{\text{P-}\beta}$ | | | $\mathbf{g}_{\text{P-}\alpha\text{CCSL}}$ $\mathbf{g}_{\text{P-}\beta\text{CCSL}}$ | | $\mathbf{g}_{\text{P-}\alpha\text{CCSL}}$ $\mathbf{g}_{\text{P-}\beta\text{CCSL}}$ | | | $\mathbf{g}_{\text{P-}\alpha\text{CCSL}}$ $\mathbf{g}_{\text{P-}\beta\text{CCSL}}$ | |
| Secondary O-lattice | | $\Delta\mathbf{g}_{\text{P-II}}$'s (small) $\Delta\mathbf{g}'_{\parallel}s = \mathbf{g}_{\text{step}} - \Delta\mathbf{g}_{\text{II}}$ | $\mathbf{g}_{\text{P-CDSCL}}$ | | All $\Delta\mathbf{g}_{\text{P-II}}$'s | $\Delta\mathbf{g}_{\text{P-II}}$'s in 1-ZX | $\Delta\mathbf{g}_{\text{P-II}}$'s in 1-ZX | $\Delta\mathbf{g}_{\text{P-II}}$'s in 1-ZX $\Delta\mathbf{g}_{\parallel}$'s | One $\Delta\mathbf{g}_{\text{P-II}}$ | $\Delta\mathbf{g}_{\parallel}$'s |

*Note*. 1-ZX ($m$-ZX) means that the $\mathbf{g}$ vectors connected by the corresponding $\Delta\mathbf{g}$'s are defined in one (many) zone axis (ZX).

misfit strain field for determining the dislocations, will the result of extra planes (in the correlated pairs) be consistent with that of the $\mathbf{g} \cdot \mathbf{b}$ criterion.

As a summary for singular interfaces in the secondary preferred states, Table 3 lists the principal planes of model lattices and their related $\Delta\mathbf{g}$'s for the singular interfaces in secondary preferred states. When an ideal CSL is definable, identification of important CSL planes from a diffraction pattern is usually straightforward. Otherwise, identification of $\Delta\mathbf{g}_{\text{P-II}}$'s, $\Delta\mathbf{g}_{\text{P-CCSL}}$'s and $\Delta\mathbf{g}_{\parallel}$'s in a diffraction pattern depends on the 3D CCSL construction. However, as discussed above, while the suggestion of the 2D CCSL for the secondary preferred state is important, the ambiguity in the construction of the 3D CCSL may not affect crystallographic features of the singular interface. Though some singular interfaces in Table 3 have been classified according to different descriptions for steps, the difference in the interpretations of the steps is not substantial. The following section presents a more practicable method, in which the attribution of the $\Delta\mathbf{g}$'s for systems in the secondary preferred state is ignored.

## 5. Macroscopic descriptions of singular interfaces

From an experimental point of view, it is often easier to conduct accurate measurements of $\Delta\mathbf{g}$'s, the OR and habit plane orientation from a superimposed diffraction pattern, than to obtain a quantitative description of the interfacial structure. As can be seen from Tables 2 and 3, any singular interface is associated with at least one $\Delta\mathbf{g}$, irrespective of the preferred state, of whether the interface has a rational or irrational orientation, and of how many sets of periodic dislocations might exist in the interface. Since, as hypothesized, the habit plane is a singular interface, identification of plausible singular interfaces in terms of measurable $\Delta\mathbf{g}$'s will allow one to rationalize the habit plane directly from the measured crystallographic data. Because any "useful" $\Delta\mathbf{g}$ that defines a singular interface must be subject to the constraint imposed by the optimum conditions, it is possible to investigate singular interfaces according to a characteristic arrangement of the $\Delta\mathbf{g}$ with other reciprocal vectors, which can be realized only at special ORs. All three optimum conditions suggested in Section 3.4 for specifying the singularities can be described by the alignment of a $\Delta\mathbf{g}$ with at least one more measurable reciprocal vector. Simply by studying the arrangement of reciprocal vectors, one may be able to identify a singular interface with a macroscopic parameter and to rationalize the precipitation crystallography at the same time.

### 5.1. Three $\Delta\mathbf{g}$ parallelism rules

It would be desirable to link each optimum condition with a particular $\Delta\mathbf{g}$ parallelism rule, but the ambiguity in determining the preferred state prevents such a one-to-one correspondence. While the first and second optimum conditions are applicable to interfaces regardless of the preferred state, the third condition is principally applicable to interfaces in a secondary preferred state. For the simplicity

of application, three $\Delta\mathbf{g}$ parallelism rules are suggested below. They are closely related to the optimum conditions, providing a link between the precipitation crystallography and possible optimum interfacial structures. When an ambiguity in the preferred state is encountered, the dilemma can often be bypassed by simply examining parallelism of a group of measurable reciprocal vectors in a diffraction pattern and by disregarding the identities of the parallel $\Delta\mathbf{g}$'s. If the OR fulfills the condition of parallelism of reciprocal vectors specified by any one of the rules, it implies that an interface must be normal to the parallel vectors.

**Rule I** ($\Delta\mathbf{g}$ *is parallel to a rational* $\mathbf{g}$). Rule I mainly expresses the first optimum condition, i.e. the elimination of interfacial singularities represented by atomic steps or steps with terrace planes defined by $\mathbf{g}_{\text{P-}\alpha\text{CCSL}}$ and $\mathbf{g}_{\text{P-}\beta\text{CCSL}}$. An interface that follows Rule I may exhibit either primary or secondary preferred state. In a system in the primary preferred state, Rule I requires that $\Delta\mathbf{g}_{\text{P-I}}$ be parallel to either $\mathbf{g}_{\text{P-}\alpha}$ *and/or* $\mathbf{g}_{\text{P-}\beta}$. It is possible that an interface that obeys Rule I is parallel to a dense atomic plane in only one phase, and is irrational with respect to the crystal coordinates of the other phase. In contrast, in a system in a secondary preferred state, Rule I implies that $\Delta\mathbf{g}_{\text{P-II}}$ is parallel to $\mathbf{g}_{\text{P-}\alpha\text{CCSL}}$ and $\mathbf{g}_{\text{P-}\beta\text{CCSL}}$, or that $\Delta\mathbf{g}_{\text{P-CSL}}$ is parallel to $\mathbf{g}_{\text{P-}\alpha\text{CSL}}$ and $\mathbf{g}_{\text{P-}\beta\text{CSL}}$ when an ideal CSL exists. Thus, an interface that obeys Rule I must be parallel to rational planes in both phases. Rule I can be satisfied in any system, without being subject to any restrictions imposed by the lattice parameters of the two phases. If this rule is not observed, another optimum condition must have prevailed over the first optimum condition.

**Rule II** (*Two* $\Delta\mathbf{g}_{\text{P-I}}$*'s are parallel*). This rule corresponds to the second optimum condition, applied only to the primary preferred state—eliminating interfacial linear defects represented by the primary misfit dislocations. Being equivalent to the condition of a primary O-line strain, satisfaction of this rule is possible only when $\text{rank}(T) < 3$ is allowed by the lattice constants, and the lattice correspondence is limited by the primary preferred state (a one-to-one lattice point correspondence with small misfit in the interface). [17] This rule applies to those cases in which meaningful $\mathbf{g}_{\text{P-I}}$'s are readily recognized as small difference vectors connecting neighboring principal $\mathbf{g}$'s from the two crystal lattices. An OR that allows two $\mathbf{g}_{\text{P-I}}$'s to be parallel cannot usually be expressed using parallelism of rational indices. Consequently, a singular interface that follows Rule II alone is typically in an irrational orientation, and, on the other hand, an irrational semicoherent habit plane is likely formed due to this rule.

[17] According to the criterion set by Christian [84], an invariant line strain is possible only when $\lambda_1 < 1$, $\lambda_2 > 1$, and $\lambda_3 \neq 1$, where $\lambda_i$ are the eigenvalues that define the principal strains. The principal strains can be decomposed from $\mathbf{A}$, which depends on the lattice correspondence and lattice constants.

**Rule III** (*Two* $\Delta\mathbf{g}$*'s are parallel*). At first sight Rule III appears to be covered by Rule II. However, Rule III is mainly reserved for those cases in which the $\Delta\mathbf{g}_{P\text{-}I}$'s cannot be defined, and the system is then in a secondary preferred state. An interface following Rule III may be governed by either the second or third optimum condition. While the classification of $\Delta\mathbf{g}$ depends on the CCSL construction, use of Rule III is a simple approach for rationalizing the precipitation crystallography without calculating the CCSL. However, when the parallel $\Delta\mathbf{g}$'s lie in a rational orientation (Rule I must be applied simultaneously), the singular interface must be governed by the second optimum condition, since the third optimum condition only applies to stepped interfaces. When the parallel $\Delta\mathbf{g}$'s do not lie in a rational orientation, the singular interface normal to the parallel $\Delta\mathbf{g}$'s contains steps. The misfit in at least one direction in the interface should be cancelled by the displacement associated with the steps, no matter whether the second or third optimum condition is active.

If we take two axes to represent the OR related variables and the IO related variables, the association of the $\Delta\mathbf{g}$ parallelism rules with the local energy ($E$) minima in the BGP space can be demonstrated schematically, as shown in Figs. 9 and 10. In

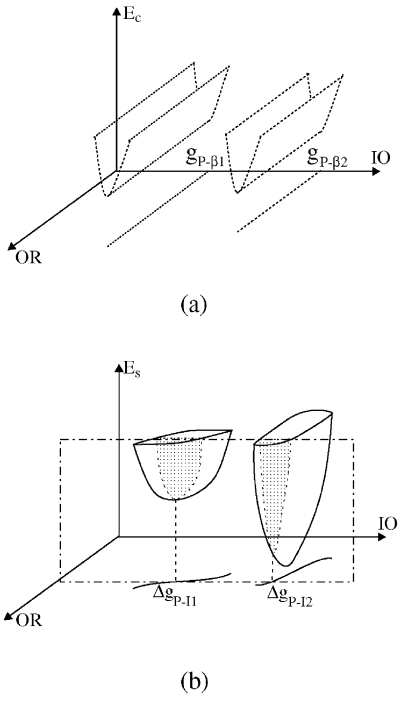


Fig. 9. Illustrations of the variation of a component of interfacial energy with the orientation-relationship (OR) and the interface-orientation (IO): (a) a minimum in the chemical component of the interfacial energy ($E_C$) is associated with low index planes in lattice $\beta$, $\mathbf{g}_{P\text{-}\beta i}$ and (b) a minimum in the structural component of the interfacial energy ($E_s$) is associated with $\Delta\mathbf{g}_{P\text{-}Ii}$ ($i = 1, 2$).

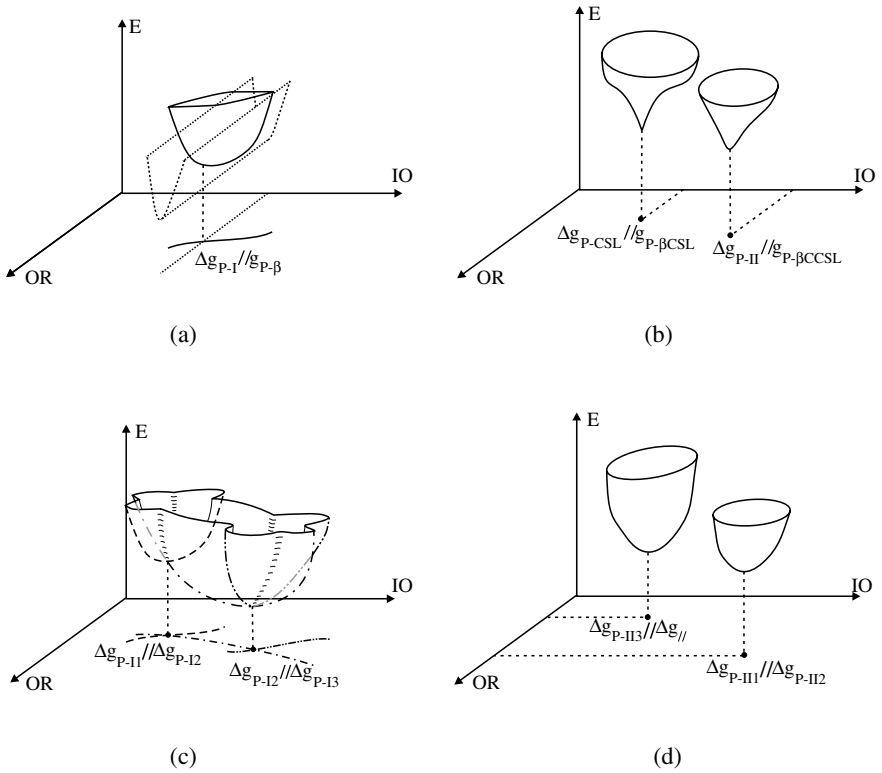


Fig. 10. Illustrations of the $\Delta\mathbf{g}$ parallelism rules: (a) Rule I is realized in an interface (in the primary state) which is defined by the intersection of curves identified by $\mathbf{g}_{P\text{-}\beta}$ and $\Delta\mathbf{g}_{P\text{-}I}$; (b) Rule I is realized in an interface (in a secondary state) defined by either $\Delta\mathbf{g}_{P\text{-}CSL}\|\mathbf{g}_{P\text{-}\beta CSL}$ (sharp cusp), or $\Delta\mathbf{g}_{P\text{-}II}\|\mathbf{g}_{P\text{-}\beta CCSL}$ (rounded cusp); (c) Rule II is realized in an interface which is defined by the intersection of curves identified by $\Delta\mathbf{g}_{P\text{-}Ii}$, $i = 1, 2$, or 3, associated with the different $\mathbf{g}_{P\text{-}\alpha}$'s and (d) Rule III is realized in an interface (in a secondary state) defined by $\Delta\mathbf{g}_{P\text{-}II3}\|\Delta\mathbf{g}_{\|}$, or $\Delta\mathbf{g}_{P\text{-}II1}\|\Delta\mathbf{g}_{P\text{-}II2}$.

these figures, a point on the IO axis represents a direction referred to one of the crystals, arbitrarily chosen as lattice $\beta$. Therefore a straight line parallel to the OR axis represents the interfaces whose indices are fixed with respect to lattice $\beta$. Fig. 9a shows an example where the chemical component of the interfacial energy ($E_c$) is at a local minimum when the interfacial orientation is in a particular orientation $\mathbf{g}_{P\text{-}\beta i}$ (the subscripts $i = 1$, 2 in Figs. 9 and 10 indicate different planes). Fig. 9b shows the variation of the structural component of the interfacial energy ($E_s$). For any OR, the energy reaches a local minimum when the interface is normal to the $\Delta\mathbf{g}_{P\text{-}Ii}$. The locus of a series of energy cusps corresponding to different ORs is represented by a curve in the OR–IO plane. Each curve is identified by the characteristic IOs, namely by $\mathbf{g}_{P\text{-}\beta i}$ in Fig. 9a and by $\Delta\mathbf{g}_{P\text{-}Ii}$ associated with a particular $\mathbf{g}_{P\text{-}\alpha i}$ in Fig. 9b. However, these interfaces are singular only with respect to the IO.

At the intersection point of any two curves, the interface must be normal to both reciprocal vectors that define the curves, and is now singular with respect to the OR (but it may not be fully confined, as explained later). This type of plot can be used to illustrate a $\Delta\mathbf{g}$ parallelism rule, as is the case for Fig. 10. Rule I is illustrated in Fig. 10a and b for the primary and secondary preferred states respectively. While the energy cusp associated with a $\mathbf{g}_{\text{P-}\beta i}$ is independent of the OR, the energy cusp associated with $\mathbf{g}_{\text{P-}\beta\text{CSL}}$ or $\mathbf{g}_{\text{P-}\beta\text{CCSL}}$ corresponds to a point in the OR axis, emphasizing the sensitivity of the energy to the OR in a secondary preferred state. Fig. 10c illustrates Rule II, with two $\Delta\mathbf{g}_{\text{P-II}}$'s being parallel at the intersection points of the curves. The minima in the energy surface in Fig. 10d, for interfaces in secondary preferred states, are not extended from continuous valleys (see also Fig. 10b). The implication is that while each periodic structure of primary dislocations in an interface normal to $\Delta\mathbf{g}_{\text{P-I}i}$ is associated with a local energy minimum (singular with respect to the IO) for any given OR (Fig. 9b), this may not be true for the secondary dislocations.

All singular interfaces listed in Table 1 can be classified in terms of $\Delta\mathbf{g}$ parallelism rules. More specifically, all singular interfaces are normal to either $\Delta\mathbf{g}_{\text{P-I}}$ or $\Delta\mathbf{g}_{\text{P-II}}$, depending on the preferred state, except for the $A_{\text{II}}$ interface, which may be normal to a $\Delta\mathbf{g}_{\text{P-CSL}}$ rather than $\Delta\mathbf{g}_{\text{P-II}}$ if an ideal CSL exists and hence no $\Delta\mathbf{g}_{\text{P-II}}$ is definable (in this case a $\Delta\mathbf{g}_{\text{P-CSL}}$ may be identical to a small $\mathbf{g}$ of a crystal lattice). Table 4 lists all the singular interfaces classified previously in Table 1 in terms of the $\Delta\mathbf{g}$ parallelism rule(s). In the table, the tick mark "✔" denotes whether a corresponding rule is applied to the type of interface specified at the top of each column. The presence of two or more ticks in any column indicates that the corresponding rule is applied to vectors in two or more zone axes independently. Multiple applications of the rules are possible only when the lattice constants of the two lattices are specially related.

Most singular interfaces in the table can be uniquely identified by different combinations of the rules, but in three cases, different types of interfaces are identified by the same rule(s). One case involves the $E_{\text{I}}$ and $E_{\text{II}}$ interfaces, as they both follow Rule I. Since identification of the $\Delta\mathbf{g}_{\text{P-I}}$'s is usually obvious, distinguishing an $E_{\text{I}}$ from an $E_{\text{II}}$ interface is often straightforward. On the other hand, both $B_{\text{II}}$ and $F_{\text{II}}$ interfaces follow Rule III twice, and both $D_{\text{II}}$ and $G_{\text{II}}$ interfaces follow Rule III once. Theoretically, parallel $\Delta\mathbf{g}$'s defining a $D_{\text{II}}$ (or $B_{\text{II}}$) interface must be among $\Delta\mathbf{g}_{\text{II}}$'s, but the parallel $\Delta\mathbf{g}$'s defining a $G_{\text{II}}$ (or $F_{\text{II}}$) interface should include $\Delta\mathbf{g}_{\parallel}$ vectors in the characteristic triangles, plus some restored $\Delta\mathbf{g}_{\text{CCSL}}$'s that are parallel to $\Delta\mathbf{g}_{\parallel}$'s because of the linear relationship. However, difference in the interfacial structure between $B_{\text{II}}$ and $F_{\text{II}}$ interfaces and between $D_{\text{II}}$ and $G_{\text{II}}$ interface may not be substantial, since any steps in these interfaces are considered as linear defects, as discussed in Section 4.5. In general, an interface that follows (and only follows) Rule III twice must contain an array of steps, any interface that follows Rule III once usually contains an array of steps plus a set of secondary dislocations.

Since any singular interface obeys at least one $\Delta\mathbf{g}$ parallelism rule, we consider the $\Delta\mathbf{g}$ parallelism rules as defining "the rules of precipitation crystallography, including the description of the OR and the habit plane orientation". *A habit plane, as a singular interface, must be normal to at least one* $\Delta\mathbf{g}$, *and the corresponding OR must*

Table 4
Descriptions of singular interfaces with the $\Delta\mathbf{g}$ parallelism rules

| Rules | | Opt. Con. | $A_I$ | $A_{II}$ | $B_I$ | $B_{II}$ | $C_I$ | $C_{II}$ | $D_I$ | $D_{II}$ | $E_I$ & $E_{II}$ | $F_{II}$ | $G_{II}$ |
|---|---|---|---|---|---|---|---|---|---|---|---|---|---|
| I | $\Delta\mathbf{g}_{P\text{-}I,II} \parallel \mathbf{g}_{P\text{-}\alpha,\beta}$ | Second | ✓ | ✓ | | | ✓ | ✓ | | | ✓ | | |
| II | $\Delta\mathbf{g}_{P\text{-}I1} \parallel \Delta\mathbf{g}_{P\text{-}I2}$ | First (I) | ✓✓ | | ✓✓ | | ✓ | | ✓ | | | | |
| III | $\Delta\mathbf{g}_{P\text{-}II1} \parallel \Delta\mathbf{g}_{P\text{-}II2}$ | First (II) | | ✓✓ | | ✓✓ | | ✓ | | ✓ | | ✓ | |
| | $\Delta\mathbf{g}_{P\text{-}II} \parallel \Delta\mathbf{g}_{\parallel}$ | Third | | | | | | | | | | ✓ | ✓ |

*permit this* $\Delta\mathbf{g}$ *to be parallel to other* $\Delta\mathbf{g}'$*s or* $\mathbf{g}('s)$ *so that one or more optimum conditions are fulfilled.* Using these simple rules, one may be able to interpret the precipitation crystallography directly from measurements made from electron diffraction patterns without recourse to an initial modeling or experimental determination of the interfacial structure. Parallelism of $\Delta\mathbf{g}$'s can also be examined by calculation, when the parallelism is not directly visible from the available experimental data. Such calculations are simple by use of matrix algebra, and do not require specification of the model lattice. This situation is especially applicable to cases obeying either Rule II or III. Then a numerical method or analytical approach [73,97,98] for determining primary O-lines can be employed, while the physical interpretation of the strain can be ignored. On the other hand, since the result from a comparison between the $\Delta\mathbf{g}$ parallelism rules and observations often suggests a possible singular interface according to Table 4, this may in turn provide help in construction of proper model lattices and selection of the right Burgers vectors to specify the interfacial structure in the habit plane.

Before ending this section it is worthwhile to discuss the special situation in which a $\Delta\mathbf{g}$ is a zero vector, i.e. this $\Delta\mathbf{g}$ connects identical $\mathbf{g}$ vectors from different lattices. Although it is almost impossible that the $\mathbf{g}$ vectors from different lattices have exactly the same length, some $\mathbf{g}$'s may be so close that the corresponding $\Delta\mathbf{g}$ is not visible. In this special situation a singular interface can be identified by two ways. One way is to define the zero vector as a virtual $\Delta\mathbf{g}$ that has an infinitesimal length and can be treated to have any orientation. In practice a non-zero length of $\Delta\mathbf{g}$ often truly exists from a precise calculation. Since the length almost vanishes, a considerable change of the $\Delta\mathbf{g}$ direction may not be accompanied with a detectable variation in the OR. Thus, it is reasonable and convenient to use a virtual $\Delta\mathbf{g}$, when the length of a $\Delta\mathbf{g}$ is smaller than the experimental uncertainty. The $\Delta\mathbf{g}$ parallelism rules can be applied as usual when the virtual $\Delta\mathbf{g}$ is taken into consideration. Another way to bypass the problem of zero vector is to use an equivalent description corresponding to each rule. For example, parallelism of two (identical) $\mathbf{g}$'s from different lattices should be equivalent to Rule I. An alternative expression for Rule II is that all $\Delta\mathbf{g}_{\mathrm{I}}$'s whose related $\mathbf{g}_{\alpha}$'s lie in a zone axis parallel to a Burgers vector, including at least one non-zero $\Delta\mathbf{g}_{\mathrm{P\text{-}I}}$, should be parallel to one another. Since the parallelism of two $\Delta\mathbf{g}$'s implies the existence of a group of parallel $\Delta\mathbf{g}$'s, the existence of zero $\Delta\mathbf{g}$ vector does not affect the application of Rule III. However, the conception of the virtual $\Delta\mathbf{g}$ is also helpful especially when one needs to identify a $\Delta\mathbf{g}_{\mathrm{P\text{-}II}}$ to which $\Delta\mathbf{g}_{\|}$'s must be parallel (as is the case in Appendix A).

### *5.2. Further constraints on the orientation relationships*

While the OR characterized by a $\Delta\mathbf{g}$ parallelism rule appears unique in the pseudo 3D illustration in Fig. 10, it is not actually so in the 5D BGP space. Although a $\Delta\mathbf{g}$ is not explicitly defined in either crystal basis, the degree of freedom imposed on the OR by parallelism of one $\Delta\mathbf{g}$ with another $\Delta\mathbf{g}$ (or $\mathbf{g}$) is equivalent to that imposed by parallelism of two $\mathbf{g}$'s from the different crystal lattices. Consequently, the constraint imposed by a single $\Delta\mathbf{g}$ parallelism rule fixes four degrees of freedom in the 5D BGP

space: a pair of parallel directions in reciprocal space, which defines two degrees of freedom in the OR, and the parallel reciprocal vectors normal to the interface, which fully define the two degrees of freedom for the IO. Although genuine experimental scattering has been measured in some systems, the measured data from many systems often converge to a narrow, well-defined crystallographic region. These observations suggest that the remaining degree of freedom left after applying one of the rules is often in fact fixed. Further conditions restricting the OR may arise still from factors affecting interfacial energy, such as the distribution of misfit strain, the type of bonds etc. A number of possibilities are given below.

*5.2.1. Satisfaction of two rules in one system*

The application of two rules simultaneously implies that two independent parallelism conditions are needed to define the OR. Theoretically, redundant conditions required by two rules cannot be realized simultaneously in a general case. Nevertheless, if we allow the lattice constants to vary, which is equivalent to an extension of the dimension higher than 5D, additional degrees of freedom can be permitted. In other words, in some systems the lattice constants may be related in such a way that two parallelism conditions (specified by different rules) might be compatible with each other. In these cases, the constraint provided by the two rules will uniquely determine the OR. A system simultaneously following two rules might be realized in two ways.

*5.2.1.1. Application of two rules to a singular interface*. In this case, the major singular interface or habit plane is normal to all parallel reciprocal vectors specified by two (or more) rules. Since the structure in this singular interface will satisfy two optimum conditions, or one optimum condition twice, the driving force selecting this particular interface plane is obvious. As can be seen from Table 4, many singular interfaces (except for interfaces *D*, *E* and *F*) belong to this case. These interfaces following two or more rules are singular with respect to all degrees of freedom in the 5D BGP space.

The combination of the rules is not however arbitrary. As Rules II and III are applied to the interfaces in a primary and secondary preferred state respectively, permissible combinations only hold between Rule I and either Rule II or III. In addition, combinations are only permitted between the first and second optimum conditions. Then, an interface that follows either Rules I and II, or Rules I and III, will be parallel to a rational crystal plane, with the interface containing at least one set of primary or secondary O-lines, such as the $A_{\mathrm{I}}$, $A_{\mathrm{II}}$, $C_{\mathrm{I}}$, and $C_{\mathrm{II}}$ interfaces in Table 4. On the other hand, multiple applications of one rule for a different pair of reciprocal vectors are also possible, provided that the parallel vectors applied in one rule are not linearly dependent on those used in the other rule. However, a double application of Rule I to one interface is equivalent to the application of Rule I followed by either Rule II or III to the same interface. Both approaches lead to the parallelism of the $\Delta\mathbf{g}$'s. Therefore, only double applications of Rule II or III should be considered. In particular, when Rule II is applied twice, the corresponding interface is a $B_{\mathrm{I}}$ interface. When Rule III is applied twice, the corresponding interface

is either a $B_{II}$ or an $F_{II}$ interface. $A_I$ and $A_{II}$ interfaces also belong to this category, as they follow three rules.

*5.2.1.2. Application of the rules for different singular interfaces*. In this case, a precipitate must contain at least two singular interfaces, each of which obeys one rule. [18] The most common case is that the two interfaces follow Rule I. This situation often occurs when the two lattices have common symmetry elements lying parallel to each other. If the two lattices have the same type of crystal structure, at an OR in which all the axes of crystals are parallel (e.g. a cube/cube OR for an fcc/fcc system), all **g** vectors with identical indices will be parallel, and every $\Delta\mathbf{g}_{P\text{-}I}$ will be parallel to their associated principal **g**'s. Then, a set of equivalent singular interfaces can be formed, serving as different facets of an embedded phase. Another possible combination is that one interface follows Rule I while a second interface obeys III, corresponding to the optimum condition of coincidence of steps and secondary dislocations. It is possible that one interface follows Rule I while a second interface obeys Rule II. However, when this occurs, both interfaces must contain an invariant line. The interface that follows Rule I must also follow Rule II if its structure is to remain periodic, and therefore belongs to the case of two rules satisfied by one interface. This implies satisfaction of three rules in a system, and is possible only when the lattice constants are specially related.

The precipitation crystallography leading to two singular interfaces, each following one rule (commonly Rule I), is not necessarily more favored than the alternative possibility that leads to a major singular interface. The choice depends on various factors, including the overall minimization of the interfacial energy and perhaps the growth kinetics, and it is not predictable from the present approach.

*5.2.2. Supplementary constraints*

When an interface does not fit into the framework of two rules simultaneously, an additional constraint is required to fix the OR for a singular interface. This occurs for those interfaces that follow a single rule in Table 4, i.e. $D_I$, $D_{II}$, $E_I$, $E_{II}$ and $G_{II}$. Fortunately, both experimental work and empirical criteria are available in the literature to guide in the selection of supplementary constraints, as outlined below. The first of these is:

*5.2.2.1. A pair of small vectors of similar lengths in the interface are parallel*. This constraint applies to all types of interfaces that follow a single rule, and is most likely to occur in practice. The set of parallel vectors are usually among the smallest or the next to smallest lattice vectors in the crystal lattices or CCSLs, [19] provided the misfit

[18] Note that observation of two facets from a precipitate does not imply that each facet follows a rule, since one of the facets may be singular only with respect to its normal.

[19] This condition is particularly convenient for a TEM study. If the interface is examined edge-on with the electron beam parallel to low index zones in the two crystals, a superimposed diffraction pattern (for examining the $\Delta\mathbf{g}$ parallelism rule(s)) and high resolution TEM image for studying the atomic structure of the interface can be recorded.

between them is small. Thus, the displacement between the parallel vectors must correspond to either a primary or secondary misfit strain. Clearly, the misfit associated with the particular pair of vectors is minimized when these vectors are parallel. Major $E_{\mathrm{I}}$ and $E_{\mathrm{II}}$ interfaces are likely to be subject to this supplementary constraint. This condition is particularly true for systems consisting of a metal/oxide combination [99]. An interface following Rule I is similar to an interface between an epitaxial film and substrate. Parallelism of small mismatching (or nearly matching) vectors was used by Kato et al. [100] as a criterion for explaining epitaxial ORs. Howe [12] also noted a strong tendency of alignment of the close-packed directions from different phases. The present condition is in principle consistent with these suggestions or observations.

For the stepped interfaces, including $D_{\mathrm{I}}$, $D_{\mathrm{II}}$, and $G_{\mathrm{II}}$, the above constraint can be considered to be a partial satisfaction of the first optimum condition. Since the parallel rational vectors should not be crossed by any interfacial steps, they must define the step risers shared by the interface and the terrace plane. Therefore, this supplementary constraint equivalently requires that the risers of all steps be free of atomic kinks, instead of eliminating all interfacial steps required by the first optimum condition. Any extra distorted or wrong bonds due to kinks associated with a step will thereby be removed. The tendency for elimination of kinks on steps is probably greater in a $D_{\mathrm{II}}$ or $G_{\mathrm{II}}$ interface than in a $D_{\mathrm{I}}$ interface, since interfacial steps and their associated kinks are expected to provide a more significant contribution to the interfacial energy when the interface is in a secondary preferred state. While stepped interfaces in a secondary preferred state are more complicated to analyze, a strong tendency for the step riser to be parallel to a pair of small vectors often allows a simplification of the 3D problem into a 2D + 1D problem (normal and parallel to the parallel vectors).

The second supplementary constraint applies when:

*5.2.2.2. No small vectors of similar length in the interface are parallel.* Among the five types of singular interfaces that are not fully constrained, the $D_{\mathrm{I}}$ interface is most likely to disobey the first constraint listed above, as the contribution of the local distortion (associated with kinks in steps) to the interfacial energy may be less significant in a $D_{\mathrm{I}}$ interface. There must be a reason for this deviation from parallelism, just as there is for those cases in which no low index planes are parallel. Two possible reasons are discussed below for $D_{\mathrm{I}}$ interfaces.

*5.2.2.2.1. Maximization of the dislocation spacing.* Since a $D_{\mathrm{I}}$ interface only contains a single set of dislocations, a simple parameter to evaluate the interfacial energy is the dislocation spacing [73]. Clearly, the dislocation spacing will vary with the remaining degree of freedom in the OR. The optimum OR, corresponding to a $D_{\mathrm{I}}$ interface characterized by a particular $\mathbf{b}_i^{\mathrm{L}}$ describing the dislocations, may be the one that leads to the maximum dislocation spacing [73]. This condition implies that the interfacial energy is minimized when the dislocation spacing is a maximum. The above principle can also be used for choosing among the possible $D_{\mathrm{I}}$ interfaces corresponding to different $\mathbf{b}_i^{\mathrm{L}}$'s. However this principle should be used with caution. The appropriate selection of the $\mathbf{b}_i^{\mathrm{L}}$'s remains a challenging problem,

particularly when the dislocation spacing is small, or the difference between the various sets of dislocations is not significant. It is often assumed that the degree of coherency strain in the areas between the dislocations varies with the periodicity of the O-elements where the good-matching regions locate. In other words, the misfit strain field around every dislocation is assumed to be identical. Based on this assumption, the interfacial energy may be expressed as a simple (monotonic) function of the dislocation density. The above assumption is valid when the dislocation spacing is large, since the distribution of the coherency strain in the regions between different pairs of dislocations is likely similar. Such a variation is sensitive not only to the dislocation spacing itself, but also to the dislocation configuration with respect to the crystal structures. However, when the dislocation spacing is small, the coherency strain could vary significantly from one area to another. In this situation, even for interfaces containing a single set of primary dislocations, it may become groundless to determine preference of the interfaces in terms of dislocation spacing, as the relative interfacial energy is not simply indicated by the values of the dislocation density.

*5.2.2.2.2. Availability and mobility of interfacial dislocations.* The phenomenological theory of martensitic crystallography (PTMC) [101] requires that the habit plane is glissile, or equivalently that the interfacial dislocations lie on a slip plane. It can be shown that the PTMC is in accord with Rule II [97], but a $D_I$ interface is more general. The constraint of the dislocation orientation can restrict fully the habit planes to discrete coordinates in the 5D BGP space. Some precipitates, for example of various metal hydrides, have been considered to form in a similar manner to martensite [63,64,102]. Plausible slip systems for the interfacial dislocations have also been considered from another viewpoint by Dahmen and Westmacott [103]. In this approach the invariant line has been required to lie at the intersection of the cone of unextended lines with a slip plane, while the Burgers vector was constrained differently from that in the PTMC. Whether or not the habit plane in a diffusional phase transformation is truly glissile in any precipitation transformation requires careful experimental work. This question has been the center of a long-standing, but as yet unresolved debate [104].

On the other hand, the availability of interfacial dislocations may affect the development of the precipitation crystallography, as suggested by observations from bcc/hcp alloy systems, in which the slip systems in the two lattices are rather different. In Zr–Nb alloys the precipitation crystallographies are different when the two phases exchange their identities as the precipitate and matrix phases [21,105,106], though both cases can be explained with the invariant line consideration. A similar observation was made by Duly [107] after an extensive survey of bcc/hcp alloy systems, although he proposed another criterion, a "surface variation" method based on growth considerations, to explain the OR. Dahmen and Westmacott [108] also noticed the change of invariant line in fcc/bcc systems as the precipitates and matrix exchange their identities. They considered that this results from the change of the slip plane in the matrix.

### 5.3. Comparison with experimental observations

It is recognized that the methodology of the $\Delta\mathbf{g}$ parallelism rules, plus the use of simple supplementary constraints when necessary, helps to identify local minima, not global minima, of the interfacial energy. Through its links with characteristic structures in singular interfaces, this method helps to elucidate *why a particular precipitation crystallography, and not one in its vicinal coordinates, is observed*. Although the $\Delta\mathbf{g}$ parameter has not been broadly used in the literature, the distribution of $\Delta\mathbf{g}$'s is often available as a "byproduct" from experimental records of the OR and the habit plane orientation. According to the arrangement of the $\Delta\mathbf{g}$'s in reported diffraction patterns, it is often possible to apply the $\Delta\mathbf{g}$ parallelism rules in a comparison with the reported habit planes.

In this section we first present examples of the application of each $\Delta\mathbf{g}$ parallelism rule. While Rule I is simple to recognize, Rules II and III are often less obvious. The validity of applying Rules II and III to these examples has relied not only upon diffraction pattern information but also on O-lattice calculations, which provided more precise comparison (the details of the calculation have been presented elsewhere). Besides these examples, the $\Delta\mathbf{g}$ parallelism rules are compared with an extensive set of experimental data, to show the general applicability of these simple rules to many systems, which may or may not have been interpreted by other models. This comparison is mainly based on visual evidence from diffraction patterns. The uncertainty in the comparison is thus of the same order of magnitude as the accuracy in the OR measurement. As discussed later, one may expect a small degree of residual long-range strain field, especially when two rules are identified. This tolerated strain could be of the same order as the measurement uncertainty. This implies that when two rules are defined within the experimental uncertainty, the interfacial structure may be described by the singular structure corresponding to the two rules, but some residual long-range strain might exist in the interface.

#### 5.3.1. A system following Rule I: TiN/Ni [42]

The crystallography of TiN precipitates produced from an internal nitridation of a Ni–Ti alloy has been studied by Savva et al. [42]. They observed five types of distinct ORs. Each of the observed ORs can be described (within the experimental uncertainty) by Rule I. Fig. 11 presents the two types of ORs that are most frequently observed in the system. The diffraction pattern in Fig. 11b exhibits a typical cube–cube OR, where the reciprocal vectors of the identical indices from different lattices are parallel to each other, and they are naturally parallel to the $\Delta\mathbf{g}$ connecting them. The facets in Fig. 11a are parallel to the plane of $\{0\,2\,0\}$ in both TiN and the matrix phase. Each facet is also normal to a $\Delta\mathbf{g}_{\text{P-I}}$ connecting a pair of $\{0\,2\,0\}$ spots from different lattices. The simple OR and facets in this case are readily understood, as they could be expected from the concept of anisotropic surface energy. However, the reason for the irrational OR in Fig. 11d is not so obvious. This OR corresponds to a well-defined habit plane in Fig. 11c, which is again parallel to the plane of $(0\,2\,0)_{\text{TiN}}$ in TiN, but in an irrational orientation $\sim(7\,{-}1\,5)_{\text{Ni–Ti}}$ with respect to the

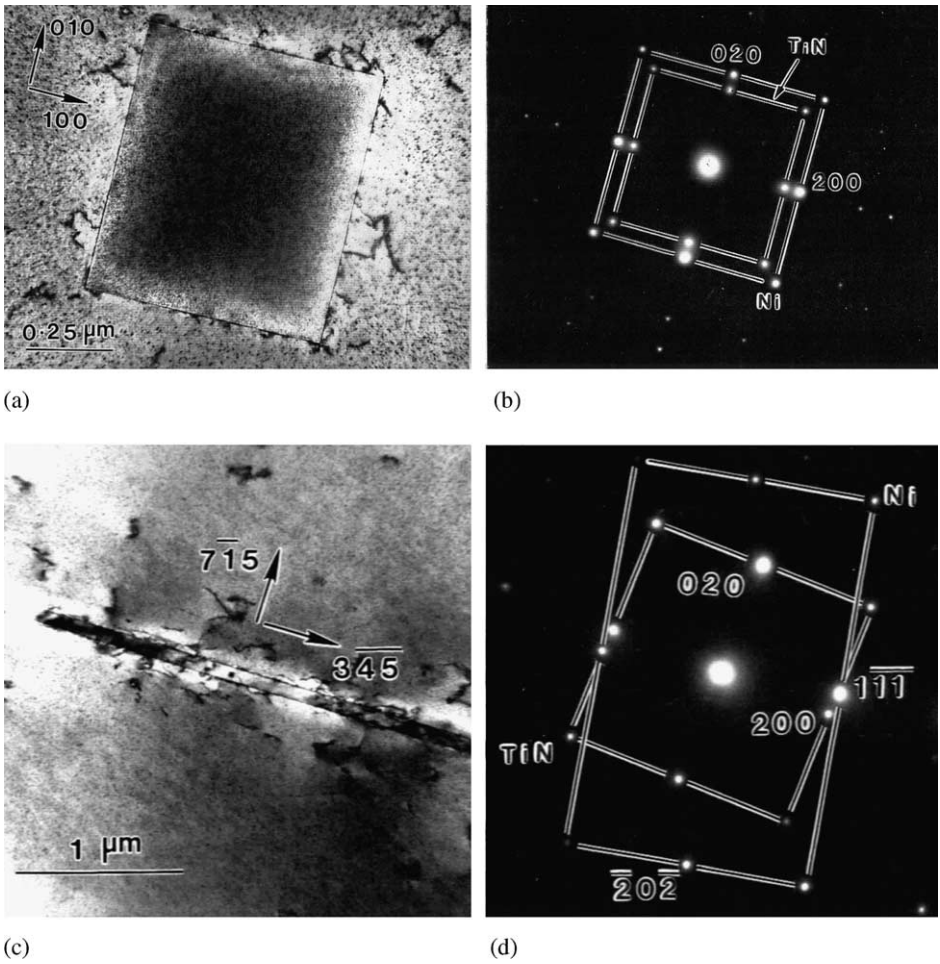


Fig. 11. TEM images of TiN precipitates in a Ni-rich matrix in (a) and (c) related by two types of ORs in the diffraction patterns in (b) and (d), respectively. Facets in (a) or habit plane (c) is normal to the vector of $(0\,2\,0)_{TiN}$ and a $\Delta\mathbf{g}_{P\text{-}I}$, as required by Rule I. (Reprinted from [42].)

matrix phase. The reason for the irrational OR becomes clear when Rule I is applied: The OR is such as to cause the particular $\Delta\mathbf{g}_{P\text{-}I1}$ $[=(2\,0\,0)_{TiN}-(1\,-1\,-1)_{Ni\text{–}Ti}]$ to be parallel to $(0\,2\,0)_{TiN}$ (Fig. 11d), so that the habit plane can be normal to the parallel vector $\Delta\mathbf{g}_{P\text{-}I}$ and $\mathbf{g}_P$. In this particular OR the vector of $(0\,2\,0)_{TiN}$ does not lie parallel to any low index direction in the matrix phase. While the habit plane has an approximately high index in the matrix, according to Rule I one would expect that it should contain a periodic good matching interfacial structure. Indeed, the observations revealed that this habit plane contain a single set of dislocations, with a spacing of about 8 nm (the Burgers vector was not characterized). The observation

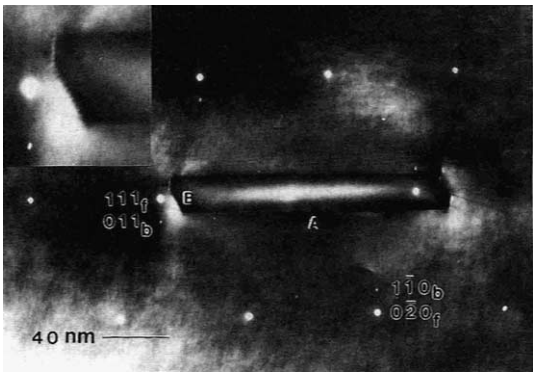


Fig. 12. A TEM image of a Cr-rich precipitate in a Ni-rich matrix, superimposed with the diffraction patterns from both phases with correct alignment (Reprinted from [24]). The habit plane between the two phases is normal to two parallel $\Delta\mathbf{g}_{\text{P-I}}$'s, as required by Rule II.

implies that this interface might also follow approximately Rule II. [20] This is likely, though no diffraction pattern from other orientations is available, since the authors [42] noted that a rotation of 1.1° from the nominal OR in Fig. 11c will bring $\Delta\mathbf{g}_{\text{P-I2}}$ $[=(-1\,1\,-1)_{\text{TiN}}-(1\,1\,1)_{\text{Ni–Ti}}]$ to be parallel to $(0\,2\,0)_{\text{TiN}}$. It is possible to find an OR near the nominal OR (since a slight deviation was actually observed, but not quantitatively determined), so that both $\mathbf{g}_{\text{P-I}}$'s are approximately parallel to $(0\,2\,0)_{\text{TiN}}$. Parallelism of the $\Delta\mathbf{g}_{\text{P-I}}$'s can lead to the suggestion that the Burgers vector of the dislocations should be $[0\,1\,-1]_{\text{Ni–Ti}}/2$ or $[0\,1\,1]_{\text{TiN}}/2$, provided that the interface is in the primary preferred state.

*5.3.2. A system following Rule II: Cr/Ni [17,24]*

Precipitation of Cr-rich lath-shaped particles in Ni alloys has been studied intensively by several authors [17,91,92]. Fig. 12 was taken from the direction of $[1\,0\,-1]_{\text{f}}\|[1\,1\,-1]_{\text{b}}$ [24]. In this figure the image of the edge-on habit plane is superimposed with the diffraction patterns from both phases with correct alignment. The OR can be described (approximately) by the K–S OR, i.e. $(1\,-1\,1)_{\text{f}}\|(1\,0\,1)_{\text{b}}$ and $[1\,0\,-1]_{\text{f}}\|[1\,1\,-1]_{\text{b}}$, since the spots of $(1\,-1\,1)_{\text{f}}$ and $(1\,0\,1)_{\text{b}}$ are not distinguishable. The habit plane does not lie normal to any point in the superimposed diffraction patterns in Fig. 12, but it is approximately normal to $(1\,-2\,1)_{\text{f}}$. When attention is paid to the alignment of $\Delta\mathbf{g}_{\text{P-I}}$, it is quickly noticed that $\Delta\mathbf{g}_{\text{P-I1}}$ $[=(1\,1\,1)_{\text{f}}-(0\,1\,1)_{\text{b}}]$ and $\Delta\mathbf{g}_{\text{P-I2}}$ $[=(0\,-2\,0)_{\text{f}}-(1\,-1\,0)_{\text{b}}]$ are parallel to each other, and that the habit plane is normal to these parallel $\Delta\mathbf{g}_{\text{P-I}}$'s. Interpretation of this irrational habit plane is straightforward when Rule II is applied. Following Rule II, this habit plane should

[20] For a singular interface to obey Rule II and I truly, the lattice constants of the phases must be specially related. The chance of a system consisting of equilibrium phases to fulfill exactly the above condition is rare. However, an approximate holding of two rules might be possible, so that a strained singular structure might be realized.

contain the O-lines. A strict O-line calculation has been made for this particular system, and the calculated result of the OR, the invariant line direction and the habit plane normal are consistent with the observed crystallography within the experimental uncertainty [24].

Despite the consistency in the precipitation crystallography, the periodic single set of dislocations has not been observed from this habit plane. One reason may be that the spacing of the dislocations is small, i.e. ~1 nm, so that the strained volume associated with individual dislocations is too small to cause visibility by diffraction contrast in TEM. These dislocations are also invisible in image of a high resolution TEM [91,92]. The proper beam direction to view the nearly edge-on dislocations is when the beam lies parallel to the low index zone axes of $[1\,0\,-1]_f \| [1\,1\,-1]_b$ as in Fig. 12. However, as seen from Fig. 6, all related planes from different lattices should be coherent, since the habit plane is normal to all $\Delta\mathbf{g}_{P\text{-}I}$'s in the zone axes. The invisibility can also be understood from the dislocation characteristic. Because the viewing direction would be parallel to the Burgers vector, no lattice discontinuity could be identified. A proper experimental method is required therefore to examine the interfacial structure of the habit plane in the Cr/Ni system. Selection of the Cr/Ni system as the example for Rule II is mainly because parallelism of the $\Delta\mathbf{g}_{P\text{-}I}$'s is visible in a single diffraction pattern. In more general cases, the edge-on irrational habit plane is normal to parallel $\Delta\mathbf{g}_{P\text{-}I}$'s that are visible from different beam directions, as the Burgers vectors for the O-lines defined in the different phases are not exactly parallel. This situation occurs in a Zr–Nb alloy system, in which a single set of dislocations in the habit plane (the faceted part of broad interface) was observed [21], in agreement with an O-line calculation [73].

*5.3.3. A system following Rule III: cementite/austenite [66,96]*

Investigation of the crystallography of Widmanstätten cementite precipitated from austenite in hypereutectoid steels was pioneered by Pitsch [109,110], and has been followed by many researchers [30,32,66,94,111–113]. Both the Pitsch OR [109,110] and the Thompson-Howell (T–H) OR [94] can be rationalized by Rule III [45,96]. We take the Pitsch OR for example, since high resolution TEM experimental results of the interfacial structures are available [66]. The Pitsch OR is usually described as $(1\,0\,0)_C \| (5\,-5\,4)_A$, $(0\,1\,0)_C \| (1\,1\,0)_A$ and $(0\,0\,1)_C \| (-2\,2\,5)_A$. Fig. 13a is the superimposed diffraction pattern from the parallel zone axes of $[0\,1\,0]_C$ and $[1\,1\,0]_A$ reported by Howe and Spanos [66]. A deviation of $(2\,0\,0)_C$ from $(1\,-1\,1)_A$ toward $(2\,-2\,0)_A$ is evident. The authors noted that the habit plane is normal to $\Delta\mathbf{g}$ of $(1\,-1\,1)_A - (2\,0\,0)_C$. According to the model of $CCSL_A$ in reciprocal space for the Pitsch OR in Fig. 8b, this $\Delta\mathbf{g}$ is classified as a $\Delta\mathbf{g}_{P\text{-}II}$ as identified in Fig. 8d. Parallelism of this $\Delta\mathbf{g}_{P\text{-}II}$ with other $\Delta\mathbf{g}$'s is not obvious at the first glance, because the size of the other parallel $\Delta\mathbf{g}$'s in the diffraction pattern is large. By referring to Fig. 8d, one finds that the $\Delta\mathbf{g}$ connecting $(0\,0\,2)_A$ with $(2\,0\,4)_C$ and that connecting $(-1\,1\,1)_A$ with $(0\,0\,4)_C$ in diffraction pattern in Fig. 13a are also normal to the average habit plane trace specified in Fig. 13a. The careful experimental measurement by Howe and Spanos [66] provided clear evidence that the Pitsch OR and corresponding habit plane obey Rule III. Moreover, they were able to determine the step and dislocation

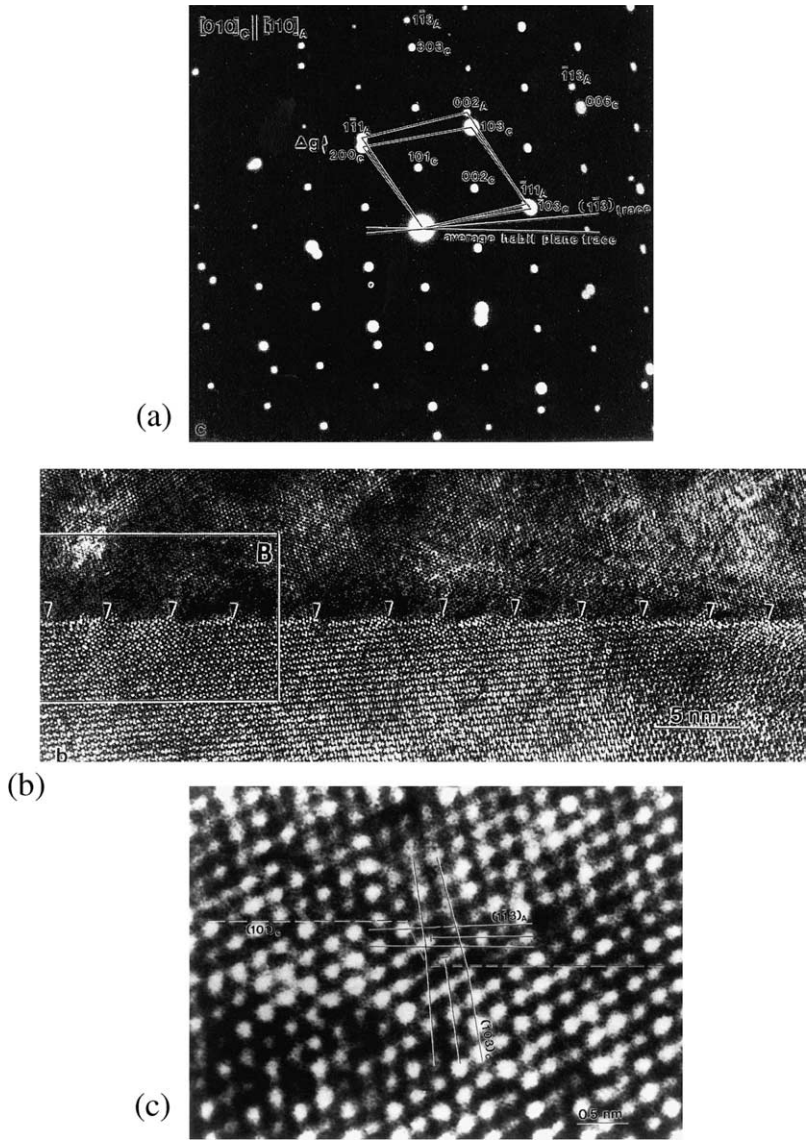


Fig. 13. The superimposed diffraction pattern taken from zone axes of $[0\,1\,0]_C$ of cementite and $[1\,1\,0]_A$ of austenite in the Pitsch OR in (a), and the high resolution image of the habit plane between the two phases in (b) showing periodic d-steps, with an enlarged image of extra planes associated with the d-step in (c). The habit plane is normal to a group of parallel $\Delta\mathbf{g}$'s, including the $\Delta\mathbf{g}$ indicated in (a) and the $\Delta\mathbf{g}$ connecting $(0\,0\,2)_A$ with $(2\,0\,4)_C$, as required by Rule III. (Reprinted from [66] with permission from Taylor and Francis Ltd.)

structure of the habit plane with high resolution TEM, as given in Fig. 13b and c. The calculated d-step interfacial structure in Fig. 8c [45], including the geometry and

Burgers vector characteristic, is in good agreement with the experimental observation [66]. The comparison indicates that the Pitsch OR can be rationalized by the third optimum condition.

It is worth noticing the difference between Figs. 12 and 13a, which reflects the different effects of 3D primary preferred state and 2D secondary preferred state on the development of the interfacial structure. Every parallel $\Delta\mathbf{g}$ in Fig. 12 (or Fig. 6a), as a $\Delta\mathbf{g}_{\mathrm{I}}$, connects the nearest neighbors, as required by the nearest neighbor principle for determining the primary misfit strain [37]. Most parallel $\Delta\mathbf{g}$'s in Fig. 13a (or 8b) do not connect the nearest neighbors. The OR that permits the parallel $\Delta\mathbf{g}$'s to connect the nearest neighbors is possible (Fig. 8e), but it is not preferred by nature in this system. The difference suggests the importance of distinguishing the preferred state for rationalizing precipitation crystallography. While only the second optimum condition is applicable to a stepped singular interface in the primary preferred state, both the second and third optimum conditions may be applicable for interfaces in a secondary preferred state. Under either condition in the latter case, a singular interface can be conveniently identified by using Rule III. As discussed in Section 4.5, distinction of the optimum conditions for a stepped interface in a secondary preferred state is unimportant, since it is the density of the steps rather than the association of the secondary dislocations with the steps has a major effect on the OR.

*5.3.4. General comparisons*

Table 5 compares the $\Delta\mathbf{g}$ parallelism rules with a number of experimental observations in the literature. While a single diffraction pattern can be sufficient for describing an OR (often defined by one rule plus a set of parallel small vectors), the full identification of the applicable rule(s) requires a 3D distribution of the reciprocal vectors. However, in many cases only a 2D configuration of $\Delta\mathbf{g}$'s, e.g. in a single diffraction pattern was reported. Identification of the $\Delta\mathbf{g}$ rule(s) has been made from the available 2D data, unless additional information, e.g. the crystal symmetry, clearly suggests the orientations of the correlated $\Delta\mathbf{g}$'s in other zone axes. Although the 3D distribution of the reciprocal vectors can be computed from the measured OR, this was not done for individual cases, except for a few examples (in which the O-lattice calculation was made). Strictly speaking therefore, the results presented in Table 5 should be regarded as a test of the $\Delta\mathbf{g}$ rules against the available experimental results, rather than a complete classification of systems with applicable rules.

The following outlines the shorthand notation used in Table 5:

1. 'HP' stands for 'habit plane', or prominent facet of a plate or lath-shaped precipitate; 'F' stands for 'facet', applied to precipitates whose interfaces include several well-defined facets; 't = ' stands for 'the terrace plane is', which is only applicable to Rule III.
2. Subscripts 'm' and 'p' denote matrix and precipitate respectively; OR$i$ ($i = 1, 2, \ldots$) indicates a particular OR in a system in which more than one ORs are observed; '$n$' associated with F or ($n$) associated with a rule indicates that '$n$' numbers of equivalent facets that obey the same rule; $i$ ($= 1, 2, \ldots$) indicates different type of facets.

Table 5
Comparison of the $\Delta\mathbf{g}$ parallelism rules with experimental observations

| Systems: precipitate/matrix | | Orientations of habit planes or major facets | | | $\Delta\mathbf{g}$ Rules | Reference(s) |
|---|---|---|---|---|---|---|
| | | $\Delta\mathbf{g}_1 = \mathbf{g}_{m1} - \mathbf{g}_{p1}$ | $\Delta\mathbf{g}_2 = \mathbf{g}_{m2} - \mathbf{g}_{p2}$ | $\mathbf{g}$ | | |
| Ni/Ag | $F_n$ | $\{111\}_m - \{111\}_p$ | | $\{111\}_p$ | (n)I | [114] |
| MgO/Pd | $F_{n-1\text{-OR1}}$ | $\{111\}_m - \{111\}_p$ | | $\{111\}_p$ | (n)I | [44,115] |
| | $F_{n-2\text{-OR1}}$ | $\{200\}_m - \{200\}_p^*$ | | $\{200\}_p$ | (n)I | [44,115] |
| | $HP_{OR2}$ | $\{111\}_m - \{111\}_p$ | | $\{111\}_p$ | I | [115] |
| MgO/Cu | $F_n$ | $\{111\}_m - \{111\}_p$ | | $\{111\}_p$ | (n)I | [44,115] |
| MnO/Cu | $F_{n\text{-OR1}}$ | $\{111\}_m - \{111\}_p$ | | $\{111\}_p$ | (n)I | [116] |
| | $HP_{OR2}$ | $(111)_m - (111)_p$ | | $(111)_p$ | I | |
| $Mn_3O_4$/Ag | HP | $\{111\}_m - \{222\}_p$ | | $\{111\}_p$ | I | [117] |
| $Mn_3O_4$/Pd | $HP_{OR1}$ | $(111)_m - (222)_p$ | | $(111)_p$ | I | [118] |
| | $HP_{OR2}$ | $(002)_m - (004)_p$ | | $(002)_p$ | I | |
| $\eta'$-$Al_2O_3$/Cu | HP | $\{111\}_m - \{222\}_p$ | | $\{111\}_p$ | (n)I | [119] |
| A-$Al_2O_3$/Nb | HP | $(110)_m - (0006)_p$ | | $(0003)_p$ | I | [99] |
| ZnO/Pd | HP | $(111)_m - (0001)_p$ | | $(0001)_p$ | I | [120] |
| $Al_3Sc$/Al alloy | $F_n$ | $\{200\}_m - \{200\}_p$ | | $\{100\}_p$ | (n)I | [10] |
| VC/$\gamma$-steel | $F_n$ | $\{111\}_m - \{111\}_p$ | | $\{111\}_p$ | (n)I | [121] |
| MnS/$\gamma$-steel | HP | $(002)_m - (002)_p^*$ | | $(002)_p$ | I | [121] |
| | $F_{n-1}$ | $\{200\}_m - \{220\}_p$ | | $\{220\}_p$ | | |
| | $F_{n-2}$ | $\{220\}_m - \{400\}_p$ | | $\{200\}_p$ | | |
| Mo/$Mo_5SiB_2$ | HP | $(-330)_m - (-211)_p$ | | $(1-10)_m$ | I | [69] |
| $\delta$-$Ni_3Nb$/Ni alloy | HP | $(111)_m - (020)_p$ | | $(020)_p$ | I | [33,122] |

Table 5 (*continued*)

| Systems: precipitate/matrix | | Orientations of habit planes or major facets | | | Δg Rules | Reference(s) |
|---|---|---|---|---|---|---|
| | | $\Delta\mathbf{g}_1 = \mathbf{g}_{m1} - \mathbf{g}_{p1}$ | $\Delta\mathbf{g}_2 = \mathbf{g}_{m2} - \mathbf{g}_{p2}$ | $\mathbf{g}$ | | |
| TiN/Ni | $F_{n\text{-}OR1}$ | $\{200\}_m - \{200\}_p$ | | $\{200\}_p$ | (n)I | [42] |
| | $HP_{OR2}$ | $(111)_m - (020)_p$ | | $(020)_p$ | I | |
| | $HP_{OR3}$ | $(1\,-1\,-1)_m - (200)_p$ | | $(020)_p$ | I | |
| | $HP_{OR4}$ | $(11\,-1)_m - (11\,-1)_p$ | | $(020)_p$ | I | |
| | $HP_{OR5}$ | $(-111)_m - (020)_p$ | | $(020)_p$ | I | |
| Ag/Cu | HP | $(-111)_m - (-11\,-1)_p$ | $(002)_m - (-111)_p$ | | II | [123] |
| Cr/Cu | $F_{1\text{-}OR1}$ | $(11\,-1)_m - (011)_p$ | | | | [22,23,86,124] |
| | $F_{2\text{-}OR1}$ | $(111)_m - (110)_p$ | | $(110)_p$ | I | [22,23,86] |
| | $F_{3\text{-}OR1}$ | $(-111)_m - (1\,-10)^*_p$ | | | | [22] |
| | $F_{OR2}$ | $(-111)_m - (110)_p$ | $(200)_m - (-101)_p$ | | II | [86] |
| | $F_{OR3}$ | $(-111)_m - (0\,-11)_p$ | $(200)_m - (020)_p$ | | II | [86] |
| Cr/Ni | HP | $(111)_m - (011)_p$ | $(0\,-20)_m - (1\,-10)_p$ | | II | [17,24,92] |
| $\alpha/\beta$(Zr-Nb) | HP | $(101)_m - (10\,-11)_p$ | $(200)_m - (01\,-12)_p$ | | II | [21] |
| (Ti,V)N/Ti-V-N alloy | $F_1$ | $(-101)_m - (-1\,-11)_p$ | | | | [125] |
| | $F_2$ | $(-110)_m - (-111)_p$ | $(110)_m - (111)_p$ | | II | |
| $\gamma$-TiH/Ti | HP | $(01\,-10)_m - (-110)_p$ | $(10\,-10)_m - (200)_p$ | $(-110)_p$ | I + II | [126] |
| $\gamma$-ZrH/Zr | HP | $(10\,-10)_m - (110)_p$ | $(1\,-100)_m - (200)_p$ | $(110)_p$ | I + II | [63] |
| $\beta'$/Al alloy | HP | $(111)_m - (111)_p$ | $(002)_m - (11\,-1)_p$ | $(111)_p$ | I + II | [127] |
| $Ti_3SiC_2$ /TiC | HP | $(111)_m - (0008)_p$ | $(11\,-1)_m - (10\,-1\,-2)_p$ | $(111)_m$ | I + II | [128] |
| $\gamma'$/Al-Ag | HP | $(11\,-1)_m - (0002)_p$ | $(020)_m - (0\,-111)_p$<br>$(002)_m - (1\,-10\,-1)^*_p$ | $(0002)_p$ | I + 2II | [129,130] |
| $\theta'$/Al alloys | HP | $(002)_m - (002)_p$ | $(202)_m - (202)_p$<br>$(022)_m - (022)^*_p$ | $(002)_p$ | I + 2II | [124,131] |
| $Ti(CN)/TiB_2$ | $HP_{OR1}$ | $(0001)_m - (111)_p$ | $(01\,-10)_m - (11\,-1)_p$ | $(0001)_m$ | I + II | [132] |
| | $F_{n\text{-}OR1}$ | $\{2\,-1\,-10\}_m - \{2\,-20\}_p$ | | $\{2\,-1\,-10\}_m$ | | |
| | $HP_{OR2}$ | $(01\,-10)_m - (002)_p$ | $(10\,-10)_m - (-111)_p$ | $(01\,-10)_m$ | I + II | |

| | | | | | | |
|---|---|---|---|---|---|---|
| $Mo_5Si_3/MoSi_2$ | $HP_{OR1}$ | $(002)_m - (220)_p$ | | $(220)_p$ | I | [81,133] |
| | $HP_{OR2}$ | $(002)_m - (220)_p$ | $(110)_m - (112)_p$ | $t = (220)_p$ | III | |
| $Mg_7Al_{12}/Mg\text{-}Al$ | $F_{1-OR1}$ | $(0002)_m - (033)_p$ | | $(011)_p$ | I | [85,134] |
| | $F_{2-OR1}$ | $(1\,-1\,0\,0)_m - (0\,-3\,3)_p$ | $(0\,-2\,2\,0)_m - (-6\,3\,3)_p$ | $t = (-2\,1\,1)_p$ | III | [85] |
| | $F_{3-OR1}$ | $(-1\,0\,1\,0)_m - (-4\,1\,-1)_p$ | | | | [85] |
| | $HP_{OR2}$ | $(1\,-2\,1\,0)_m - (3\,-3\,-6)_p$ | | $(1\,-1\,-2)_p$ | I | [134] |
| $Fe_3C/\gamma$-steels | $HP_{OR1}$ | $(1\,-1\,1)_m - (2\,0\,0)_p$ | $(1\,-1\,3)_m - (4\,0\,4)_p$<br>$(3\,1\,1)_m - (2\,4\,0)_p^*$ | $t = (1\,0\,1)_p$ | 2III | [66,96] |
| | $HP_{OR2}$ | $(002)_m - (200)_p$ | $(1\,1\,-3)_m - (-3\,0\,3)_p$<br>$(2\,-2\,2)_m - (2\,4\,0)_p^*$ | $t = (-1\,0\,1)_p$ | 2III | [94,96] |
| S/Al alloy | $HP_{OR1}$ | $(002)_m - (023)_p$ | | $(001)_p$ | I | [135] |
| | $HP_{OR2}$ | $(020)_m - (002)_p$ | $(022)_m - (062)_p^*$ | $t = (021)_p$ | III | |
| Ge/Al | $F_{n\text{-}OR1}$ | $\{111\}_m - \{111\}_p$ | | $\{111\}_p$ | (n)I | [136] |
| | $F_{1\text{-}OR2}$ | $(002)_m - (-2\,2\,2)_p$ | $(202)_m - (042)_p$ | $(-1\,1\,1)_p$ | I + III | |
| | $F_{2\text{-}OR2}$ | $(040)_m - (-2\,2\,-4)_p$ | $(240)_m - (0\,4\,-4)_p$ | $(-2\,2\,-4)_p$ | I + III | |
| $Ti_5Si_3/TiAl$ | HP | $(111)_m - (0002)_p$ | $(-1\,1\,1)_m - (2\,-3\,11)_p$ | $(0001)_p$ | I + III | [137] |
| $\beta_1$/Mg alloy | HP | $(0\,-1\,1\,0)_m - (-2\,2\,0)_p$ | $(2\,-2\,0\,0)_m - (-2\,2\,4)_p^*$ | $(-1\,1\,2)_p$ | I + III | [138] |
| $Al_2Ti/Al_{24}Cr_9Ti_{27}$ | HP | $(002)_m - (0012)_p$ | $(202)_m - (2012)_p$ | $(004)_p$ | I + III | [68] |
| Ω/Al alloy | HP | $(111)_m - (004)_p$ | $(0\,2\,0)_m - (-2\,0\,2)_p$<br>$(0\,0\,2)_m - (1\,-3\,1)_p$ | $(001)_p$ | I + 2III | [127] |
| H/Al alloy | HP | $(1\,-1\,1)_m - (0\,0\,0\,2)_p$ | $(2\,0\,0)_m - (-2\,2\,0\,1)_p$ | $(0\,0\,0\,1)_p$ | I + III | [139] |
| Q/Al alloy | HP | $(2\,0\,0)_m - (4\,-5\,1\,0)_p$ | $(0\,2\,0)_m - (-4\,-1\,5\,0)_p$ | $(1\,-1\,0\,0)_p$ | I + III | [140] |
| NiHfSi/NiAl-0.5Hf | $F_1$ | $(111)_m - (400)_p$ | $(0\,1\,0)_m - (1\,0\,-2)_p$ | $(200)_p$ | I + III | [141] |
| | $F_2$ | $(-1\,0\,1)_m - (0\,2\,0)_p$ | $(-1\,1\,0)_m - (0\,1\,-3)_p$ | $(0\,2\,0)_p$ | I + III | |

3. Superscript '*' indicates that the particular $\Delta\mathbf{g}$ was not observed, but its existence can be deduced by extending the array of spots in the reported diffraction patterns or by calculation.
4. The indices for crystal planes in the original reports have been adopted. They are given in the crystal reference, either in a 3- or 4-index convention.

The results in Table 5 demonstrate that in a wide range of systems the crystallography obeys at least one $\Delta\mathbf{g}$ parallelism rule. Most of the precipitation systems in Table 5 follow Rule I, i.e. the habit planes or major facets of the precipitates are parallel to a low index plane in at least one crystal. These rational singular interfaces are readily understood, as may be expected from surface energy viewpoint. At the same time, many systems that obey Rule I also follow one or more rules, indicating a strong tendency for the precipitation crystallography to obey $\Delta\mathbf{g}$ parallelism rules, wherever this is permitted by the lattice constants. It is always the interface obeying two rules that defines the habit plane, although other rational planes, from the same precipitate and matrix, could also be parallel to each other in a given rational OR. This arrangement is due to the prevailing singular structure in the interface that obeys two optimum conditions and cannot be solely understood from a surface energy viewpoint.

While in most cases only one prominent facet (the habit plane) is found, in some special systems two or more equivalent interfaces follow the same rule(s), with an embedded particle being enclosed by equivalent singular interfaces. In other examples, secondary facets may be developed in addition to the interface(s) that obey the rule(s). These facets may follow a different rule, or they may also be defined by $\Delta\mathbf{g}$'s that are not parallel to the other measurable reciprocal vectors. As discussed earlier, the facet defined by a single $\Delta\mathbf{g}$ is singular only with respect to the IO, while the OR is fixed by the $\Delta\mathbf{g}$ parallelism rule(s), with or without a supplementary constraint. In a few alloy systems, several different ORs may coexist, each being consistent with Rule I. Though the variety of the observations in one system can be explained from the $\Delta\mathbf{g}$ approach, why a unique OR is observed in one system and several distinct ORs coexist in other systems remains to be a challenging question.

Interfaces resulted from other types of phase transformations, e.g. eutectics, eutectoids and discontinuous precipitates having lamellar structures appear to follow $\Delta\mathbf{g}$ rules but have not been included in Table 5. The flat interfaces in lamellar structures have been found to obey at least one $\Delta\mathbf{g}$ parallelism rule. Examples include $NiO/ZrO_2$ [142], $\gamma/B_2$ in Ti–Al–Mo alloy [143] and $M_7C_3$ pearlite structures [144]. In an as-cast eutectic Cr–Cu alloy, the broad facets of the lath-shaped Cr particles are also normal to parallel $\Delta\mathbf{g}$'s [145]. Though eutectic reactions are out of the scope of the present work, the OR between the solid phases is likely to be governed by principles similar to those considered for the precipitation reactions. On the other hand, some precipitates with needle or rod morphology also obey a $\Delta\mathbf{g}$ parallelism rule, e.g. needle-shaped particles in a quenched Zr–Nb alloy [106], and rod-shaped $Cr_2Nb$ precipitates in a Cr alloy [146]. Since well-defined facets have not been identified from these precipitates, these cases have not been listed in Table 5.

However, agreement with the $\Delta\mathbf{g}$ parallelism rules suggests that an optimum interfacial structure might nevertheless be developed in these systems.

### 5.4. Discussions on the Application of the $\Delta\mathbf{g}$ Parallelism Rules

While the $\Delta\mathbf{g}$ parallelism rules, plus supplementary constraints, can lead to discrete coordinates for singular interfaces in the BGP space, the possible combinations of different rules with supplementary constraints still leave open a number of choices. However, our comparison does indicate that certain types of systems tend to follow a particular rule. The tendencies summarized below may provide some guidelines that help to limit the plausible precipitation crystallography in a given system. The possible deviation of real systems from strict satisfaction of the rule(s) will be also discussed.

#### 5.4.1. Selections of singular interfaces

Though preference for a particular rule is not strictly predicable, singular interfaces that obey more than one rule should take priority, because these interfaces satisfy two optimum conditions simultaneously, which are presumably associated with deep energy cusps. It is convenient to rank the order of preference using the classification in Table 1. Depending on the appropriate preferred state, priority for realization of the singular interfaces should first include those that follow three rules, i.e. $A_{\mathrm{I}}$ or $A_{\mathrm{II}}$; then those that follow two rules, i.e. $B_{\mathrm{I}}$, $C_{\mathrm{I}}$, $C_{\mathrm{II}}$, $B_{\mathrm{II}}$, and $F_{\mathrm{II}}$; and finally those that follow only a single rule. Therefore, when two or more rules are permitted by the lattice constants of the two phases, a prediction of the crystallography is possible, since the number of such interfaces in the BGP space is limited.

When only a single rule is applicable, preference for a particular rule would depend on which of the optimum conditions, described in Section 3.4, has the dominant effect in the given system. Among the three rules, Rule I is the most general. Any system, whether the lattice misfit is large or small, always has the freedom to follow this rule. Rule I will be realized, when the first optimum condition prevails or the second optimum condition is not feasible (For example, when the primary misfit strain is isotropic, the rank of $\mathbf{T}$ is constantly three and no invariant element can be solved). The majority of interfaces that follow Rule I (Table 5) belong to the first case. These systems contain a ceramic phase with directional covalent or ionic bonds, so that the strong influence of the chemical component of the interfacial energy results in dominance of the first optimum condition over the others.

Though rational habit planes form the majority of the observations in Table 5, the small, but persistent, rotation away from a rational OR, and the irrational orientation of the interface plane itself in several well-characterized systems, can also be interpreted consistently in terms of parallelism of two $\Delta\mathbf{g}$'s. (The relative paucity of these observations is probably related to the facet that irrational habit planes are found in only a minority of the precipitation systems studied so far.) Preference for formation of interfacial steps in a singular interface is due to a dominant tendency for realizing certain characteristic structures, described by either the second or third optimum condition. A system consisting of phases of metallic solid solutions (with small misfit) tends to prefer Rule II, since the chemical component of the interfacial

energy in such systems is not expected to be strongly anisotropic. These systems probably obtain a large reduction in the structural component of the interfacial energy at a small expense in the rise of the chemical component due to the steps. This hypothesis is consistent with a recent atomic simulation of the interfacial energy for a $(1\,{-}2\,1)_f$ habit plane in fcc/bcc Ni–Cr alloys by Chen et al. [147], where the chemical contribution to the interfacial energy was found to be less than 20%. Rule III is preferred to Rule I for a system of large misfit, where a compromise between dense CCSL points and small secondary misfit in the interface can be achieved by the formation of interfacial steps. Again, this occurs only if the balance between the rise of chemical component and the reduction of the structural component of the interfacial energy is in favor of the steps. Systems consisting of an intermetallic compound and a metallic phase may tend to obey this rule, provided that the surface energy of the compound phase is not strongly anisotropic.

In special systems where the terrace planes defined in different phases have identical spacing, an OR can satisfy Rules I and Rule III simultaneously, and the terrace planes for the stepped interface that obey Rule III are parallel to the rational crystal planes that obey Rule I. The interface in Fig. 15d is a typical example for this special case. In this system, two sets of $\Delta\mathbf{g}$'s obey Rule III and they are symmetrically equivalent. If they were not symmetrically equivalent, the one type of steps may be preferred than the other, and the resultant stepped interface would likely follow Rule III. However, because of the symmetry preference cannot be made for any set of $\Delta\mathbf{g}$'s (so an arbitrary one is chosen for illustrating the stepped interface). It is likely that up-and-down steps are equally developed. In principle, the development of the stepped interface is mainly governed by the third optimum condition, though the first optimum condition may appear active. In the microscopic scale the interface follows Rule III, but the average interface orientation follows Rule I. In real systems, the case in Fig. 15 is rare. However, it remains possible that a structure is microscopically controlled by the third optimum condition but macroscopically controlled by Rule I. As discussed in the following subsection, any ideal singular structure that can only be present in systems of special lattice constants might be developed in other systems with a residual long range strain being allowed. When the terrace planes defined in different phases have different spacing, up-and-down d-steps may be developed with a residual misfit strain between the interplanar spacing being tolerated elastically at each step, so that the overall misfit in the interface is minimized [132]. This residual misfit strain is alternating and is not in a long range, but it is not accommodated by the secondary dislocation associated with the step. Such an up-and-down step structure is also favored when wrong bonds between intermetallic compounds can be avoided [81,133]. Because of the difference in the interplanar spacing, the OR between the phases only follows Rule I, but the interface contains d-steps, that are usually present in an interface following Rule III.

Fig. 14 schematically summarizes the influences of various conditions on the tendency of a precipitation system to obey a particular $\Delta\mathbf{g}$ parallelism rule. It is hoped that this empirical chart will provide some guidelines for investigations of precipitation crystallography. According to the guidelines, together with the avail-

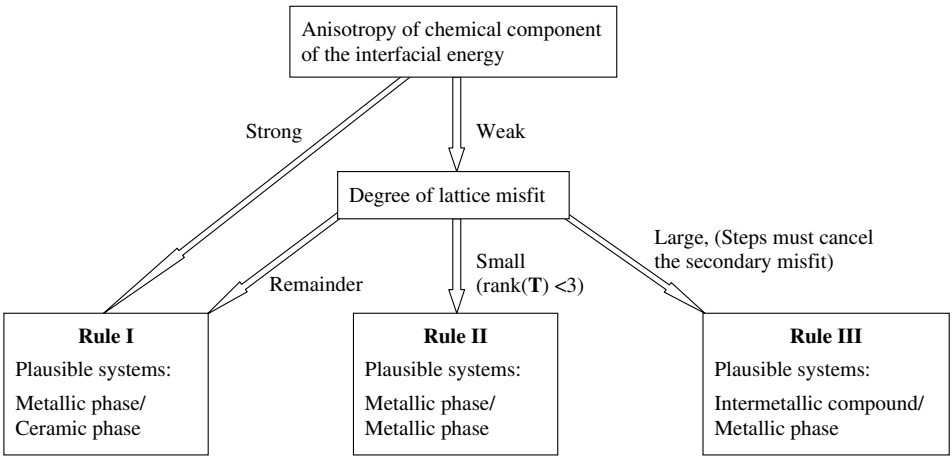


Fig. 14. A chart schematically summarized the influences of different conditions on the selection among the possible $\Delta\mathbf{g}$ parallelism rules.

able crystallographic data and the nature of the chemical bonding in a given system, one may be able to deduce the $\Delta\mathbf{g}$ parallelism rule applicable to a system and to identify the possible singular interfaces correspondingly.

Although the knowledge of active rules greatly limits the possible crystallography, there are still a number of candidates of singular interfaces, each of which can follow a selected rule. Which one $\Delta\mathbf{g}$, or a set of $\Delta\mathbf{g}$'s, should define the singular interface in a given system is not always obvious. In principle, the preferred singular interface should be the one in which the deviation from the preferred state (i.e. the primary or secondary misfit strain) is small. The misfit distribution can be investigated by a systematic study based on the O-lattice, or an appropriate CCSL. Therefore, though a calculation may be avoided for interpretation of precipitation crystallography, it must be used for prediction of plausible precipitation crystallography. Such an approach requires only the input of lattice constants of the two phases. It may serve as a first step for a fast and rough quantitative search for the possible precipitation crystallography in the 5D GBP space, before more sophisticated (physical) models are tried. The result of the misfit distribution might also be used to suggest the possible morphology of the precipitates, which is a critically important microstructural feature for engineering materials. When the model lattice is properly determined, the predicted precipitation crystallography and morphology can potentially be applied to microstructural design, both guiding and accelerating the development of materials with improved properties.

*5.4.2. Possible tolerance of a small long-range strain*

Although a singular interface that obeys two rules should most likely be favored, in practice, however, strict satisfaction of two rules is unlikely. Simultaneous

satisfaction of two rules is equivalent to the condition that two pairs of directions from different phases are parallel. As explained earlier, two pairs of parallel directions in a general system must be dependent (for example, a rational OR is defined by a pair of parallel planes and a pair of parallel directions in the parallel planes), so that they only define three degrees of freedom, rather than the four degrees that would be defined if they were independent. However, if we allow the lattice parameters to vary, more degrees of freedom become available and satisfaction of multiple rules is possible. In this hypothetical space of higher degrees of freedom, one would be able define a set of points corresponding to strict satisfaction of two rules that are presumably associated with deep energy cusps. If the lattice parameters of a real system are close enough to those that are associated with a deep energy cusp, the singular interface in the real system will contain the structure that is permitted by the condition of two rules, albeit at the expense of a small degree of long-range strain. A common example of strained singular interface is the elastically forced coherent ($A_1$) interface around small precipitates (in Al–Sc alloys for example), whose morphology is also influenced by the strain energy [10].

More general singular interfaces that satisfy two optimum conditions (or one condition twice) may contain a single set of periodic dislocations (Table 4). The prevailing singular structure in these interfaces can also be realized, in a slightly strained form. Those cases in Table 5 that have been identified by multiple rules may not strictly satisfy the corresponding rules if their lattice constants are used for calculations. However, allowing a certain degree of residual long-range strain to be tolerated, the corresponding habit plane in each case probably contains the singular structure associated with satisfaction of multiple rules. Singular structure may also be realized in different facets when a small amount of long-range strain is tolerated. For example, an interface can consist of several facets in the zone axis of the invariant line, with a facet following Rule I and another following approximately Rule II [22,23] though the lattice constants in the system do not permit satisfaction of two rules simultaneously. Other habit planes, which do not follow multiple rules, may also carry some residual long-range strain. When the total energy is taken into a thermodynamic consideration, the present of a certain degree of residual long-range strain, with the spacing of the interfacial dislocations being smaller than the value determined from a long-range strain free state may be preferred [148]. It is also possible that some parts of the interface will carry a long-range strain greater than that in the other parts. The surface relief effect associated with precipitates in some systems [104,149–151] provides evidence of the existence of long-range strain. Similar to the surface relief effect associated with martensitic transformations, the habit planes of the precipitates are usually undistorted, i.e. they are macroscopic invariant planes. This means that the habit plane itself in this situation can be regarded free from a long-range strain.

The degree of long-range strain that can be tolerated varies from one case to another. In practice, a long-range strain usually exists in the course of precipitation, especially when the precipitates are small. The strain may diminish with the growth of the precipitates, as the strain is affected by the balance of total energy

(interfacial energy and strain energy). Therefore, the long-range strain that can be tolerated depends not only on the deviation of the equilibrium lattice constants from the "ideal" constants for the prevailed singular structure and the depth of the associated energy cusp, but also on the precipitate size and the details of the precipitation process. The singular structures in Table 1 can be considered as ideal structures corresponding to energy cusps. When derived with the long-range strain free assumption, these structures are permitted only when at least one $\Delta\mathbf{g}$ parallelism rule is followed (Table 4). Once a long-range strain is allowed, the satisfaction of the rules may not be strictly observed. However, since the residual long-range strain virtually enhances preservation of a singular structure, an observed habit plane or facet should be normal to the near parallel $\Delta\mathbf{g}$('s) or $\mathbf{g}$'s. It is convenient to take the allowable extent of a possible long-range strain of the same order of magnitude as the experimental uncertainty in the diffraction patterns. Thus, the association between the singular structure and habit planes can be examined by visual inspection of parallelism of $\Delta\mathbf{g}$ with other $\Delta\mathbf{g}$'s or $\mathbf{g}$'s, as was carried out for construction of Table 5. However, minimization of experimental uncertainty is always desirable for quantitative description of the precipitation crystallography. [21]

*5.4.3. Possible scattering of precipitation crystallography*

A true scattering of OR's and of habit plane orientations has been reported, especially in metallic systems that exhibit an irrational crystallography [27,86,152]. When the scattering of precipitation crystallography is due to residual strain during precipitation, as discussed in the above, the scattering must be somehow related to the size of the precipitates, and the precipitation crystallography must converge to a unique description for well-developed precipitates. However, there might be other causes for the variation of the transformation crystallography. Although any change in the parameters describing the crystallography of a singular interface may cause the interfacial energy to rise, the persistence of the singular interface against perturbation is likely to vary with direction in the BGP space. Since constraints in different directions are normally not equivalent, the partial derivatives of energy with respect to any change in direction (i.e. the slope of the Wulff plot at the cusp) will not be identical. Under these circumstances one might expect some experimental scattering to be found in one or more of the parameters needed to define the precipitation crystallography.

When two rules can be applied simultaneously, the energy cusp associated with the singular interface is likely sharp with respect to any direction in the BGP space, and the probability of scattering to occur in the OR or the facet orientation is expected to be small. If a singular interface is restricted by a rule together with a supplementary constraint, the chance of some deviation from the condition imposed

[21] Since a precise $\Delta\mathbf{g}$ can only be measured at the cross point of Kikuchi bands associated with the correlated $\mathbf{g}$'s, Kikuchi lines will be particularly useful for a systematic and accurate measurement of $\Delta\mathbf{g}$'s for a given system.

by the supplementary constraint may be larger than any deviation from the $\Delta\mathbf{g}$ parallelism rule. While the supplementary constraint of parallel low index directions imposes clearly specified crystallographic requirements to the OR, any criterion that makes use of the dislocation spacing is less rigorous. Provided that a local minimum of interfacial energy is associated with the maximum spacing of the dislocations in a $D_I$ interface, the local minimum may be rather shallow since the dislocation spacing changes only gradually with a change in the OR. In addition, the dislocation spacing is often observed to vary in the habit plane, suggesting that a small deviation of the average dislocation spacing from the optimum value likely occurs. This implies that the OR and habit plane normal for a $D_I$ interface might display some scattering along a line defined by Rule II in the 5D BGP space. This argument might help to explain the scattering found in the OR and habit plane in those systems that exhibit an irrational crystallography. On the other hand, as discussed in Section 5.2, when the dislocation spacing is not significantly larger than the atomic spacing, selection of the OR according to the dislocation spacing may not be justified and selection condition may become uncertain. Several $D_I$ interfaces, selected by using various conditions, corresponding to different Burgers vectors can be determined in a small range of OR for a given fcc/bcc system [98]. However, whether each combination of a condition and a Burgers vector is associated with a shallow local energy minimum requires further examination.

#### *5.4.4. Information extended from the $\Delta\mathbf{g}$ parallelism rule(s)*

While the principal application of the $\Delta\mathbf{g}$ parallelism rules lies in the quantitative interpretation of observed precipitation crystallography, the unambiguous identification of the $\Delta\mathbf{g}$ parallelism rule(s) can be extended to provide further insight into the precipitation crystallography. The optimum condition(s) that govern the development of the precipitation crystallography may be deduced from the effective parallelism rule(s) and any additional information from the system. For example, in a two-phase couple that follows Rule I, the chemical component of the interfacial energy probably has a dominant effect. On the other hand, although the interpretation of precipitation crystallography with the $\Delta\mathbf{g}$ parallelism rules does not require any calculation or observation of the interfacial structure, knowledge of the interfacial structure is essential to fully understand the precipitation crystallography. When $\Delta\mathbf{g}_{P\text{-}I}$'s are distinguishable (as those connecting the nearest low index $\mathbf{g}$'s in a one-to-one fashion), the interfacial structures for the habit planes can be proposed by following the one-to-one associations of different combination of the rules with the singular structures given in Table 4. Though systems in secondary preferred states are more complicated, one can also establish a one-to-one relationship between different combinations of the rules with the singular structures, if any step in the singular interfaces is treated to be of the same type. The interfacial structure can then be suggested based on the relationship and the identified $\Delta\mathbf{g}$ parallelism rule(s).

In addition, the Burgers vector(s) of the interfacial dislocations can be suggested according to the intrinsic relationship between $\Delta\mathbf{g}_{P\text{-}I}$('s) or $\Delta\mathbf{g}_{P\text{-}II}$('s) normal to the singular interface and the Burgers vector(s) of the dislocations contained in the

interface. For example, if a system follows Rule II once, the Burgers vector of the single set of dislocations in the habit plane should lie in the planes defined by the $\mathbf{g}_P$'s associated with the parallel $\Delta\mathbf{g}_{P\text{-}I}$'s (Section 4.2). The theoretical result is particularly helpful for experimental studies of interfacial structures, because experimental confirmation of predicted Burgers vectors is often much simpler than an "ab initio" determination of the Burgers vectors, especially when secondary dislocations are present.

More quantitative description of the interfacial structure usually requires a calculation with a model lattice. The information available from the parallel $\Delta\mathbf{g}$'s can be used to guide the construction of proper model lattices, including determination of the preferred state (in particular, the orientation of the parallel $\Delta\mathbf{g}$'s will indicate the plane for construction of the 2D CCSL for a secondary preferred state) and the lattice correspondence for the transformation strain. Testing of calculated principal planes in a model lattice with experimental results is straightforward when this is done in terms of the $\Delta\mathbf{g}$'s; any uncertainty in both calculation and experiment in the comparison can often be avoided.

## 6. Other approaches and links described in the O-lattice

As briefly reviewed in the introduction, observations of precipitation crystallography in different systems have been interpreted by various models. While the present study emphasizes the roles of periodicity and singularity of interfacial structure, together with the degree of misfit strain, in determining the precipitation crystallography, other models address the same problem from different perspectives. The present study has intended to integrate useful concepts developed from different models. Many characteristic features proposed by different models can be accounted for by using the present approach. In literature, one often finds that the same set of observations can be interpreted by different models. It is convenient to use the present approach as a link to discuss several broadly-adopted models. Our discussion will also address the assumptions and approximations in the different models, and the intrinsic similarities and differences between the models, to elucidate why and in what circumstances these different models might yield equivalent results.

### *6.1. Symmetry-dictated criterion*

Cahn and Kalonji [46] suggested the association of a symmetry-dictated energy extremum with the OR and the morphology of a faceted precipitate. The extremum corresponds to the parallelism of common symmetry axes, and may be a minimum, a maximum or a saddle point in energy. According to the suggestion by Cahn and Kalonji [46], when a symmetry dictated extremum is observed, the OR should correspond to an energy minimum. Since the alignment of common symmetry axes will result in a rational OR, the criterion of symmetry-dictated energy extremum (symmetry-dictated criterion) may explain the observations of rational ORs. While this criterion emphasizes parallelism of the symmetry elements common to both

crystalline phases, the present approach specifies parallelism of either $\mathbf{g}_{P\text{-}\alpha}$ and $\mathbf{g}_{P\text{-}\beta}$, or $\mathbf{g}_{P\text{-}\alpha CCSL}$ and $\mathbf{g}_{P\text{-}\beta CCSL}$ for rational habit plane (or facets) (Rule I). An observed rational OR and interface may be explained by both approaches, if the observations meet the specifications in both approaches. While there are possible overlaps between the candidates suggested from the parallelism principal $\mathbf{g}$ vectors and that expected from the symmetry parallelism, the candidates in the former case are usually fewer than that in the latter. All candidates in the former case are associated with local minima of energy in the present consideration, but those in the latter may or may not be associated with local minima [46], and they may or may not be described by Rule I. In this aspect, the candidates suggested by the present approach are more concentrated. These candidates can be further narrowed according to the degrees of the interfacial misfit. However, the present model assumes that the OR is developed for the realization of at least one singular interface, whereas the symmetry criterion is not subject to this assumption. Since the present survey has focused on systems in which a well-defined habit plane (or facets) was observed, full consistency between the model and the observations has been obtained. Whether some rational ORs (e.g. those corresponding to precipitates with needle or rod shapes) can be explained by the symmetry criterion but cannot be interpreted by the present approach requires further test. On the other hand, while the observations of rational ORs may be explained by the symmetry-dictated criterion, the observations of irrational ORs cannot be interpreted from this approach. In this aspect, the present approach offers a more complete scope of applications, including both rational and irrational ORs.

Though the symmetry-dictated criterion may not be general in determining the OR, the relationship between the intersection group of symmetry with the precipitate morphology proposed by Cahn and Kalonji [46] is completely general. When the symmetry-dictated criterion is not applicable, the precipitate morphology is not likely to carry any symmetry element from either crystal, unless the effect of the structural component of the interfacial energy is negligibly small (then the symmetry of one crystal with strongly anisotropic surface energy may have a dominant effect on the shape of the precipitates). Once certain symmetry operations are common to both crystals for a given OR, the morphology of the precipitate (and the interfacial structure) must be in accord with the survived symmetry. Any correct prediction of a model must be in agreement with this general and simple relationship. The results from the present approach are consistent with this relationship. As emphasized in the symmetry consideration [46], it is the bi-crystal crystallography, rather than the crystallography of individual crystal lattices, that plays a crucial role for the present analysis of precipitation crystallography. Each of the model lattices, which serve as the basis in the present analysis, carries the information of the superimposed crystal lattices. When the common symmetry elements can be found in an OR, these elements must be conserved in the model lattice. They will be inherited in the distribution of the $\Delta\mathbf{g}$'s, as the reciprocal vectors of the model lattice, and will be reflected in the interfacial structure, as determined by the model lattice. The crystallographic equivalent facets of a precipitate, determined by the equivalent $\Delta\mathbf{g}_{P\text{-}I}$'s (or $\Delta\mathbf{g}_{P\text{-}II}$'s), should be in accord with the intersection point symmetry (Fig. 11). The information

from $\Delta\mathbf{g}_{\text{P-I}}$ (or $\Delta\mathbf{g}_{\text{P-II}}$) vectors not only indicates the surviving symmetry but also specifies the orientations of the facets, which is an advantage over the symmetry approach. In addition, the distribution of $\Delta\mathbf{g}$'s (e.g. parallelism) and their magnitudes also carry information about the lattice misfit (e.g. as indicated by the density of the O-points [83]) in the interface normal to the $\Delta\mathbf{g}$'s. Because the relative values of the interfacial energy cusps are probably affected by the lattice misfit, it is possible to discriminate corresponding facets based on an analysis of $\Delta\mathbf{g}$'s. For example, when the symmetry consideration predicts a rectangular cross-section for a precipitate, the $\Delta\mathbf{g}$ approach can specify the orientations of the facets, and which facet has a broad area, as the habit plane or the prominent facet.

Though the present approach is more quantitative, the simple and general relationship between the intersection group of symmetry with the precipitate morphology is always valuable in analysis of the precipitate morphology. For example, by examining the measurement of the OR and the precipitate shape against this relationship, one can quickly test the validity of the measurement, especially for identifying a small deviation from exact parallelism of symmetry elements. Furthermore, one may be able to make useful suggestions for the crystal structure of unknown precipitates simply based on the OR and the measured precipitate shape.

### *6.2. Parametric methods*

Parametric methods explain or predict the precipitation crystallography by finding minimum or maximum values of selected parameters [34–36]. Searching for optimum boundary structures using a simple parameter was pioneered by Bollmann and Nissen [35]. In their method, local minimum values of a simple parameter $P$ (where $P$ is a function of $b_i/d_i$, with $d_i$ being the dislocation spacing and $b_i$ the magnitude of the Burgers vector) were used to represent the interfacial energy. Another parameter $R$, suggested by Ecob and Ralph [36], has been used for representing the energy, and is also a function of $b_i/d_i$. Since primary dislocations are assumed in these models, the primary preferred state is implied by the methods. These parameters essentially serve as estimations of the primary misfit in different interfaces, and their values were believed to represent the interfacial energy (i.e. the structural component).

Applications of the parameters $P$ or $R$ have been based the O-lattice construction. The results have shown that the minimum value of $P$ or $R$ corresponds to planes containing two sets of dislocations, determined by two principal O-lattice vectors [35,36]. According to the present definition, these are the principal planes of the O-lattice. In the study of the precipitation crystallography, the potential local minima, rather than the absolute values of $P$ and $R$, are the most important. The results from applications of the parameter $P$ or $R$, concerning the principal O-lattice planes are incorporated directly into the present approach, though our selection of the principal O-lattice planes as the candidates for the singular interfaces was rationalized by a different argument, namely the dislocation periodicity. Without using numerical calculations, we identify all principal O-lattice planes directly from $\Delta\mathbf{g}_{\text{P-I}}$ vectors, the reciprocal vectors of principal planes of the O-lattice. Despite that common results

may be produced from either approach, the result of the principal planes of the O-lattice suggested by parametric method is often incomplete. This is because the parametric method employed the simplification that the lattice misfit is completely accommodated by three sets of misfit dislocations, with non-coplanar Burgers vectors. In real systems, the number of Burgers vectors usually exceeds three (e.g. there are totally six $\langle 1\,1\,0\rangle/2$ Burgers vectors for an fcc lattice). Therefore, some important candidates for the singular interfaces might be missed due to this simplification. Even if a useful principal O-lattice plane is determined via a correct selection of the Burgers vectors, the dislocation structure may not be represented by the description based on a simplified O-cell structure, consisting of just three sets of walls. The complete O-cell structure should consist of the same number of walls as the possible Burgers vectors [37]. Only when the O-lattice plane indeed contains only two sets of dislocations, can the description of the dislocation structure from the simplified method be valid.

Although the dislocation structure determined by the parametric methods is often oversimplified, the values of $P$ or $R$ may indicate the relative densities of the dislocations in the interfaces parallel to the principal O-lattice planes. The values of $P$ or $R$ are determined as functions of the magnitudes of the principal O-lattice vectors in the planes [35,36], and they should somehow reflect the densities of the O-points on these planes. Because each O-point on a principal O-lattice plane should correspond to a dislocation cell, the planar density of O-points could be used as a relative measure of the density of the interfacial dislocations [83]. Since the calculation details are different, the results of ORs predicted by different parameters may be different. The results may also be different from the result expected from the **g** parallelism rules. However, when the parametric methods are applied to select the optimum boundary for a given OR, the selection is usually made among the principal O-lattice planes, and the optimum boundary selected by different parameters from a set of discrete values may be similar. For example, $P$ and $R$ were used to evaluate different principal O-lattice planes in an fcc/bcc system, and each led to the same rank [153]. A similar result can also be obtained from the magnitude of $\mathbf{g}_{\text{P-I}}$. As the reciprocal vector, the value of $1/|\Delta\mathbf{g}_{\text{P-I}}|$ indicates relative density of the O-points in a plane normal to $\Delta\mathbf{g}_{\text{P-I}}$. Provided that the O-point densities in the different principal O-lattice planes are significantly different, the same habit plane containing dislocations of the lowest density could be distinguished from the principal O-lattice plane(s) by the use of any one of the parameters, $1/|\Delta\mathbf{g}_{\text{P-I}}|$, $P$ or $R$. Among the three parameters, $1/|\Delta\mathbf{g}_{\text{P-I}}|$ is the simplest to calculate, and it is the only one that is measurable. However, it should be remembered that such a comparison is valid, only if the O-lattice is a point lattice in 3D.

A similar choice might be made from a still different parameter, the net Burgers vector content, as suggested by Knowles and Smith [34]. The interface with a minimum Burgers vector content is defined by the plane containing two smaller axes in the **B** ellipsoid, describing the misfit associated with any unit vector [34]. This interface, as a plane of the smallest misfit, has not taken the discrete Burgers vectors into consideration, and it may be close but not exactly identical to a principal O-lattice plane containing periodic dislocations of the lowest density. The discrepancy

of the interfaces predicted by different approaches could be quantitatively analyzed in reciprocal space [83]. Let $\mathbf{r}$ be a general unit reciprocal vector. One can determine $\Delta\mathbf{r}$ as the displacement associated with $\mathbf{r}$ by Eq. (7a). The plane with the minimum Burgers vector content is normal to the $\Delta\mathbf{r}$ that has the largest magnitude [83]. On the other hand, the plane containing the lowest density of dislocations may be defined by the largest $\Delta\mathbf{g}_{\text{P-I}}$ [83], or by $\Delta\mathbf{g}_{\text{P-I}}/|\mathbf{g}_{\text{P}}|$ to be comparable with $\Delta\mathbf{r}$, as $\Delta\mathbf{g}_{\text{P-I}}/|\mathbf{g}_{\text{P}}|$ is the displacement associated with a unit vector $\mathbf{g}_{\text{P}}/|\mathbf{g}_{\text{P}}|$. The largest $\Delta\mathbf{r}$ based on a continuum approach rarely agrees with $\Delta\mathbf{g}_{\text{P-I}}/|\mathbf{g}_{\text{P}}|$ that can have only a discrete orientation determined by the O-lattice construction. However, the difference between the two vectors may be in the range of experimental uncertainty, if an observed irrational habit plane is expressed in an approximate high index. While both approaches may account for the observation indexed in a crystal basis, the validity of the models can be distinguished by using measurable $\Delta\mathbf{g}_{\text{P-I}}$'s.

It is implied by various parametric methods that the degree of lattice misfit, in terms of dislocation density or net Burgers vector content, should have a dominant effect on the determination of the habit plane. The present study has regarded the degree of lattice misfit as an important factor in the determination of the precipitation crystallography. However, the general predictability of any geometric parameter remains in doubt. No simple and general parameter can effectively represent the interfacial energy over the whole range of possible lattice misfit in crystalline materials. Maximizing the dislocation spacing has been considered in Section 5.2 only as a possible supplementary constraint for a $D_{\text{I}}$ interface, containing a single set of dislocations, as this does not always lead to a correct prediction of the habit plane in fcc/bcc systems [24]. Considerations based on the dislocation density or net Burgers vector content neglect: (a) the contribution of the chemical component of the interfacial energy, (b) the topography of the interface at the atomic scale which determines the microscopic distribution of the interface misfit, and (c) the possible variation of dislocation core energy with the dislocation spacing, especially likely when the spacing is small. Therefore, the validity of using a parametric method is probably limited to metallic systems in the primary preferred state when the dislocation spacing is considerably larger than the size of the dislocation core, as neglecting the above factors may not significantly alter the order of the preference of the singular interfaces. Real systems are often complicated, and any parameter must be used very carefully. In the present study, the condition of maximum dislocation spacing has been regarded only to define a possible shallow minimum in the interfacial energy, while the conditions imposed by the optimum conditions or $\Delta\mathbf{g}$ parallelism rule(s) have been considered to be associated with shape cusps in the interfacial energy. It should be also recognized that the second optimum condition does not necessarily lead to a reduction of dislocation density. For a given interface, when the misfit strain in the direction along the invariant line vanishes, the misfit strain in the direction normal to the invariant line will increase [24], so that there might be no net effect on the dislocation density. In practice, it is also possible that a realized habit plane may be associated with a local minimum rather than the global minimum of interfacial energy. No matter what the absolute value of the interfacial

energy is, the habit plane, as a singular interface, should be identified by the $\Delta\mathbf{g}$ parallelism rule(s).

### 6.3. Invariant line criterion

As noted in the introduction, a large body of evidence suggests that an invariant line plays an important role in the development of the OR in many alloys. The application of the invariant line criterion to precipitation crystallography was first emphasized by Dahmen in his systematic study of OR's in various precipitation systems in 1982 [16]. The earlier applications [74,154] of the invariant line criterion for rationalizing ORs have shown a close relationship with the parametric approach based on the O-lattice model [35]. The condition of an invariant line strain does not uniquely define the OR, as an invariant line can be produced in numerous ORs [84]. However, if the calculation is restricted to two dimensions, a single invariant line is uniquely predicted. This approach was used by Dahmen to rationalize the observations from different precipitation systems, limiting the invariant line to lie in parallel close packed planes in the two crystals [16]. The precipitates in the applicable examples were mostly transition metal carbides or nitrides, and their experimental ORs with the corresponding metal matrixes were reported as being rational. While the selections from among the rational ORs are in good general agreement with the OR predicted from the invariant line criterion, further testing using precise experimental data is required to decide whether a strict invariant line truly exists with the OR (which is usually irrational) predicted from the invariant line calculation, or whether otherwise, the OR in a selected system is strictly rational (with the selection of parallel in-plane low index directions among possible candidates probably being governed by the small directional misfit criterion [100]). While the 2D model has the advantage of being simple and providing an analytical solution of the OR, it is limited to systems in which the close packed planes are parallel. Moreover this method alone only predicts the possible ORs, not the habit planes. Unless the lattice constants are special, the invariant line predicted from a 2D model does usually not satisfy the O-line condition. The 2D model will yield an invariant line that only lies in the parallel close-packed planes. This restricted invariant line is not always supported by experimental observations, though the precision in the measurement of the OR does not often allow a close examination of the parallelism.

An alternative approach, adopted by Luo and Weatherly [17], determines the invariant line in a Ni–Cr system from a three dimensional calculation, using the observed OR (K–S) in an fcc/bcc system. These authors also showed that the habit plane corresponded to an unrotated plane of the transformation, and contained the invariant line. They determined the candidates for the invariant line from the intersection points of the initial and final cones of the unextended lines, associated by the Bain strain. Their result is consistent with the observed invariant line inclined to the conjugate planes, which is presumably parallel to the long axis of the precipitate lath. However, while the invariant line must be at an intersecting point between the initial and final cones of the unextended lines, as an intersecting point to define an invariant line, the vectors from different lattices meeting at the intersecting point

must be related by the Bain strain. As noted by the authors [17], not all intersecting points can define invariant lines. The intersection points related by the K–S OR can define invariant lines only when the lattice parameters are special [155]. Though the observation of the K–S OR in the Ni–Cr system was reported [17], the strict K–S OR for the lattice parameter ratio in this system does not permit realization of any invariant line. On the other hand, the habit plane was observed to obey Rule II (e.g. Fig. 12). The habit plane containing the O-lines could be obtained when the conjugate planes are rotated by 0.4° about the close packed direction from the K–S OR, and in this case the resulting habit plane and the invariant line are in good agreement with the observations [24,98]. Clearly, if this O-line OR is taken as the input in the method for 3D calculation of the invariant line, the invariant line can be determined from the intersection point between the initial and final cones of the unextended lines. If the input OR carried some experimental uncertainty, say about 0.5°, the invariant line determined by the intersection point will be close (or identical within the experimental error) to the true invariant line, since the intersection point will change smoothly with the small variation of the OR. This dependence explains why the intersection point determined from the exact K–S OR, 0.4° from the O-line OR, could give an approximate invariant line, close to the measured one [17].

The restriction of the Bain strain to the solution(s) of invariant line can be used to test the observed OR and invariant line. For convenience we denote the displacement associated with unextended line as a rotation displacement. [22] The starting OR may be given by any rational OR, e.g. N–W or K–S. The necessary condition for a rotation, **R**, to bring a particular unextended line into an invariant line is that the rotation axis is normal to the rotation displacement associated with this unextended line. While a particular invariant line can be realized by various rotations that fulfill the above condition, usually each rotation axis is normal to two rotation displacement vectors, and it can only render at most a pair of unextended lines into invariant lines. Only when the rotation axis is an invariant line in reciprocal space, will all displacement vectors lie in the plane normal to the rotation axis [73], and numerous invariant lines may be produced through small rotations around the axis. In the Bain correspondence, any vector in one of the conjugate planes (e.g. $\{1\,1\,1\}_{\mathrm{f}}$) must be correlated with a vector in the other conjugate plane (e.g. $\{1\,1\,0\}_{\mathrm{b}}$) and the correlation is the same for both 2D and 3D calculations. If the conjugate planes remain parallel and have different interplanar spacing, only the displacement between the correlated inplane vectors will lie in the plane. Among them there may be zero, one, or two rotation displacement vectors. Assuming that at least one rotation displacement vector is available in the plane, its associated unextended vectors, the potential invariant line, must also lie in the plane. Therefore, the requirement of parallelism of the conjugate planes in a general fcc/bcc system will only yield the

[22] The condition of invariant line is $\mathbf{R}\mathbf{A}_0\mathbf{x}_i = \mathbf{x}_i$ or $\mathbf{A}_0\mathbf{x}_i = \mathbf{R}'\mathbf{x}_i$, where $\mathbf{A}_0$ is either Bain strain or another strain before the rotation. The displacement caused by the strain and the invert rotation is same: $(\mathbf{I} - \mathbf{A}_0)\mathbf{x}_i = (\mathbf{I} - \mathbf{R}')\mathbf{x}_i$. Because the displacement due to any rotation must be normal to the rotation axis, an invariant line can be realized by a rotation only if the rotation axis is normal to the initial displacement.

invariant line lying in the conjugate planes, [23] identical to that determined from the 2D model [16]. On the other hand, a rotation around a pair of parallel conjugate Burgers vectors does not necessarily cause an invariant line to form in the plane normal to the rotation axis, as the planes normal to the Burgers vectors may not be related by the lattice correspondence. When the Burgers vectors are not identical, i.e. when they do not define an invariant line, only one (or two) unique rotation around the parallel Burgers vectors can lead to an invariant line strain. This rotation must allow an invariant line in reciprocal space to form in the plane normal to the Burgers vector. The projection of the invariant line in direct space onto the plane normal to the Burgers vectors must lie normal to the parallel displacement vectors ($\Delta\mathbf{g}$'s) between the reciprocal vectors in the plane, but the angle between the Burgers vectors and the invariant line will vary with the specific misfit strain field.

The following relationships may be concluded from the above analysis for the condition of the conjugate planes being parallel. (1) Only in an ideal case in which the conjugate planes have identical interplanar spacing, the intersection point produced from the 3D model [17] is a strict invariant line, which can have any orientation depending on the specific OR. The 3D model may effectively produce an approximate invariant line inclined to the conjugate plane, only if the conjugate planes have almost identical interplanar spacing, as in a Ni–Cr alloy system [17]. (2) In a usual case, the conjugate planes have different interplanar spacing, and the possible invariant line only lies in the conjugate planes. If the invariant line was observed to lie in the conjugate planes, the conjugate planes are likely parallel and a 2D model can yield correct result of the invariant line. More strictly, an angular deviation must exist between the conjugate planes though it may be too small to be detectable (Fig. 12), when an invariant line is observed (e.g. according to parallel linear defects or the axis of precipitate lath) to incline with respect to the conjugate planes. If a pair of Burgers vectors are parallel in the condition of the habit plane containing an invariant line, usually these Burgers vectors should be that (defined in the different phases) for the dislocations in the habit plane and should lie in the habit plane. The OR and the IO of the habit plane can be determined by a 2D calculation in the plane normal to the Burgers vectors.

In the application of the O-line criterion, or the second optimum condition, an equilibrium periodic dislocation structure is assumed. How the misfit dislocations were generated was not considered, though this factor may play a crucial role in the preference of the Burgers vector. This important aspect has been emphasized in several investigations by Dahmen and Westmacott [18,103,108]. In their analyses, the invariant lines associated with coherent and semicoherent particles were different. Considering the role of the slip plane in determination of the nucleation of the dislocations along the invariant line, the invariant line was determined at the intersection of the cone of unextended lines with a slip plane. The habit plane would

[23] When conjugate planes have identical interplanar spacing, the plane normal will define the invariant line in reciprocal space. Then different rotations around the plane normal will lead to various invariant lines, and the 3D invariant line approach is strictly valid only for this special case.

contain this invariant line and a tensile axis of the strain (possibly an unrotated direction) [18,108]. On noticing the role of discrete Burgers vectors in determining the crystallography of the semicoherent precipitates, Dahmen and Westmacott [108] also suggested another condition for restricting the invariant line for precipitates that have lost coherency. They postulated that the shear direction in the shear matrix (**S**) decomposed from the invariant line strain ($\mathbf{A} = \mathbf{PS}$, where **P** is a pure deformation) must be determined by a Burgers vector. They argued that a shear loop is preferred over a prismatic loop in the dislocation nucleation process. While both shear loop approach and the O-line condition take the important constraint of the Burgers vector into consideration, the details are different. The O-line condition focuses on the habit plane, which should be accommodated fully by a single set of dislocations, no matter whether the dislocations are dominated by screw or edge character. The shear loop approach emphasizes the overall shear field, but it does not explain how the pure deformation is accommodated in any part of the interface. On the other hand, both approaches share one of two conditions in the PTMC, i.e. (1) the invariant line must lie in the slip plane, and (2) the invariant line in reciprocal space must be normal to the Burgers vector [101]. While the shear loop approach adopted condition (1), the O-line condition is equivalent with condition (2). However, unlike the decomposition in the PTMC, the relationship between the invariant line and the slip plane was not specified in the shear matrix [108].

Although the arguments advanced for predicting invariant lines and semicoherent habit planes vary from one model to the next, the results may converge, in agreement with the experimental observations. For example, a habit plane containing a pair of parallel small vectors in good match, plus an invariant line, fulfills the conditions of several different models. If the small vectors define the Burgers vector, which is likely, this habit plane is a $D_I$ interface subject to the supplementary constraint of parallelism of small vectors, as discussed above. This habit plane itself will be an unrotated plane of the transformation [17], since it contains two unrotated directions, the set of parallel vectors and the invariant line. The parallel small vectors may define a tensile axis of a small strain (as implied in many examples [103]). In addition, the habit plane could also be explained from approaches in terms of concepts other than the invariant lines, such as the structural ledge model [27], edge-to-edge matching model [156], discussed in later sections.

Although it is widely accepted that interfaces in many systems contain an invariant line, there is as yet no general consensus as to what the controlling factors are related to the formation of the invariant line. While an observed habit plane may be explained by different models, the conditions in the models usually do not uniquely fix the ORs or the habit planes. The second optimum condition (or Rule II) suggested in the present work also does not fully constrain the $D_I$ interface. It must be recognized, as pointed out by Dahmen and Westmacott [18,103,108], that intermediate states lying between a fully coherent state and a complete long-range free state might be observed in practice. In addition, long-range strains arising from some precipitations, especially in metallic systems (which are possibly associated with invariant line strains), may remain after the precipitates have grown to considerably large sizes. The existence of the long-range strain can be tested by observations of the

surface relief effect associated with precipitates [149–151]. Nevertheless, how the residual long-range strain might constrain the remaining degree of freedom in determining the $D_I$ interface remains to be an open question.

### 6.4. Structural ledge model

The structural ledge model, proposed by Aaronson and colleagues [27–29], offers an effective approach to understanding some observations of irrational habit planes. In contrast to models that rely heavily on vector and matrix algebra, the structural ledge model is mainly based on a graphical analysis. The clear and amenable pictures from the model provide great help for many readers in visualizing why some interfaces tend to have irrational orientations, and have been adopted in several well-known books [11,157]. In the original proposed model, applied to fcc/bcc system, the conjugate planes ($\{1\,1\,1\}_f$ and $\{1\,1\,0\}_b$) are assumed to be parallel [27]. The habit plane is then defined by a vector (in-plane) lying along a row of good matching "patches" within the parallel planes, and a second vector (the terrace vector) lying along a row of good matching "patches" crossing different layers of the set of parallel planes. The latter vector thereby defines the structural ledges. While the terrace vector is fixed for a given OR, its combination with different in-plane vectors leads to the prediction of various possible irrational habit planes. The habit planes in different systems have been explained by this model [19,27,158]. Van der Merwe et al. [78,79] conducted a detailed energy analysis of interfaces containing structural ledges. In describing the accommodation of misfit by structural ledges, they proposed a cancellation criterion, i.e. the misfit in the terrace is cancelled by the "pattern advance" associated with the step, and were able to justify the occurrence of some stepped interfaces in terms of the minimum energy requirements.

The graphical method of the structural ledge model is similar to the O-lattice construction in 2D, since both involve overlapping of a pair of rational planes from different lattices. As recognized by Hall et al. [153], the center of each good matching "patch" lying in the plane is located at an O-point. While a 3D O-lattice is formed by interpenetration of two 3D lattices, the good matching "patches" in different planes in the structural ledges are equivalent to a set of planes of 2D O-lattice stacked according to the in-plane translation of the crystal points in different pairs of planes [24,159]. In such a construction, the misfit between the spacing of conjugate planes e.g., $\{1\,1\,1\}_f$ and $\{1\,1\,0\}_b$ in an fcc/bcc system, is neglected. By applying the standard O-lattice translation formula [37], one can also determine the terrace vector $\mathbf{d}_0$, [24] which connects the O-point at the origin to the shifted O-point (or shifted origin) at the center of the nearest good matching "patch" in the subsequent plane. It has proved that the misfit associated with $\mathbf{d}_0$ is simply the misfit ($\Delta d$) between the interplanar spacing of the conjugate planes in its normal direction $\mathbf{k}$(unit vector), as related by Eq. (3), i.e. $\mathbf{d}_0 = -\mathbf{T}^{-1}(\Delta d\mathbf{k})$ [24,159]. This result is understandable, since

[24] The terrace vector $\mathbf{d}_0$ was called step vector in a previous publication [24]. It is more properly called a terrace vector, and the step vector is differently defined in this paper.

if the misfit $\Delta d$ is zero, $\mathbf{d}_0$ will define a true invariant line, i.e. the terrace vector will lie along the invariant line, as also noted by different authors [160,161]. If $\Delta d$ were neglected, as in the structural ledge construction, a line along $\mathbf{d}_0$ would define a row of good (in-plane) matching "patches". It is recognized that structural ledges effectively play a role in the compensation of the interfacial misfit [159], but the tacit assumption that misfit dislocations can be replaced by structural ledges should be exercised with caution. Since $\mathbf{d}_0$ is unique, one cannot find another set of structural ledges to replace the remaining dislocations (unless an irrational invariant plane, or a $B_I$ interface, is possible in the system).

In the consideration of the structural ledge model or the cancellation criterion, the misfit normal to the terrace is either neglected or treated separately. In practice, this part of the misfit may be present in different forms. The possibilities include (1) planes remain parallel and meet at the steps with the misfit strain in the form of a long-range elastic strain; (2) the misfit strain is relaxed by an additional set of dislocations; or (3) a small rotation is introduced to meet the geometric condition for the planes matching at the steps. While the second possibility has been suggested by different investigators [28,79], the structures corresponding to the cases (1) and (3) may consist of a single set of dislocations. In the early growth stage of a plate, the misfit between the parallel close packed planes might be accommodated elastically. Then, the dislocation free direction may be defined by the terrace vector, or a forced invariant line. The residual long-range strain field associated with the forced invariant line at opposing faces of the plate may cause a spontaneous rotation as the particle thickness, so that the close packed planes from the two phases can exactly meet in an edge-to-edge fashion [162]. A small rotation has been allowed in recent extensions of the structural ledge model, so that the corresponding habit plane contains a single set of dislocations along the invariant line [29,159]. In practice, cases (1) and (3) may both occur, for small and large particles respectively. An intermediate state between the two extreme cases might also occur for particles of transitional sizes.

The vector connecting the good matching "patches" lying in the conjugate planes may or may not be a principal O-lattice vector, $\mathbf{x}_i^{\mathrm{O}}$, as pointed out by Ecob and Ralph (in terms of a unit vector of the O-lattice) [36]. If an $\mathbf{x}_i^{\mathrm{O}}$ is chosen for determining the habit plane in the structural ledge model, as was done by Hall et al. [153] in a study of an fcc/bcc system, the interface is then determined by $\mathbf{x}_i^{\mathrm{O}}$ and by $\mathbf{d}_0$. Such an interface can be expressed by $\Delta\mathbf{g}_{\{22-4\}\mathrm{f}}$, which is the $\Delta\mathbf{g}$ associated with planes normal to $\mathbf{k}$ and $\mathbf{b}_i^{\mathrm{L}}$, i.e. $\{22-4\}_{\mathrm{f}}$ in an fcc/bcc system. When the O-lattice is a point lattice, $\Delta\mathbf{g}_{\{22-4\}\mathrm{f}}$ does not define a principal O-lattice plane. If a particular rotation around $\mathbf{x}_i^{\mathrm{O}}$, which presumably remains unrotated, is added to let the conjugate planes to meet at the steps of the O-line habit plane, the OR will become close to the condition required by Rule II. The rotation seems to cause the formation of the invariant line, as the remaining interplanar misfit is now removed. However, in the strict mathematic sense, the rotation may also slightly change the positions of the good matching patches, so that $\mathbf{d}_0$ does not give an invariant line direction. Nevertheless, when both $\Delta d$ and rotation are small, the rotated OR could be very close to the condition for a $D_I$ interface and the dislocation structures from the two

approaches should be similar. Then, the $\Delta\mathbf{g}_{\{2\,2\,-4\}\mathrm{f}}$ becomes one of the parallel $\Delta\mathbf{g}_{\mathrm{I}}$'s normal to the habit plane.

Even if the rotation is not allowed, the resultant habit plane from the two approaches might also be similar when the conjugate planes have similar spacing. Fig. 12 can be used to illustrate this point. In this figure, the diffraction spots of the conjugate planes are not distinguishable. Thus one may consider this OR to be the K–S OR, i.e., no rotation between the spots for the conjugate planes. At the same time, the association of the habit plane with parallelism of the measurable $\Delta\mathbf{g}_{\mathrm{P\text{-}I}}$'s is obvious. If the OR were strictly the K–S OR, the two $\Delta\mathbf{g}_{\mathrm{P\text{-}I}}$'s would be almost parallel to each other. The $\Delta\mathbf{g}_{\{2\,2\,-4\}\mathrm{f}}$ vector, which must be normal to the plane suggested by the structural ledge model, is not visible from the figure, but it should also lie approximately in the direction of the nearly parallel $\Delta\mathbf{g}_{\mathrm{P\text{-}I}}$'s, as can be derived from the figure by a linear relationship. Therefore, the habit plane can be described by either the (nearly) parallel $\Delta\mathbf{g}_{\mathrm{P\text{-}I}}$'s or $\Delta\mathbf{g}_{\{2\,2\,-4\}\mathrm{f}}$. The fcc/bcc systems with the lattice parameter ratio ($a_{\mathrm{f}}/a_{\mathrm{b}}$) near 1.25, as in Fig. 12, have been studied by many investigators [17,22,23,27,28,153]. However, these systems are special. A recent systematic study of this system [98] indicated that when the lattice parameter ratio is close to 1.25, the Burgers vectors for all possible O-lines always lie in the conjugate planes. In this study, the conjugate planes have been defined by the pair of the most closely oriented $\{1\,1\,1\}_{\mathrm{f}}$ and $\{1\,1\,0\}_{\mathrm{b}}$, since usually none of such related planes can be parallel in the O-line condition. If a rational OR (in which the conjugate planes are parallel) near an O-line OR is taken as the input for the structural ledge model, and the habit plane resulted from the structural ledge model, $\Delta\mathbf{g}_{\{2\,2\,-4\}\mathrm{f}}$, could be close to the parallel $\Delta\mathbf{g}_{\mathrm{P\text{-}I}}$ vectors at the O-line OR. As the value of $\Delta d$ approaches zero, which occurs when $a_{\mathrm{f}}/a_{\mathrm{b}} = 1.225$, the angle between $\Delta\mathbf{g}_{\{2\,2\,-4\}\mathrm{f}}$ and the $\Delta\mathbf{g}_{\mathrm{P\text{-}I}}$ vectors will vanish. Then, all $\Delta\mathbf{g}_{\mathrm{I}}$'s, including $\mathbf{g}_{\{2\,2\,-4\}\mathrm{f}}$, in the zone axis of $\mathbf{b}_i^{\mathrm{L}}$ will be normal to the interface that obey Rule II (Figs. 6 and 12). In this special case, many O-line habit planes are possible. Because the special lattice parameter ratio permits different $\mathbf{x}_i^{\mathrm{O}}$ to be solved from all of the three in-plane Burgers vectors [98], three O-line habit planes will coexist, as resulted from the structural ledge model. When the O-line is inclined to the conjugate planes, any interface containing the O-lines would be strictly consistent with the descriptions of either the structural ledge model or Rule II. For a system with a more general lattice parameter, the OR for the O-lines corresponding to each Burgers vector is distinct. This is different from the structural ledge model, which can predict different habit planes for the same OR, because the model virtually neglects the effect of $\Delta d$.

Despite some limitations due to simplification and special requirement, the concept of the structural ledge model has drawn attention to the distribution of good matching patches as a critical factor in the structures of a singular interface and an important role of steps on enhancement of overall good matching in the interfaces. The energetic compromise between the introduction of steps and minimization of interfacial misfit has been confirmed by van der Merwe et al. in a more sophisticated energy analysis [78,79]. This useful concept has been extended recently in construction of the good matching regions under more general conditions, as discussed in the following section.

### 6.5. Near-coincidence site model

Liang and Reynolds proposed the model of near-coincidence sites (NCS) [33]. Near-coincidence (the nearest atomic neighbor distance <15%) is another term for good matching, where atomic matching rather than lattice matching is usually used. It has been suggested in the NCS model that the OR should lead to the greatest areal density of the NCS, and that the habit plane should contain the greatest area of continuous NCS [33]. A unique advantage of the NCS approach is that it is easy to adopt, since calculation of the NCS only requires input of the coordinates of the atoms in the joining phases, and does not require knowledge of lattice correspondence and matrix operation. In addition, the calculation is greatly facilitated by advanced computer software. The NCS approach has been followed by a number of recent investigations [163–167], confirming the association of the observed habit plane or facets with densely distributed NCS.

While the principle behind the NCS model is essentially inherited from the structural ledge model, the applicability range of the new model is greatly extended. Unlike the structural ledge model, a 3D distribution of the NCS can be examined without being subject to the selection of the terrace planes [164], although a pair of conjugate planes can be suggested based on the high areal density of the NCS for a given OR. Thus, the limitation of parallelism of any planes in the OR in the structural ledge model can be removed. While the structural ledge model was mainly applied to the primary preferred state, the NCS model is in principle applicable to any system since the continuity of the NCS in an area (within an NCS cluster) can be evaluated either on a strict one-to-one basis (for a system in primary preferred state) or on a basis in which only a fraction of the regularly distributed points can be regarded near coincident (for a system in a secondary preferred state). On the one hand, the structural ledge model provides a dislocation description of the interface, but the defects between the NCS clusters are unidentified. On the other hand, the validity of the NCS model is not limited by the assumption of the Burgers vectors lying in the terrace plane suggested in the structural ledge model.

A relationship between the NCS model and the O-lattice model will help to determine the defects between the NCS. Both the NCS and the O-lattice are based on the same construction interpenetrating two lattices in 3D. The O-lattice applies when the pattern of good and poor misfit is periodic, while the NCS model is applicable to any situation. However, when the NCS model is applied to investigate a singular interface, which must contain a periodic structure, the two models should yield similar result. A complete description of the regions between the adjacent NCS clusters must be analyzed according to the preferred state. Consider first the case in which a strict continuity of a one-to-one correspondence, as described by the primary preferred state, is sustained within an NCS cluster. When the misfit strain is general, i.e. $\mathrm{rank}(\mathbf{T}) = 3$, each good matching region must be centered at an O-point, and the volume near the O-point will contain dense NCS. Whether the NCS within an O-cell are considered continuous depends on the criterion for evaluating coincidence, since possible atomic steps within the cell may be associated with a relatively large local misfit. If the NCS clusters are confined within a certain

close packed plane, the regions between the adjacent NCS clusters within an O-cell may be separated by steps, or structural ledges. In this definition, the NCS clusters connected by the steps only repeat within an O-cell. (When the OR permits the formation of an invariant line strain, the clusters connected by the structural ledges can repeat indefinitely, provided that the terrace vector is parallel to the invariant line.) If various steps are allowed within an NCS cluster, a one-to-one relationship can be established between each NCS cluster and a primary O-point. In this definition, the NCS clusters can repeat indefinitely, as the O-lattice points. If an interface is determined by passing the adjacent NCS clusters, the interface is likely (but not necessarily) parallel to a principal O-lattice plane, since the adjacent O-points are usually connected by principal O-lattice vectors. Then, each region between a pair of adjacent NCS clusters will contain a primary dislocation, whose configuration can be determined by the intersections of O-cell walls by the interface plane (Eqs. (12)–(13)). In general, however, if the continuity of NCS within a cluster of a considerable area is evaluated on a one-to-one basis, the regions between the adjacent NCS clusters may possibly contain: (1) a step without a misfit dislocation characteristic, i.e., a typical structural ledge; (2) a primary misfit dislocation only; (3) a primary misfit dislocation associated with a step; (4) a knot of several primary misfit dislocations if the adjacent NCS clusters are not connected by a principal O-lattice vector; or (5) a highly mismatched band that cannot be defined by any primary misfit dislocation (then a secondary preferred state should be considered).

If missing points are allowed within an NCS cluster (e.g, Fig. 12c in [33]), then the identification of the defects in the regions between the NCS cluster are more complicated, depending on the preferred state. If continuous NCS on the one-to-one basis can be identified over an area whose dimension is at least several atomic distances, then the regions of poor matching, missed in the NCS configuration, may contain a set of primary dislocations. The single flat NCS cluster that defines the habit plane in a Ni–Cr alloy by Liang and Reynolds (in Fig. 12c in [33]) contains many narrow continuous NCS bands. The example for Rule II is also taken from this alloy system. The index for the observed habit plane in this system is usually expressed as $(1\,{-2}\,1)_{\mathrm{f}}$ [17,43] at the K–S OR. The parallel $\Delta\mathbf{g}$'s in the zone axes of $[1\,0\,{-1}]_{\mathrm{f}}\|[1\,1\,{-1}]_{\mathrm{b}}$ in Fig. 12 are approximately perpendicular to $(1\,1\,1)_{\mathrm{f}}$, indicating that their directions are close to $(1\,{-2}\,1)_{\mathrm{f}}$. The calculated O-lines (a single set of dislocations) in the habit plane for this system have the spacing of 0.97 nm [24], which agrees with the distance ($\sim$1 nm) between the narrow NCS bands within the flat cluster. Chen and Reynolds [43] have considered the neighboring NCS in the $(1\,{-2}\,1)_{\mathrm{f}}$ plane to form a 2D CCSL cell, and virtually analyzed the habit plane with the secondary misfit strain. Liang and Reynolds [33] have also neglected the defects between the flat clusters of NCS, but expected defects between the broad and flat NCS. According to the description of the O-lines, the periodic narrow bands of NCS can be spread endlessly in the habit plane approximately parallel to $(1\,{-2}\,1)_{\mathrm{f}}$, normal to the parallel $\Delta\mathbf{g}$'s (Fig. 12). The reason for the limited size of the flat NCS is that the input OR for the NCS construction is very close but not identical to the O-line OR. In this situation the unit cell of the O-point lattice becomes strongly anisotropic,

elongated towards the small misfit (near invariant line) direction. According to the O-lattice model for the rational OR, the border of the flat clusters should consist of segments of dislocations of different Burgers vectors. However, the real OR may have fulfilled the invariant line condition [17], though the measurement uncertainty may cause the discrepancy in the OR, so that this complicated dislocation structure is not present in the habit plane. As can be expected, if the O-line OR (0.4° from the K–S OR) were input for the NCS construction, one would obtain the broad flat shape of periodic NCS clusters over an unlimited area. Liang and Reynolds [33] have attempted to modify a few factors in order to extend the NCS region in $(1\,{-}2\,1)_f$, but none of the modifications is effective. Their introduction of dislocations has caused a variation of the distribution of the NCS. According to the O-lattice construction, the dislocations must be located at the poor matching regions (Figs. 2 and 4) and the existence of the dislocations should not alter the distribution of the O-lattice elements.

The same consideration can be extended to systems with large lattice misfit. In this case, a "unit cell" of the NCS will consist of missing points, or crystal lattice points that are not near coincident. If each near coincidence site is forced to become coincident, the unit cell of NCS will be equivalent to a unit cell of the CCSL. One face of the cell likely defines the 2D CCSL for a secondary preferred state. In such a system the region between the adjacent NCS clusters possibly contains (1) a step which is either associated with a secondary dislocation (d-step) or not (when crossed by a secondary invariant line); (2) a secondary dislocation which is not associated with a step; (3) a band of highly mismatch that cannot be defined as a single misfit dislocation. Various methods for determining near coincident site lattice (**NCSL**) have been suggested in literature [40,43,132,168]. The description of the interfacial structure from the model depends on the selection of the unit cell. If the points in the adjacent NCS clusters are chosen to form a unit cell of the NCSL, the defects discussed above would be contained within an NCSL cell. Selection of an NCSL model implies a secondary preferred state in the interface. The periodicity for this case is considered in two levels in the present approach. An NCSL or CCSL should yield a small unit cell of 2D CCSL that is consistent with the nearest neighbors of NCS within a cluster in a terrace plane, rather than across the clusters. The unit cell of the secondary O-lattice consists of points (or lines) from different NCS clusters. The defect structure is determined for the secondary O-lattice model.

Depending on the criterion for the coincidence, the steps could be included within or excluded from an NCS cluster. When an OR following Rule III is taken as the input for the calculation of the NCS, the corresponding interface will contain periodic and endless rows of NCS (with steps being allowed in the rows). When a deviation from the ideal OR is carried in the input data for the OR, the habit plane determined by passing the adjacent elongated clusters spread in a rather large area should give a good approximate orientation of the habit plane defined by Rule III. Rule III apparently agrees with the OR between $\delta$ and $\gamma$ in a 718 alloy in the diffraction pattern provided by Liang and Reynolds (Fig. 1 in [33]). The plane passing the adjacent NCS clusters in Fig. 16 in [33] should be normal to a group of parallel

$\Delta\mathbf{g}$'s, but the experimental data was not sufficiently precise for a strict comparison. [25] Unlike the structural ledges which are not associated with discontinuity to the primary preferred state, the steps with respect to the terrace plane parallel to the 2D CCSL representing the secondary preferred state should always be treated as defects no matter whether the steps are included within an NCS cluster or not.

It must be recognized that the border between NCS clusters in an interface in the primary preferred state may also contain a step associated with a dislocation. According to the terrace plane with respect to the O-lattice structure, we may classify the steps into two types. The first type of terrace plane (or facet) is parallel to a principal O-lattice plane, which contains periodic NCS clusters. The misfit in terrace planes is accommodated by the dislocations lying in the principal O-lattice plane. The dislocation located at a step connecting the adjacent NCS clusters at different levels of the terraces must have a Burgers vector that accommodates the misfit associated with the riser of the step. These steps do not have regular spacing; their distribution depends on the interfacial curvature. They are often called growth ledges because their position change effectively causes the volume change between phases. The second type of terrace planes is parallel to a pair of conjugate low index planes, and each terrace plane contains a single O-element at the center of an NCS cluster. The average interface is parallel to a principal O-lattice plane, having a unique orientation. If the conjugate planes are parallel and have different interplanar spacing, the Burgers vector associated with the dislocations at steps must be different from those associated with the dislocations between the clusters in the conjugate planes. This type of step is similar to the misfit compensation ledges suggested by Furuhara et al. [19], but our conclusion on the Burgers vector is different from theirs. In their model, the introduction of the steps effectively changes the average interface orientation, but does not affect the Burgers vector of the dislocations. Our starting point is that a long-range strain free interface containing periodic dislocations must have a fixed orientation. It is determined by the relaxation of specific system whether an irrational singular interface will be smooth in microscopic scale (containing fine atomic steps), or will be decomposed into a sharp step-terrace structure, where each step is associated with a dislocation. The spacing and the Burgers vector of the dislocations are not affected by the ways of decomposition. The main difference is in the step spacing. The spacing in the smooth interface depends only on the inclination of the interface and the crystal structures, and that in the sharply stepped interface depends only on the dislocation spacing. This is in contrast to the d-step structure, for which the OR must allow the dislocation spacing to coincide with the step spacing determined by the inclination of the habit plane.

While the NCS structure can be described in the framework of the O-lattice, the criteria for the selections of the OR and the habit plane are not completely equivalent. Local planar density of an NCS cluster is an important concern in the NCS

[25] The experimental evidence supported the conclusion that the habit plane must contain the conjugate direction of $[1\,-1\,0]_\gamma$, but the reported average habit plane is $(1\,1.05\,1.03)_\gamma$, inconsistent with the above result.

model, which suggests an OR to produce *the greatest areal density of the NCS* in some conjugate planes [33]. This simple criterion essentially confines the terrace plane, but the OR in the plane is not precisely fixed, since the maximum density of NCS within a local area can always be fulfilled with the OR varying in a small range. A high density of NCS implies small unit cells. This criterion effectively suggests a lattice correspondence for the interfacial strain. The habit plane suggested by the NCS model should contain *the greatest area of continuous NCS*, but maximization of the area is not considered in the optimum condition for the OR [33]. The areal density of the NCS within a cluster and the area of a single NCS cluster can provide an indication of a degree of interfacial misfit. These conditions are equivalent to the considerations made for the preferred state and for the shape of an O-element. While these aspects are important in optimization of the OR and IO, the present approach emphasizes the singularity and periodicity of the O-elements in any singular interface. Satisfaction of either the second optimum or third condition effectively ensures each NCS cluster (including steps) to have an unlimited size in one direction, and the endless NCS bands to spread periodically in the singular interface.

It is an advantage to combine the NCS construction with the O-lattice calculation for singular interfaces. On the one hand, the NCS construction opens a transparent 3D view of the misfit distribution, which greatly helps in visualizing the misfit distribution in an irrational habit plane. Though the O-lattice can also be illustrated graphically, it is usually limited to 2D in a rational plane (Figs. 2 and 4). For more complicated cases, the O-lattice is determined through a "black-box" of a matrix calculation. In addition, the "unit cell" of the NCS within a cluster, constructed at an observed OR, can effectively suggest a proper lattice correspondence for the O-lattice calculation. On the other hand, the uncertainty in the OR and IO measurements may restrict the correct distribution of the NCS clusters over a large area. The $\Delta\mathbf{g}$ parallelism rules can guide the selection of an appropriate OR that permits endless bands of NCS. The dislocation structure between the endless NCS bands is readily determined from an O-lattice calculation. A strict 3D distribution of the O-elements is often unavailable when the singular interface contains an invariant element. This drawback can be compensated by a construction of 3D NCS, since the NCS distribution remains irrespective of the periodicity of the clusters. The distribution of the 3D NCS may also provide useful hints for suggesting other facet(s) than the O-line habit plane [165]. The possible dislocation structure in these facets may be further derived through an O-lattice analysis.

### *6.6. Row matching model*

The row matching concept was originally developed from investigations of epitaxial ORs. An epitaxial OR is developed between a substrate and a deposited film. For the importance of film technology in modern industry, this type of ORs has been extensively studied, leading to suggestions of various criteria, such as the matching of close packed atomic rows (the "lock-in" model) [70,169], or the matching of close packed directions [100], to explain the observed epitaxial orientations. Van der Merwe [170] has proposed that energetically favorable epitaxial configurations occur

when the matching of sets of parallel atomic rows from different lattices is realized. Using a static distortion wave model, Fecht [70] has shown that energy cusps are characterized by commensuration of reciprocal vectors defined in the interface, i.e. normal to the atomic rows. The same approach has been applied to interfaces between precipitates and matrix. For example, Shiflet and van der Merwe [79] have found that energy minima correspond to row matching for the N–W or K–S OR between fcc and bcc phases, when their lattice parameter ratio meets the requirement of the row matching. In his review article and book, Howe [12,15] also considered the atomic row matching as a criterion in analysis of low energy interface and the associated ORs in general crystalline interfaces.

The interface between a substrate and a deposited film is usually parallel to low index planes in both lattices. This constraint is equivalent to Rule I. The row matching criterion is equivalent to the condition that an interface must follow Rules I and II or Rules I and III simultaneously. While Rule I ensures rows of dense points to lie in the interface, Rule II or Rule III renders exact row matching. This relationship can be explained by using the property of Moiré planes. Consider first a $C_{\mathrm{I}}$ interface, which follows Rules I and II. In the zone axes defined by the Burgers vectors for the O-lines in the interface, one finds at least two sets of principal planes. One set of planes, $\mathbf{g}_{P1}$, is parallel to the interface. The $\Delta\mathbf{g}_{\mathrm{P\text{-}I1}}$ vector associated with this $\mathbf{g}_{P1}$, is parallel to $\mathbf{g}_{P1}$, normal to the interface. The $\Delta\mathbf{g}_{\mathrm{P\text{-}I2}}$ vector associated with the other set of planes, $\mathbf{g}_{P2}$, is also normal to the interface, as required by Rule II. According to the property of Moiré planes (Fig. 5), the planes related by $\Delta\mathbf{g}_{\mathrm{P\text{-}I2}}$ must meet in an edge-to-edge fashion in a Moiré plane normal to $\Delta\mathbf{g}_{\mathrm{P\text{-}I2}}$. On the other hand, the $\mathbf{g}_{P2}$ planes only meet the interface plane $\mathbf{g}_{P1}$ at every row of dense points along the Burgers vector for the O-lines, and their related planes in the other lattice are in the same situation. Consequently, the planes related by $\Delta\mathbf{g}_{\mathrm{P\text{-}I2}}$ should meet each other at every row of dense points along the Burgers vector in the interface. Therefore, the requirement of Rules I and II to be followed by an interface plus the condition of parallelism of two Burgers vectors is entirely consistent with the criterion of row matching.

While satisfaction of two rules is expected to define a shape energy minimum, its application is limited to systems in which the lattice constants bear a special relationship between each other. In a more general system, few parallel rows can be found in good matching condition in an interface parallel to low index planes. Kelly and Zhang [32,156] have extended the association between the row matching and low energy to the case of stepped interfaces using a model of edge-to-edge matching. They found that the probability of row matching in a general system would be increased by introducing steps to the interface. The interface plane is then determined by two directions: the vector connecting the matching rows in different planes and the direction of the matching rows, along parallel close packed or nearly close packed directions. Their model still requires row matching condition to be fulfilled as far as possible in the interface, while the edge-to-edge matching criterion is a necessary condition for (approximate) row matching. They also require that the matching planes should have almost identical interplanar spacing. In a systematic manner, they could select the candidates of the matching pairs according to the

interplanar spacing and suggest the preferred ORs, without examining the degree of in-plane misfit [156].

It is a crucial condition for the matching planes to have almost identical interplanar spacing. Consider first an ideal case, in which the parallel principal planes from different lattices have identical interplanar spacing, in the OR that a pair of Burgers vectors from different phases lie parallel to define the direction of the matching edges. This condition implies that the normal of the parallel principal planes defines an invariant line in reciprocal space, and that the parallel Burgers vectors are normal to this invariant line. This is an O-line condition, which ensures a group of $\Delta\mathbf{g}$'s to lie parallel. Though the edge-to-edge matching condition for the parallel planes can be fulfilled in any interface inclined to these planes, row matching can only be achieved in the interface normal to the parallel $\Delta\mathbf{g}$'s, because edge matching in common principal Moiré planes is the necessary condition for row matching. This argument can be explained using Fig. 6b, where knots of lines in the same lattice represent the locations of edge-on rows of lattice points. The interface in this figure follows Rule II; its mathematic position is indicated by a dashed and dotted line in the figure. Three sets of (edge-on) principal planes from different lattices all meet the edge-to-edge matching condition in the interface, the common principal Moiré planes. However, the related planes usually match at different locations, unless a matching edge coincides with a row of points located in the "mathematic" interface. At each row a plane from different sets must meet. When the interface has an irrational orientation with respect to both lattices, it only contains occasional rather than regular matching rows in its mathematic position. If a local relaxation is allowed, a band of elastically forced matching rows can be formed, and a stepped interface connecting the forced matching rows can be defined. By a rigid graphic method, approximate matching rows can be defined in the orientation normal to the parallel $\Delta\mathbf{g}$'s, as shown by Kelly and Zhang [156], leading to the prediction of the habit plane. Usually, the vectors connecting approximate matching rows will lie in different directions, and the geometric method may bring a certain degree of scattering in the predicted habit plane.

For more general systems, in which the parallel planes from different phases do not have identical interplanar spacing, Kelly and Zhang [156] have permitted a small rotation around the parallel close-packed directions to accommodate small difference in the spacing so that planes can match at the interface. The further condition to fix the habit plane or the OR is that the matching planes must meet at or approximately at matching rows. However, unlike the special case with a rational invariant line in reciprocal space, approximate matching rows do not usually exist. If the interface is normal to a single $\Delta\mathbf{g}_{\text{P-I}}$, the edge-to-edge matching condition only holds for this pair of related planes. Even when a row of lattice points is located at the Moiré plane, this row does not usually match with a row from the other lattice. According to the analysis in Section 4.2, an interface parallel to the single principal Moiré plane will contain at least two sets of dislocations, which also accommodate the misfit between the rows. On the other hand, as explained above, approximate matching rows can be defined in the common principal Moiré planes. Rule II with the supplementary constraint of parallel Burgers vectors offers a simple restriction to

fix the OR and the habit plane, the latter of which contains steps along the Burgers vectors. The $\{1\,1\,2\}_f$ habit plane in an fcc/bcc system near the K–S OR is a typical example of Rule II (Fig. 12). The edge-to-edge model [156] explains this habit plane in terms of good matching rows at the edges (the steps) where nearly parallel conjugate planes meet (Fig. 5 in [156]). In contrast, good matching regions in terrace planes are essential in the structural ledge model [27,28]. Similarly, the greatest planar density of NCS in the parallel planes is preferred in the NCS model [33]. Nevertheless, given the same OR in the O-line condition with parallel Burgers vectors, the habit plane orientations from different models should be consistent. In a real interface, every row in the $\{1\,1\,2\}_f$ habit plane may become an elastically forced matching row [91].

However, the row matching model, or edge-to-edge matching model, has ignored the possible defects in the matching rows. The essence of interfacial structure considered from the O-lattice approach is the dislocation structure. Observations of dislocations in numerous interfaces tend to support that it is the local elastically forced point matching, instead of row matching, that controls the preferred state. As stated earlier, a position of good atomic matching must be defined by three sets of independent principal Moiré planes. An interface defined by the row matching criterion is parallel to only two sets. It must contain some regions in poor lattice point matching along the matching rows. The graphical method of the NCS model is particularly helpful for one to see how point misfit is distributed within each matching row, and how good matching regions in different matching rows are connected by an (approximately) invariant line in a $\{1\,1\,2\}_f$ habit plane (Fig. 12 in [33]). Though the dislocations in the $\{1\,1\,2\}_f$ habit plane were not observed probably because of the small spacing ($\sim$1 nm [24]), the direction of the invariant line, as the axis of a lath precipitate, contained in the $\{1\,1\,2\}_f$ habit plane in a Ni–Cr alloy has been reported repeatedly [17,43]. In general, the direction of the invariant line will vary with respect to the matching row, depending on the details of the misfit strain field. Theoretically, misfit displacement of any vector in the interface must lie parallel to the direction of the matching row, i.e. the Burgers vector of the dislocations. Therefore, the row matching condition may not be destroyed by the development of the dislocations.

The row matching criterion is also applicable to systems in secondary preferred states. The above analysis can be extended to these systems, but some modifications should be added. One would also expect that in this case the matching rows will contain dense CCSL points, and that may or may not be parallel to rows containing the densest points in either crystal lattice. Exact row matching should be observed from an interface when Rule I and Rule III are followed by the interface. Such a step free interface must be normal to $\mathbf{g}_{\text{P-}\alpha\text{CCSL}}$ and $\mathbf{g}_{\text{P-}\beta\text{CCSL}}$, plus at least one $\Delta\mathbf{g}$. Because of linear combination, the interface should be normal to a group of parallel $\Delta\mathbf{g}$'s, including $\Delta\mathbf{g}_{\text{P-II}}$'s and restored $\Delta\mathbf{g}_{\text{P-CCSL}}$'s. It is often convenient to choose a restored $\Delta\mathbf{g}_{\text{P-CCSL}}$ associated with a low index plane for describing the row matching condition. As explained for a $C_I$ interface, the planes related by this $\Delta\mathbf{g}_{\text{P-CCSL}}$ must meet at the interface at rows of dense CCSL points. In contrast to a $C_I$ interface, not every parallel row will find its counterpart in the other lattice, because the one-to-one

nearest neighbor principle is not applicable to the related planes in this case. Usually, only a fraction of parallel rows may match regularly their related rows in the interface parallel to common Moiré planes.

A stepped interface may contain elastically forced matching rows, if it obeys only Rule III, and if the directions of dense CCSL points defined in different lattices are parallel to serve the direction of the matching rows (the step riser). If the interface contains a set of secondary O-lines, the row matching condition can be understood in the same way as the interface following Rule II. However, the steps may be associated with secondary dislocations whose Burgers vector is not parallel to the matching rows. As demonstrated in Figs. 8c and 14d, the secondary dislocations are defined in the framework of the CDSCL. Unlike the principal planes of crystal lattices, where one finds a row of lattice points at every knot where planes meet, the knots where principal planes in the CDSCL meet do not always define a row of points of crystal lattice. Misfit between the CDSCL does not necessarily cause mismatching between rows in crystal lattices. Instead, the translation of a secondary Burgers vector associated with a d-step effectively causes a shift of the regular partner relationship of near matching from one terrace to the next (Figs. 8c and 14d). On the other hand, despite conservation of the forced row matching condition over the interface, extra (or missing) planes may still be found at d-steps (Fig. 8c). When $\Delta\mathbf{g}$'s are not related by a fixed lattice correspondence, one can always find numerous $\Delta\mathbf{g}$'s in various directions in the same zone axis of the matching rows. The planes related by the $\Delta\mathbf{g}$'s that are not normal to the interface cannot match at the interface, as demonstrated in Appendix A. In particular, because of the relationship defined in the characteristic triangles (Fig. 8d) an extra plane should be associated with every d-step, when the planes related by a non-parallel $\Delta\mathbf{g}_{\Pi}$ are taken into consideration.

The above results illustrated that some particular types of singular interfaces, i.e. those follow Rule II or III with the constraint of parallel rational vectors, can be identified or explained by the row matching criterion or its extended version of edge-to-edge matching. While row matching can be treated as 1D preferred state, it is considered here as a sufficient condition for a singular interface to obtain a structure described in 3D (primary) or 2D (secondary) preferred state. Though evidence from numerous systems can be found to support the requirement of parallelism of two rational vectors of small misfit, this condition is not completely general, since cases that disobey the condition have also been reported [21,22,152]. However, when two low index directions are observed parallel in nearly parallel planes of similar interplanar spacing, the simple model of row matching is convenient for explaining the observations of irrational habit plane and the associated OR. The application range covers systems either in the primary or secondary preferred state, independent of the lattice correspondence for describing the misfit strain [156].

### *6.7. General remarks*

A common implication of all approaches reviewed above is that the observed ORs and habit planes should correspond to low interfacial energy. However, the

determination of the variation of the interfacial energy in the 5D BGP space for a general system remains a challenging task from either a theoretical or experimental perspective. Except for the symmetry approach, all reviewed approaches rationalize the habit plane or facets in terms of some characteristic features in interfacial structures, including the dislocation spacing, net Burgers vector content, an invariant line, good matching patches connected by structural ledges, dense NCS clusters, and (near) matching rows. While the detailed features are different, the results of the models overlap with one another to some extent, because of the shared common principle of optimizing good matching. A simple example in the overlapped zone is a fully coherent interface in a low index orientation (i.e. $A_I$ interface), as it can be interpreted by almost all models. Given an observed singular interface in a more general system, various characteristic features have been proposed by different models. Because the emphases placed by different models and overall constraints applied to a system are not completely equivalent, predictions from the different models may diverge when the characteristic structures suggested by different model cannot coexist in a given system.

A typical example in the overlapped zone is the $(1\,{-}2\,1)_f$ habit plane in a Ni–Cr alloy. This observed habit plane has been explained by the 3D invariant line model [17], structural ledge model [91], near-CSL model [43,92] and its modified version of NCS model [33], extended row matching approach [156], and O-line model [24] or Rule II. In this system the conjugate planes in different lattices have almost, but not exactly, identical spacing (Fig. 12). As discussed earlier, the approaches of the 3D invariant line model [17], structural ledge model [90], and extended row matching approach [156] can apply mainly under this special condition. In addition to the parallel Burgers vectors, another direction to restrict the habit plane in these models is the vector connecting approximately matching rows [156], or is an approximate invariant line, inclined to the conjugate planes. This approximate invariant line can be determined by an intersection point between unextended cones [17] or a line connecting good matching patches [90]. However, if the conjugate planes had exactly identical spacing, the invariant line would become parallel to the Burgers vector. In this case, the 3D invariant line and structural ledge models may fail to identify the habit plane, because a single direction is not sufficient to define a plane. In this special case, the NCS model [33], extended row matching approach [156] and O-line model [24] remain valid, and these models should produce identical predictions of the habit plane with the exact K–S OR. If the conjugate planes have obviously different spacing, these three models are still applicable. The O-line model predicts a rotation between the conjugate planes, with the supplementary condition of parallel Burgers vectors, in the condition that the lattice parameters allow the O-lines to form. With the K–S OR, the NCS (and equivalently the structural ledge model) model will predict an interface containing at least two sets of dislocations [33], and the 3D invariant line model [17] does not produce a true invariant line. If a true invariant line is generated by an in-plane rotation (2D model), the predicted habit plane will contain more than one set of parallel dislocations. However, given an O-line OR as an input, the habit plane containing O-lines can be predicted by the NCS model [33], 3D invariant line model [17], structural ledge model [90] and extended

row matching approach [156]. In other words, characteristic structures suggested by different models coexist in the habit plane containing the O-lines. Under the O-line condition, preferences of different models may still differ, since the O-line solutions are discrete but not unique. For example, areas of good matching patches in the terrace planes should be optimized in the structural ledge or NCS model, dense matching rows may be preferred by the row matching approach, without considering the misfit between lattice points in the interface. The structural ledge model requests that the Burgers vector of the dislocations lie in the terrace planes, but general O-lines are not subject to this constraint.

The O-line structure represents the essence only in one type of singular structures classified in Table 1. The present approach intends to identify singular interfaces with their general features, in order not to lose generality. A general singular interface is characterized by singularity and periodicity; it can be directly identified by the $\Delta\mathbf{g}$ parallelism rules. Any one of the three optimum conditions can be applied independently, so as to rationalize singular interfaces in different systems. For example of an $E_I$ interface, this simple interface is often observed (Table 5), and is accounted for by Rule I. However, it cannot be explained from criteria mainly developed for irrational habit planes, such as the invariant line criterion or the structural ledge model. The candidates for the singular interfaces can be further discriminated by different supplementary constraints, such as parallelism of two vectors of small misfit (as used in row-matching model), or low dislocation density (as applied by parametric models). However, the supplementary constraints are not considered general conditions for singular interfaces. When a supplementary constraint is considered as the prerequisite by a model, it also limits the application range of the particular model.

It is worth noticing two classes of parameters used in evaluating interfacial fit/misfit. While the parametric methods discussed in Section 6.2 addressed the density of defects, as high energy contributors; the graphic methods in NCS and structural ledge models focused on the good matching sites, as low energy contributors. In principle, it is the good matching regions, the low energy features, that bring the overall interfacial energy to a local minimum. When the dislocation spacing is considerably larger than the atomic spacing, it may be valid to assume a homogenous and periodic distribution of misfit displacement between the dislocations, as described in a continuum dislocation theory. It is then reasonable to consider that minimizing the density of interfacial defects is equivalent to maximizing the areas of good matching. However, when primary misfit strain is rather large (towards the fuzzy limit for the primary preferred state), the misfit distribution may not strictly repeat from one dislocation cell to another. The interfacial energy may become very sensitive to the misfit state in the region between the dislocations, rather than be a simple function of the dislocation configuration. This situation can be more prominent in a system in a secondary preferred state, since the interfacial energy is known to depend strongly on the structure in the areas between the secondary dislocations [39,52]. While investigation of interfacial structure in the atomic scale requires using high resolution TEM and advanced modeling [171], misfit distribution and step structure determined using rigid graphic methods can be particularly useful for

investigating systems with large misfit strain. In this case, maximizing good matching regions might become a more effective criterion than minimizing dislocation density. This argument might explain the preference of some ORs, such as the K–S OR over the N–W OR in some fcc/bcc systems, that cannot be explained in terms of the dislocation spacing [24,98].

The models based on good matching criteria usually input the observed ORs, though in principle these criteria may be used to search for the optimum results by allowing the OR to vary. When the OR corresponding to the Rule II or III is typically irrational, systematic and numerical adjustments of the OR, which may involves in a heavy calculation, may not yield the precise OR satisfying Rules. In this aspect, the $\Delta\mathbf{g}$ parallelism rules are particularly practical and simple. However, analysis using the reciprocal vectors alone does not present perceptible features in interfaces. Using the input OR determined from the $\Delta\mathbf{g}$ parallelism rules, one gets the periodic distribution of the NCS in the corresponding singular interface. It is possible to suggest qualitatively the configuration of defects in the singular interface based on the relationships between the singular structures and the $\Delta\mathbf{g}$ parallelism rules, and between the Burgers vectors of dislocations and the $\mathbf{g}$('s) associated with the parallel $\Delta\mathbf{g}$('s). Though intricate task of constructing model lattices may be bypassed at an early stage of an investigation, a more quantitative description of the interfacial structure must be determined by a calculation with a model lattice. This information is often useful for in-depth understanding of various properties of interfaces. An advantage claimed by the models with graphic methods is the avoidance of selecting the lattice correspondence, but a further advantage of the methods is to guide the selection of a proper lattice correspondence with the atomic structure in good matching regions, e.g. in an NCS cluster. When the NCS model is combined with calculation of model lattices, as well as the $\Delta\mathbf{g}$ parallelism rules, one gets the descriptions of a singular interface in the atomic, microscopic and macroscopic scales. The property of Moiré planes provides useful links between the descriptions in the three levels of scales.

## 7. Summary

In this paper we have presented a systematic analysis for precipitation crystallography. While the approach has a strong geometric basis, the suggested discrete singular interfaces help to rationalize the observations of particular OR and IO, rather than their vicinal coordinates. The central hypothesis is that a habit plane or major facet associated with a precipitation reaction is the physical realization of a singular interface whose interfacial energy corresponds to a local minimum in the 5D BGP space. Though the chemical component of the interfacial energy may influence the choice of a specific precipitation crystallography, the structural component of the interfacial energy is considered to be the dictating factor, responsible for a reproducible, and often unique, OR.

The local minima of the structural component can be associated with a characteristic structure of a singular interface. The common characteristics are periodicity

and singularity. The periodicity, in terms of the (primary or secondary) misfit dislocations or structural units, ensures the low energy features to repeat over a variable area in a singular interface. The singularities are specified by one or more of three optimum conditions that require: (i) a singular interface free of interfacial steps, (ii) elimination of dislocations in one direction and (iii) a set of interfacial steps and secondary dislocations in coincidence. Combinations of different optimum conditions, or repeated applications of a particular condition, result in twelve types of possible singular structures. Any array of linear defects, dislocations or steps, in a singular structure must fully accommodate the interfacial misfit in a particular direction. While periodicity exerts the geometric requirement to fix the IO, the singularity imposes the constraint to restrict the OR, which may be further fixed by various supplementary constraints. Though physical basis for these conditions was discussed, the optimum conditions are largely empirical in nature.

Characterizing a singular interface with its structure (the microscopic description) may often be a non-trivial task. It is often much simpler to identify the interface with its characteristic IO and OR (the macroscopic parameters). Several model lattices: the primary or secondary O-lattice, or the CSL, have been applied to establish and to explain the links between the microscopic and macroscopic descriptions of various singular structures. The geometrical condition for an interface to contain a periodic structure is that it must be parallel to a principal plane in one of the model lattices, represented by a measurable $\Delta\mathbf{g}$ vector. The OR of a singular interface must permit this $\Delta\mathbf{g}$ to be parallel to one or more reciprocal vectors to provide the necessary geometric condition for the singularity to be realized in the interface. The parallelism relationships have been expressed by three rules for practical convenience. They are: (I) parallelism of a $\Delta\mathbf{g}$ with a rational $\mathbf{g}$; (II) parallelism of two principal primary $\Delta\mathbf{g}$'s; and (III) parallelism of two $\Delta\mathbf{g}$'s, which applies interfaces in a secondary preferred state. A comparison of these rules with a broad range of experimental results suggests that naturally formed habit planes or facets have a strong tendency to follow one or more of the $\Delta\mathbf{g}$ parallelism rules.

This work also reviewed other major approaches to the precipitation crystallography and discussed their connections with the present one. Some singular interfaces can be rationalized by different models. While the overall conditions proposed by different models can be equivalent in special systems, some prerequisites suggested by other models were taken as the supplemental constraints in the present approach. A common optimum principle governing many models is that a singular interface should exhibit good matching, but quantities for assessing the state of matching are various. The present analysis has followed Bollmann's dislocation description of interfacial structure classified in terms of the preferred state. In common with the division between small and large angle grain boundaries, the distinction between the 3D primary and 2D secondary preferred state has been specially emphasized for providing correct descriptions of the interfacial defects and specified links between the $\Delta\mathbf{g}$ parallelism rules and the singular structures.

The $\Delta\mathbf{g}$ approach can be particularly helpful at the beginning of any investigation before the details of the interfacial structure or lattice correspondence are studied experimentally or theoretically. The $\Delta\mathbf{g}$ approach can be joined with the NCS model

to suggest the proper OR for construction of NCS in a singular interface, and to deduce the possible characteristic features in a singular interface using the relationship between the $\Delta\mathbf{g}$ parallelism rules and the singular structures. However, calculations with an O-lattice model are needed in order to provide a quantitative description of the defects in the singular structure. The structure within an NCS cluster may suggest the proper lattice correspondence for the calculation of the O-lattice.

## Acknowledgements

ZWZ wishes to express her thanks to Professor G.R. Purdy, her Ph.D. supervisor, for valuable advice at the early stage of the investigation, to Drs. S. Ranganathan (Indian Institute of Science) and Y.-P. Lin (GE, Wilmington, US) for valuable suggestions which stimulated this study at the beginning stage, to Dr. A. Godfrey (Tsinghua) and to graduate students in ZWZ's research group for helpful comments on the manuscript, and especially to Mr. F. Ye and Ms. M. Zhang (graduate students) for assistance in plotting a number of figures. She also wishes to acknowledge gratefully the support from the "Cao-Guangbiao Foundation" in the early stages of this work, and from the National Natural Science Foundation of China (Grant No. 59871021 and 50271035). GCW thanks NSERC (Canada) for continued support.

## Appendix A. Interfacial misfit in a simple stepped interface

A simple system is given as an example in this Appendix A to illustrate stepped interfacial structure for the following points: (1) reduction of the overall interfacial misfit by introducing steps; (2) different interpretations of the steps; (3) association of Moiré planes with the interfacial misfit. Fig. 15d has been constructed by overlapping lattices *a* and *b*. For simplicity, there is no misfit in the vertical direction. The lattice misfit along the horizontal orientation is so large that the system must take a secondary preferred state. We have assumed that the 2D lattices repeat in the direction normal to the paper and that there is no (or is a pure expansion or contraction) misfit along this direction, so that each row of lattice points can represent an edge-on plane. Based on this assumption, we have also plotted the reciprocal lattices for lattices *a* and *b* in Fig. 15b. The secondary $\Delta\mathbf{g}$ vectors are surrounded by fine circles. The other $\Delta\mathbf{g}$ vectors have also been drawn for analysis of plane matching in terms of the Moiré planes.

Fig. 15a presents the structure of $CCSL_a$ for the system in Fig. 15d. In constructing the $CCSL_a$ lattice *b* is contracted slightly, while lattice *a* remains unchanged. In the figure each $CCSL_a$ point is indicated by a circle with a center dot. The $CCSL_a$ points are only contained in the alternating horizontal planes. Fine lines have been drawn locally to indicate the $CDSCL_a$. This $CCSL_a/CDSCL_a$ structure belongs to the second case classified in Section 3.4 for occurrence of the d-steps.

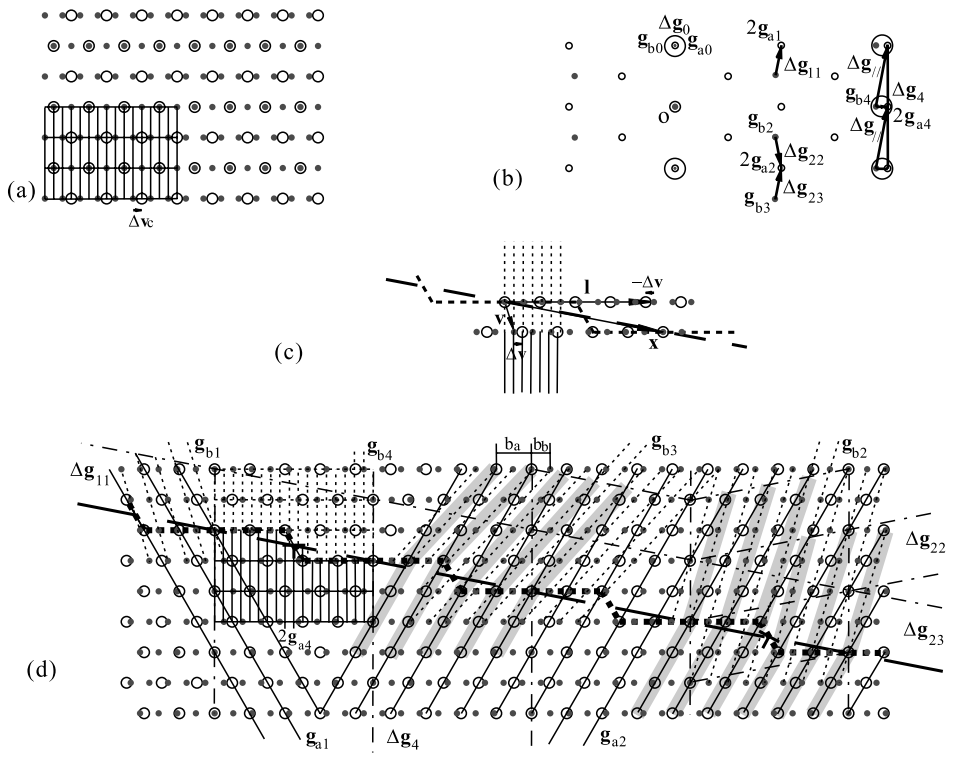


Fig. 15. (a) $CCSL_a$ and $CDSCL_a$ for system consisting of lattice $a$ (open circles) and lattice $b$ (solid circles); (b) reciprocal lattices of lattices $a$ and $b$, where restored CCSL points are enclosed by larger circles; (c) an illustration to show the definition of the step vector, $\mathbf{v}$, and its associated displacement $\Delta\mathbf{v}$ and (d) descriptions of interfacial misfit in the stepped interface (thick dotted line) in terms of d-steps and plane matching.

Namely, the planes containing dense $CCSL_a$ points and the planes containing dense $CDSCL_a$ points are parallel, but the planes actually containing the small displacement vectors that can bring a complete pattern shift do not lie in the same positions as the planes of $CCSL_a$.

The secondary misfit strain in the hypothetical system is a pure expansion in direct space (from lattice $a$ to $b$) along the horizontal direction. In this 1D strain, the plane normal to the deformation direction is virtually a plane of invariant plane. The secondary O-lattice consists of O-plane elements, which can be identified as the vertical rows of good matching points. The 1D secondary misfit strain relationship in the system in Fig. 15 can be defined in a scalar form of transformation

$$2b_{\mathrm{b}} = rb_a, \tag{A.1a}$$

$$r = 18/17. \tag{A.1b}$$

The spacing between the O-planes, or between the O-cell walls that are alternate with the O-planes, can be determined from Eq. (11) or (12) in a scalar form for the "Burgers vector" of $b_a/4$, which is the smallest $CDSCL_a$ vector in this direction:

$$d^{O} = (b_a/4)/(1 - 1/r) = 4.5b_a. \tag{A.2}$$

In this special case, the reciprocal Burgers vector $\mathbf{b}_a^*$ is equal to $2\mathbf{g}_{a4}$, which defines a set of vertical planes of $CDSCL_a$ in Fig. 15a. $d^{O}$ can be given directly as $1|\Delta\mathbf{g}_4|$ [172]. This analytical result helps identification of the periodicity of O-planes or the dislocation spacing with the Moiré plane defined by $\Delta\mathbf{g}_4$, as specified in Fig. 15d. Since all secondary $\Delta\mathbf{g}$'s must be normal to the O-planes, the singular interface suggested by the $\Delta\mathbf{g}$ parallelism rules (I and III) should be parallel to these secondary O-planes, i.e. in the vertical orientation. One will reach the same conclusion from a simple criterion of dense CSL points in the interface. However, a comparison between a horizontal (flat) interface and a stepped interface is the major concern here. This will be discussed below.

### *A.1. Reduction of the overall interfacial misfit by introducing steps*

According to the O-lattice theory any interface inclined to the O-planes will contain a set of parallel secondary dislocations, located at the intersection between the interface and the O-cell walls. An arbitrarily inclined interface is not considered as a singular interface in terms of the dislocations structure, as discussed in Section 3.3. However, singularity in the interfacial structure can be defined when the crystal structures are taken into consideration in the $\Delta\mathbf{g}$ approach. In the example in Fig. 15, the interface is singular when it intersects the O-elements in the crystal plane, e.g. the inclined interface indicated by thick dashed line. Because of the special inclination, the dislocation spacing is identical to the step spacing. Therefore, the interface contains a d-step structure. This singular interface must follow Rule III. It is normal to a set of $\Delta\mathbf{g}_{\parallel}$'s in characteristic triangles in Fig. 15b. It is also normal to a number of restored $\Delta\mathbf{g}_{\text{P-CCSL}}$'s, e.g. $\Delta\mathbf{g}_{11}$ and $\Delta\mathbf{g}_{23}$ specified in Fig. 15b. A stepped interface, having its average orientation normal to a group of $\Delta\mathbf{g}$'s, is indicated by a thick dotted line in Fig. 15d. It can be seen, from the fine vertical lines in left part of the interface in Fig. 15d, that each step is associated with a secondary dislocation with the Burgers vector of the $CDSCL_a$ vector, $b_a/4$. The projected dislocation spacing onto the terrace plane is consistent with the spacing of the O-cell walls, or that of the Moiré planes defined by $\Delta\mathbf{g}_4$.

Consider next the step-free interface parallel to the horizontal row. The spacing between the good matching points in the plane is double of the dislocation spacing from the O-plane model. Although the CDSCLs from different sides of the interface match well in the middle of the good points, it is seen from Fig. 15d that good matching of CDSCLs may or may not define good matching of lattice points. It is the latter that affects the interfacial energy. According to Fig. 15a, it is clear that the smallest $CDSCL_a$ vector in the plane of the $CCSL_a$ is $b_a/2$ rather than $b_a/4$. Though the 1D misfit strain is the same, the secondary dislocation in the flat interface plane should be determined from the Burgers vector of $b_a/2$. Therefore, the dislocation

spacing corresponding to the increased Burgers vector is also doubled, i.e. it becomes $9b_a$. By assuming validity of the simple relationship between the energy and the Burgers vector ($E \sim b^2/D$) for semicoherent interface, one would expect a reduction of energy in the stepped interface, even though the dislocation density in the stepped interface is higher compared with that in the flat interface.

Assuming that the preferred state is determined by the horizontal row of CCSL in Fig. 15a, let us compare the deviation from the preferred state in the flat and stepped interface containing the d-steps. One can compare the maximum interfacial misfit in different interfaces. As a rough indicator, the maximum misfit can be evaluated by half Burgers vector, which is especially true for cases with 1D misfit strain. The maximum misfit is $b_a/4$ in the flat interface, while it is $b_a/8$ in the stepped interface. Clearly, the fraction of good matching points, exhibiting small deviation from the preferred state, should be higher in the stepped interface than that in the flat interface. As also can be seen from Fig. 15d, the nearest NCS clusters are located in the adjacent layer, instead of in the same layer, indicating that the stepped interface consists of more good matching NCS than the flat interface. As a result of improving overall matching condition, the stepped interface is likely preferred to the flat interface in this system.

It must be noted that in this special case of the secondary invariant plane strain, it is impossible to identify a $\Delta\mathbf{g}_{\text{P-II}}$, to which the $\Delta\mathbf{g}_{\parallel}$ vectors in the characteristic triangles corresponding to these steps are parallel. However, as suggested in Section 5.1, we may consider the $\Delta\mathbf{g}_{\text{P-II}}$ connecting $\mathbf{g}_{a0}$ and $\mathbf{g}_{b0}$ as a virtual $\Delta\mathbf{g}$. This $\Delta\mathbf{g}_{\text{P-II}}$ can be considered to be parallel to $\Delta\mathbf{g}_{\parallel}$'s, but the differences between $\mathbf{g}_{a0}$ and $\mathbf{g}_{b0}$ in length and orientation are too small for the $\Delta\mathbf{g}_{\text{P-II}}$ to be noticed. Therefore, a set of characteristic triangles can still be constructed, as in Fig. 15b. The following consideration also helps to understand missing $\Delta\mathbf{g}_{\text{P-II}}$ for $\Delta\mathbf{g}_{\parallel}$'s to be parallel to. The condition of a singular interface being normal to a $\Delta\mathbf{g}_{\text{P-II}}$ is to ensure periodic dislocations in an interface, while the characteristic triangles ensure coincidence of the steps with the dislocations. When a $\Delta\mathbf{g}_{\text{P-II}}$ is a zero vector, it defines an invariant line in reciprocal space. In addition, it is a condition for existence of two sets of O-lines, though the actual secondary misfit strain could be an invariant plane (spacing of a set dislocations approaches infinity as the case in Fig. 15) or invariant line strain (if there is a misfit in the direction normal to the paper in Fig. 15). As discussed in Section 3.3, when periodic O-lines or O-planes exist, the interface that is not parallel to the O-lattice element will contain periodic dislocation. Therefore, when a $\Delta\mathbf{g}_{\text{P-II}}$ is a zero vector, a periodic dislocation structure must exist.

Moreover, when the $\mathbf{g}_{\text{step}}$ in a characteristic triangle is given by either one of the $\mathbf{g}$'s associated with the virtual $\Delta\mathbf{g}$, not only $\Delta\mathbf{g}_{\parallel}$'s but also $\Delta\mathbf{g}_{\text{II}}$'s in a row of characteristic triangles are parallel to one another. All $\Delta\mathbf{g}_{\parallel}$'s have identical length and hence all characteristic triangles become identical. At the same time, it is possible to identify a set of generalized characteristic triangles, whose edges consist of $\mathbf{g}_{\text{step}}$, $\Delta\mathbf{g}_{\parallel}$ and a general $\Delta\mathbf{g}$. The general $\Delta\mathbf{g}$'s in a row of characteristic triangles are also parallel to one another. If the length of $\Delta\mathbf{g}_{\parallel}$'s is identical to that of the parallel general $\Delta\mathbf{g}$'s, as is the case in Fig. 15b, both sets of parallel $\Delta\mathbf{g}$'s may equally define stepped interfaces, whose inclination angles with respect to the terrace plane are identical. Since the stepped

interfaces are symmetrically equivalent, the real stepped interface may contain up-and-down steps, and the average orientation of the singular interface may not be normal to either group of $\Delta\mathbf{g}$'s. If the lengths of these two groups of $\Delta\mathbf{g}$'s are different, the orientation of interface normal to the larger $\Delta\mathbf{g}$'s is closer to $\mathbf{g}_{\text{step}}$. Compared with the interface normal to the other group of $\Delta\mathbf{g}$'s, the density of the steps in this interface is lower, but the maximum misfit is larger. Among the three choices of interfaces normal to different sets of parallel $\Delta\mathbf{g}$'s, the frequent observations of the Pitsch OR [30,66,109] tend to suggest that nature favors low density of steps.

### *A.2. Different interpretations of steps*

Given a singular interface normal to a set of parallel $\Delta\mathbf{g}$'s, the attribution of the $\Delta\mathbf{g}$'s depends on the construction of the $CCSL_a$ in 3D. The interpretation of the steps is affected by the attribution. If we redefine the secondary strain so that $\Delta\mathbf{g}_{13}$ and $\Delta\mathbf{g}_{23}$ become secondary $\Delta\mathbf{g}$'s, then the same stepped interface is normal to all secondary $\Delta\mathbf{g}$'s. Consequently, the same interface, indicated by the thick dashed line, is parallel to a secondary O-plane. If the direction normal to the plane of paper is not free of misfit, then the interface trace is parallel to a secondary invariant line. Namely, the steps are crossed by a secondary invariant line. Though the redefined $CCSL_a$ is not shown, its structure is identical to the lattice $a$ in Fig. 15a. Namely, every horizontal row contains alternating $CCSL_a$ points, and the smallest $CDSCL_a$ vector is now $b_a/2$. The secondary misfit strain is no longer pure 1D expansion. It is characterized by a large shear displacement. While the nominated interfacial misfit according to this CCSL model is low, the secondary misfit in the direction normal to the interface appears rather high.

No matter how the steps are interpreted, the role of the steps is unique: The displacement associated with the step cancels the misfit in the terrace plane, in which the 2D CCSL should be preserved and undistorted as far as possible. The misfit associated with a particular step is analyzed in Fig. 15c, where vector $\mathbf{v}$ is the step vector, and $\mathbf{l}$ is a vector lying in the terrace plane. The vectors $\mathbf{v}$ and $\mathbf{l}$ are related by $\mathbf{x} = \mathbf{v} + \mathbf{l}$, with $\mathbf{x}$ connecting the nearest good matching points in the adjacent terraces. As can be seen from the figure, the displacements from the nearest neighbors associated with $\mathbf{v}$ and $\mathbf{l}$ respectively are identical in length ($|\Delta\mathbf{v}| = |\Delta\mathbf{l}| = 4b_a/17$), but opposite in direction. Consequently, no net displacement is associated with $\mathbf{x}$. If $\Delta\mathbf{v}$ and $\Delta\mathbf{l}$ are determined from the secondary misfit strain, $\mathbf{x}$ should define a secondary invariant line. This straightforward interpretation of $\mathbf{x}$ corresponds to the redefined $CCSL_a$, whose structure is identical to lattice $a$. However, when the $CCSL_a$ in Fig. 15a is taken as the reference for defining the secondary misfit strain, only $\Delta\mathbf{l}$ can be determined by the secondary misfit strain, but $\Delta\mathbf{v}$ is a restored CDSCL vector. Its form in the constrained state is $\Delta\mathbf{v}_c(= b_a/4)$, as indicated in Fig. 15a. The cancellation condition requires the Burgers vector, $\mathbf{b}_s^{\text{II}}$, for misfit dislocations associated with the d-steps be identical in length but opposite in direction to $\Delta\mathbf{v}_c$. The secondary misfit associated with $\mathbf{v}$ is $d(\mathbf{v}) = (b_a/4)/17$, as can be seen from the displacement of the DSCL at the point defined by $\mathbf{v}$ in Fig. 15c. Then, the misfit displacement associated with $\mathbf{x}$ is $(b_a/4)/17 + 4b_a/17$, which equals $b_a/4$ and is consistent

with the cancellation requirement. In this model of $CCSL_a$ (Fig. 15a) **x** defines a secondary O-element associated with the Burgers vector $\mathbf{b}_s^{II}$. In both models, **x** defines a point of good matching.

While $\Delta\mathbf{v}$ is easier to visualize than $d(\mathbf{v})$, the construction of $CCSL_a$ in Fig. 15a seems more reasonable than the one yielding a secondary invariant line, since the secondary strain in the former construction is much smaller. An appropriate selection should be such that the periodicity of the 2D CCSL agrees with the preferred state in the same terrace plane, and the secondary misfit strain associated with **v** should be small. Namely, the Burgers vector should be close to $\Delta\mathbf{v}$. For example, because of the mirror symmetry in Fig. 15b, one can also define secondary O-lattice planes, normal to the other set of parallel $\Delta\mathbf{g}$'s (e.g. $\Delta\mathbf{g}_{22}$). According to this model of $CCSL_a$, steps in Fig. 15d will again be associated with the secondary dislocations. However, the Burgers vector or $\Delta\mathbf{v}_c$ is $b_a/2$, which is significantly larger than $\Delta\mathbf{v}$. Therefore, this description of the d-steps is not appropriate.

### *A.3. Association of Moiré planes with interfacial misfit*

Since the experimental study of the step structure often requires high resolution techniques, continuity of planes has often been examined so as to characterize the steps. This method is adopted from studies of the interfaces in the primary preferred state, for which discontinuity of coherence is an important indicator of the defects. However, one must be careful when extending this method to the study of interfaces in a secondary preferred state, since observations of an extra plane associated with each step may or may not be consistent with conventional $\mathbf{g}\cdot\mathbf{b}$ practice. This is another distinct property of interfaces in secondary preferred state, because the $\Delta\mathbf{g}$ vectors in this case are often comparatively larger than the principal primary $\Delta\mathbf{g}$'s, which only connect low index **g**'s in the nearest neighborhood. The lattice correspondence is unimportant when one defines **g**'s in a system in a secondary preferred state. One particular **g** can relate to its different neighbors to form $\Delta\mathbf{g}$ vectors of similar length, as can be seen from Fig. 15b.

Whether two sets of planes will match or not at an interface depends only on the orientation of the corresponding Moiré plane with respect to the interface, as demonstrated in Fig. 5. Several sets of planes in the different lattices have been indicated by lines in Fig. 15d: lattice *a* in solid lines and lattice *b* in dashed lines. Since $\Delta\mathbf{g}_{11}$ and $\Delta\mathbf{g}_{23}$ (Fig. 15b) are normal to the selected interface, in the interface, parallel to their Moiré planes, the planes defined by $\mathbf{g}_{a1}$ (or $2\mathbf{g}_{a1}$) should match with the planes defined by $\mathbf{g}_{b1}$ /2 (or $\mathbf{g}_{b1}$), and so should the planes defined by $\mathbf{g}_{a2}$ (or $2\mathbf{g}_{a2}$) with the planes defined by $\mathbf{g}_{b3}/2$ (or $\mathbf{g}_{b3}$), as shown in different parts in Fig. 15d. Because the parallel $\Delta\mathbf{g}$'s connect $\mathbf{g}_b$ with $2\mathbf{g}_a$, rather than $\mathbf{g}_a$, only every other planes in lattice b find their matching counterparts in lattice a. This interface would be considered "coherent" in terms of these matching planes. Usually, as is the case for systems in the primary preferred state, the Burgers vector of any dislocation in the interface is considered to lie in the matching planes. This argument is valid only if the planes are related by the misfit strain. For a system in a secondary preferred state, various $\Delta\mathbf{g}$'s may not be

related by the secondary misfit strain, as in Fig. 15b. The Burgers vector of the d-steps ($\Delta\mathbf{v}_c$) in Fig. 15d does not lie in the matching planes analyzed above.

Discontinuity of the related planes will occur whenever the associated $\Delta\mathbf{g}$ is not normal to the interface. A discontinuity between two sets of planes will coincide with the step, if the $\Delta\mathbf{g}$ connecting the related $\mathbf{g}$'s can be defined in a generalized characteristic triangle. Besides the above $\Delta\mathbf{g}$, the edges of the triangle consist of a $\mathbf{g}_{\text{step}}$ and a $\Delta\mathbf{g}_{\parallel}$ that are specified in Appendix B for a typical characteristic triangle. Such a relationship ensures that the stepped interface intersects the Moiré planes in the same spacing with the steps. The Moiré planes defined by the $\Delta\mathbf{g}$ connecting $\mathbf{g}_{b2}$ and $2\mathbf{g}_{a2}$ are an example. As can be seen on the right part from Fig. 15d, there is a missing plane in $\mathbf{g}_{b2}$ planes at the step. The same set of planes, with their $\mathbf{g}$ connected by different $\Delta\mathbf{g}$'s in a characteristic triangle, will exhibit a dual feature: matching (e.g. $2\mathbf{g}_{a2}$ vs $\mathbf{g}_{b3}$) in the whole interface or mismatching (e.g. $2\mathbf{g}_{a2}$ vs $\mathbf{g}_{\text{b}}$) at the steps. When interface contains d-steps, there exist numerous typical and general characteristic triangles in reciprocal space, and many planes will possess the dual feature. Whether a set of planes will match at an interface depends on which planes in the other phase are considered.

## Appendix B. $\Delta g$ Characteristic triangles

A $\Delta\mathbf{g}$ characteristic triangle is a useful device to describe an interface in which coincidence of interfacial steps and dislocations can be realized, as required by the third optimum condition. The definition of the $\Delta\mathbf{g}$ characteristic triangle is shown in Fig. 16a. Two corners of the triangle are defined by reciprocal points of the larger lattice (arbitrarily chosen as lattice $\beta$), in which the step height is defined, while the third point is from the other reciprocal lattice. The edges of the $\Delta\mathbf{g}$ characteristic triangle consist of $\mathbf{g}_{\text{step}}$, $\Delta\mathbf{g}_{\parallel}$, and $\Delta\mathbf{g}_{\text{II}}$ vectors, that must be specified by the following

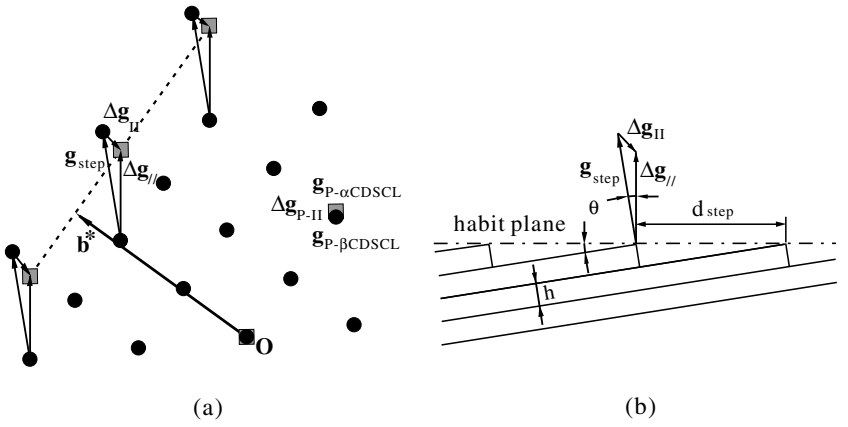


Fig. 16. (a) Definition of the $\Delta\mathbf{g}$ characteristic triangle, where black and gray dots are reciprocal points from lattices $\alpha$ and $\beta$, and (b) its relationship with the interfacial steps.

conditions. These conditions ensure the step spacing to be identical to that of the secondary dislocations in the singular interface normal to **n**.

(i) $\mathbf{g}_{\text{step}}$, a reciprocal vector in lattice $\beta$, is parallel to $\mathbf{g}_{\text{P-}\beta\text{CCSL}}$, which defines the terrace planes of the stepped interface, and its inverse magnitude $1/|\mathbf{g}_{\text{step}}|$ gives the unit of the step height $h$. Namely, $h = i/|\mathbf{g}_{\text{step}}|$, with $i$ being a small positive integer number.
(ii) $\Delta\mathbf{g}_{\parallel}$ is parallel to $\Delta\mathbf{g}_{\text{P-II}}$, so that $\Delta\mathbf{g}_{\parallel}/|\Delta\mathbf{g}_{\parallel}| = \Delta\mathbf{g}_{\text{P-II}}/|\Delta\mathbf{g}_{\text{P-II}}| = \mathbf{n}$.
(iii) $\Delta\mathbf{g}_{\text{II}}$ is a secondary $\Delta\mathbf{g}$ defined by $\Delta\mathbf{g}_{\text{II}} = (\mathbf{T}^{\text{II}})'\mathbf{g}_{\text{}\alpha\text{CDSCL}}$ (Eq. (15)), in the condition that $\mathbf{g}_{\text{}\alpha\text{CDSCL}} = i\mathbf{b}_s^{\text{II}*} + k\mathbf{g}_{\text{P-}\alpha\text{CDSCL}}$, where $\mathbf{b}_s^{\text{II}*} = \mathbf{b}_s^{\text{II}}/|\mathbf{b}_s^{\text{II}}|^2$, $\mathbf{b}_s^{\text{II}}$ is the Burgers vector of the secondary dislocations associated with the steps, and $k$ is a scalar variable. $\mathbf{g}_{\text{P-}\alpha\text{CDSCL}}$ is related to $\mathbf{b}_s^{\text{II}}$ by $\mathbf{g}'_{\text{P-}\alpha\text{CDSCL}}\mathbf{b}_s^{\text{II}} = 0$, and it is associated with the particular $\Delta\mathbf{g}_{\text{P-II}}$ normal to the singular interface.

For simplicity, we set the step height, $h$, in Fig. 16b equal to a single layer of crystal planes parallel to the terrace plane of the interface, i.e. $h = 1/|\mathbf{g}_{\text{step}}|$. As can be seen from the figure, the spacing of the steps can be determined from

$$d_{\text{step}} = h/\sin\theta = 1/|\mathbf{g}_{\text{step}} \times \mathbf{n}|. \tag{B.1a}$$

Similarly, if the step height is counted as i layers of planes i.e. $h = i/|\mathbf{g}_{\text{step}}|$, the step spacing should be

$$d_{\text{step}} = i/|\mathbf{g}_{\text{step}} \times \mathbf{n}|. \tag{B.1b}$$

From the geometry of the $\Delta\mathbf{g}$ characteristic triangle one gets:

$$|\mathbf{g}_{\text{step}} \times \Delta\mathbf{g}_{\parallel}| = |\Delta\mathbf{g}_{\text{II}} \times \Delta\mathbf{g}_{\parallel}|, \tag{B.2a}$$

or

$$|\mathbf{g}_{\text{step}} \times \mathbf{n}| = |\Delta\mathbf{g}_{\text{II}} \times \mathbf{n}|, \tag{B.2b}$$

because of condition (ii). On the other hand, according to Eqs. (12)–(13) the dislocation spacing is

$$d_{i\text{-dis}}^{\text{II}} = 1/|(\mathbf{T}^{\text{II}})'\mathbf{b}_i^{\text{II}*} \times \mathbf{n}|. \tag{B.3}$$

According to condition (iii), we can express

$$\Delta\mathbf{g}_{\text{II}} \times \mathbf{n} = (i(\mathbf{T}^{\text{II}})'\mathbf{b}_s^{\text{II}*} + k\Delta\mathbf{g}_{\text{P-II}}) \times \mathbf{n} = i\mathbf{T}^{II\prime}\mathbf{b}_s^{\text{II}*} \times \mathbf{n}, \tag{B.4a}$$

or

$$i/|\mathbf{g}_{\text{II}} \times \mathbf{n}| = 1/|(\mathbf{T}^{\text{II}})'\mathbf{b}_i^{\text{II}*} \times \mathbf{n}|. \tag{B.4b}$$

Comparing Eqs. (B.1–B.4), one finds

$$d_{i\text{-dis}}^{\text{II}} = d_{\text{step}}. \tag{B.5}$$

Because the linear relationship between reciprocal vectors associated with $\Delta\mathbf{g}_{\parallel}$ and $\mathbf{g}_{\text{II}}$, there exists a set of $\Delta\mathbf{g}$ characteristic triangles corresponding to various $k$ values. Examples of the $\Delta\mathbf{g}$ characteristic triangles in a diffraction pattern for a cementite/

austenite system is given in Fig. 13a, with a corresponding plot in Fig. 8d [45]. The corresponding model and the image of the habit plane have been shown in Figs. 8c and 13b [45,66]. While the angle bounded by $\mathbf{g}_{\text{step}}$ and $\Delta\mathbf{g}_{\parallel}$ is invariant, the shapes of the triangles can vary from one to the next. Due to condition (iii) stated above, all associated $\mathbf{g}_{\alpha\text{CDSCL}}$'s in these triangles must lie in one row (the dashed line in Figs. 16a, 7a and 8d), parallel to $\mathbf{g}_{\text{P-}\alpha\text{CDSCL}}$ and at a distance of $i|\mathbf{b}_s^{\text{II}*}|$ ($i = 1$ in all figures) from the origin. A case of $h = 2/|\mathbf{g}_{\text{step}}|$ has been noticed in a recent study of a Mg-Al alloy [173]. This condition can be used for identifying the Burgers vector from an observation of a group of parallel $\Delta\mathbf{g}$'s in an experimental diffraction pattern.

The step heights evaluated in the different lattices are often different. In this case, there must be a rotation between $\mathbf{g}_{\text{P-}\alpha\text{CCSL}}$ and $\mathbf{g}_{\text{P-}\beta\text{CCSL}}$, so that a $\Delta\mathbf{g}$ connecting $m\mathbf{g}_{\text{P-}\alpha\text{CCSL}}$ and $n\mathbf{g}_{\text{P-}\beta\text{CCSL}}$, having a similar length, can be defined either as $\Delta\mathbf{g}_{\text{P-II}}$ or $\Delta\mathbf{g}_{\parallel}$ normal to the interface. According to the property of Moiré planes in Fig. 5, the planes defined by $\mathbf{g}_{\text{P-}\alpha\text{CCSL}}/n$ and $\mathbf{g}_{\text{P-}\beta\text{CCSL}}/m$ should match at the steps because they serve as the terrace planes (refer Fig. 6b). In addition, if $m\mathbf{g}_{\text{P-}\alpha\text{CCSL}}$ and $n\mathbf{g}_{\text{P-}\beta\text{CCSL}}$ are connected by $\Delta\mathbf{g}_{\text{P-II}}$, $\mathbf{b}_s^{\text{II}}$ must lie in the terrace plane.

## References


[1] Thompson ME, Su CS, Voorhees PW. Acta Metall Mater 1994;42:2107.
[2] Wang Y, Chen R-Q, Khachaturyan A. In: Johnson WC, Howe JM, Laughlin DE, Soffa WA, editors. Solid–solid phase transformations. USA: TMS; 1994. p. 245.
[3] Lee JK. Metall Mater Trans 1996;27A:1449.
[4] Johnson WC. In: Aaronson HI, editor. Lecture on the theory of phase transformation. USA: TMS; 1999. p. 35.
[5] Howell PR, Honeycombe RWK. In: Aaronson HI, Laughlin DE, Sekerka RF, Wayman CM, editors. Proceedings of the Conference on Solid–Solid Phase Transactions. Warrendale, USA: TMS; 1981. p. 399.
[6] Aaronson HI, Lee JK. In: Aaronson HI, editor. Lecture on the theory of phase transformation. USA: TMS; 1999. p. 165.
[7] Brokman A, Balluffi RW. Acta Metall 1981;29:1703.
[8] Wolf D, Merkle KL. In: Wolf D, Yip S, editors. Materials interfaces atomic-level structure and properties. New York: Chapman and Hall; 1992. p. 87.
[9] Vitek V, Sutton AP, Smith DA, Pond RC. In: Grain-boundary structure and kinetics. USA: ASM; 1979. p. 115.
[10] Marquis EA, Seidman DN. Acta Mater 2001;49:1909.
[11] Porter DA, Easterling KE. Phase transformations in metals and alloys. New York: Chapman and Hall; 1992. 514p.
[12] Howe JM. Interfaces in materials. New York: John Wiley and Sons; 1997. 516p.
[13] Aaronson HI. J Microsc 1974;102:275.
[14] Ralph B, Randle V. In: Lorimer GW, editor. Phase transformations'87. London: Institute of Metals; 1988. p. 613.
[15] Howe JM. Mater Trans JIM 1998;39:3.
[16] Dahmen U. Acta Metall 1982;30:63.
[17] Luo CP, Weatherly GC. Acta Metall 1987;35:1963.
[18] Dahmen U, Westmacott KH. Acta Metall 1986;34:475.
[19] Furuhara T, Howe JM, Aaronson HI. Acta Metall Mater 1991;39:2873.
[20] Zhou DS, Fonda RW, Shiflet GJ. Scripta Metall 1991;25:2639.
[21] Zhang W-Z, Purdy GR. Acta Metall Mater 1993;41:543.

[22] Luo CP, Dahmen U, Westmacott KH. Acta Metall Mater 1994;42:1923.
[23] Luo CP, Dahmen U. Acta Metall Mater 1998;46:2063.
[24] Weatherly GC, Zhang W-Z. Metall Mater Trans 1994;25A:1865.
[25] Banerjee S, Dey GK, Srivastava D, Ranganathan S. Metall Mater Trans 1997;28A:2201.
[26] Ikuhara Y, Pirouz P. Mater Sci Forum 1996;207–209:121.
[27] Hall MG, Aaronson HI, Kinsman KR. Surf Sci 1972;31:257.
[28] Rigsbee JM, Aaronson HI. Acta Metall 1978;27:351.
[29] Furuhara T, Aaronson HI. Acta Metall Mater 1991;39:2857.
[30] Spanos G, Aaronson HI. Acta Metall Mater 1990;38:2721.
[31] Champion Y, Hagege S. Acta Mater 1997;45:2621.
[32] Zhang MX, Kelly PM. Acta Mater 1998;46:4617.
[33] Liang Q, Reynolds Jr WT. Metall Mater Trans 1998;29A:2059.
[34] Knowles KM, Smith DA. Acta Cryst 1982;A38:34.
[35] Bollmann W, Nissen HU. Acta Cryst 1968;A24:546.
[36] Ecob RC, Ralph B. Acta Metall 1981;29:1037.
[37] Bollmann W. Crystal defects and crystalline interfaces. Berlin: Springer; 1970. 254p.
[38] Brandon DG, Ralph B, Ranganathan S, Wald MS. Acta Metall 1964;12:813.
[39] Balluffi RW, Brokman A, King AH. Acta Metall 1982;30:1453.
[40] Bonnet R, Durand F. Philos Mag 1975;32:997.
[41] Wang R, Dunlop GL, Kuo KH. Acta Metall 1986;34:681.
[42] Savva GC, Kirkaldy JS, Weatherly GC. Philos Mag 1997;75A:315.
[43] Chen JK, Reynolds Jr WT. Acta Mater 1997;45:4423.
[44] Lu P, Cosandey F. Acta Metall Mater 1992;40:S259.
[45] Ye F, Zhang W-Z. Acta Mater 2002;50:2761.
[46] Cahn JW, Kalonji G. In: Aaronson HI, Laughlin DE, Sekerka RF, Wayman CM, editors. Proceedings of the conference on solid–solid phase transactions. Warrendale, USA: TMS; 1981. p. 3.
[47] Dahmen U, Witcomb MJ, Westmacott KH. Coll Phys 1990;51:C1–737.
[48] Champion Y, Hagege S. Acta Mater 1996;44:4169.
[49] Sutton AP, Balluffi RW. Acta Metall 1987;35:2177.
[50] Balluffi RW, Sutton AP. Mater Sci Forum 1996;207–209:1.
[51] Sutton AP, Balluffi RW. Interfaces in crystalline materials. Oxford: Oxford University Press; 1995. 819p.
[52] Goodhew PJ. In: Grain-boundary structure and kinetics. USA: ASM; 1979. p. 155.
[53] Pond RC. Can Metall Quart 1974;13:33.
[54] Randle V. Acta Mater 1997;45:1459.
[55] Bonnet R, Loubradou M, Catana A, Stadelmann P. Metall Trans 1991;22A:1145.
[56] Zhang W-Z. Scripta Mater 1997;37:187.
[57] Merkle KL, Wolf D. Philos Mag 1992;65A:513.
[58] Bollmann W. Crystal lattices, interfaces, matrices. Geneva: Bollmann; 1982. 360p.
[59] Smith DA, Hazzledine PM. Scripta Metall 1981;15:393.
[60] Read WT, Shockley W. Phys Rev 1950;78:275.
[61] Knowles KM, Smith DA, Clark WAT. Scripta Metall 1982;16:413.
[62] Howell PR, Southwick PD, Honeycombe RWK. J Microsc 1979;116:151.
[63] Weatherly GC. Acta Metall 1981;29:501.
[64] Cassidy MP, Muddle BC, Scott TE, Wayman CM, Bowles JS. Acta Metall 1977;25:829.
[65] Chen FR, Chiou SK, Chang L, Hong CS. Ultramicroscopy 1994;54:179.
[66] Howe JM, Spanos G. Philos Mag 1999;79A:9.
[67] Dehm G, Thomas J, Mayer J. Philos Mag 1998;77A:1531.
[68] Forwood CT, Gibson MA. Mater Sci Forum 1995;189–190:353.
[69] Sakidja R, Sieber H, Perepezko JH. Philos Mag Let 1999;79:351.
[70] Fecht HJ. Acta Metall Mater 1992;40:S39.
[71] Hirth JP, Nixon T, Pond RC. In: Pond RC, Clark WAT, King AH, Willams DB, editors. Boundaries and interfaces in materials: the David A Smith symposium. USA: TMS; 1998. p. 63.

[72] Aaronson HI, Clark WAT, Smith DA. Scripta Metall 1983;17:785.
[73] Zhang W-Z, Purdy GR. Philos Mag 1993;68A:291.
[74] Bonnet R, Durand F. In: Proceedings of the Conference On In situ Composites, Lakeville, USA. Publ NMAB 308-I; 1973. p. 209.
[75] Ecob RC. J Microsc 1985;137:313.
[76] Hirth JP, Balluffi RW. Acta Metall 1973;21:929.
[77] King AH. Metall Trans 1991;22A:1177.
[78] Van der Merwe JH, Shiflet GJ, Stoop PM. Metall Trans 1991;22A:1165.
[79] Shiflet GJ, van der Merwe JH. Metall Trans 1994;25A:1895.
[80] Bonnet R, Loubradou M, Pénisson JM. J Phys (Paris) 1996;6:C2–C165.
[81] Xiao SQ, Maloy SA, Heuer AH, Dahmen U. Philos Mag 1995;72A:997.
[82] Shtansky DV, Nakai K, Ohmori Y. Philos Mag 1999;79A:1655.
[83] Zhang W-Z, Purdy GR. Philos Mag 1993;68A:279.
[84] Christian JW. The theory of transformation in metals and alloys. Oxford: Pergamon Press; 1975. 586p.
[85] Duly D, Zhang W-Z, Audier M. Philos Mag 1995;71A:187.
[86] Fujii T, Nakazawa H, Kato M, Dahmen U. Acta Mater 2000;48:1033.
[87] Hytch MJ, Snoeck E, Kilaas R. Ultramicroscopy 1998;74:131.
[88] Zhang W-Z. Philos Mag 1998;78A:913.
[89] Zhang W-Z. PhD thesis. McMaster University; 1991. 198p.
[90] Khachaturyan AG. Theory of structural transformations in solids. New York: John Wiley and Sons; 1983. 574p.
[91] Furuhara T, Wada K, Maki T. Metall Mater Trans 1995;26A:1971.
[92] Chen JK, Chen G, Reynolds Jr WT. Philos Mag 1998;78A:405.
[93] Grimmer H. Scripta Metall 1974;8:1221.
[94] Thompson SW, Howell PR. In: Johnson WC, Howe JM, Laughlin DE, Soffa WA, editors. Proceedings of the conference on solid–solid phase transactions. Warrendale, USA: TMS; 1994. p. 1127.
[95] Warrington DH, Bollmann W. Philos Mag 1972;25:1195.
[96] Zhang WZ, Ye F, Zhang C, Qi Y, Fang HS. Acta Mater 2000;48:2209.
[97] Zhang W-Z, Weatherly GC. Acta Mater 1998;46:1837.
[98] Qiu D, Zhang WZ. Philos Mag 2003;83(27):3093.
[99] Mader W. Z Metall 1989;80:139.
[100] Kato M, Wada M, Sato A, Mori T. Acta Metall 1989;37:749.
[101] Wayman CM. Introduction to the crystallography of martensitic transformations. New York: MacMillan; 1964. 189p.
[102] Carpenter GJC. Acta Metall 1978;26:1225.
[103] Dahmen U, Westmacott KH. In: Lorimer GW, editor. Phase transformations'87. Institute of Metals: London; 1988. p. 511.
[104] Aaronson HI, Hall MG. Metall Mater Trans 1994;25A:1797.
[105] Perovic V, Weatherly GC. Acta Metall 1988;37:813.
[106] Luo CP, Weatherly GC. Metall Trans 1988;19A:1153.
[107] Duly D. Acta Metall 1993;41:1559.
[108] Dahmen U, Westmacott KH. In: Aaronson HI, Laughlin DE, Sekerka RF, Wayman CM, editors. Proceedings of the conference solid–solid phase transactions, Warrendale. USA: TMS; 1981. p. 433.
[109] Pitsch W. Acta Metall 1962;10:897.
[110] Pitsch W. Arch Eisenhuttenwes 1963;34:381.
[111] Yang KH, Choo WK. Acta Metall Mater 1994;42:263.
[112] Khalid FA, Edmonds DV. Acta Metall Mater 1993;41:3421.
[113] Mangan MA, Kral MV, Spanos1 G. Acta Mater 1999;47:4263.
[114] Gao Y, Merkle KL. J Mater Res 1990;5:1995.
[115] Lu P, Cosandey F. Ultramicroscopy 1992;40:271.
[116] Kooi BJ, De Hosson JTh M. Acta Mater 1998;46:1909.

[117] Kooi BJ, Groen HB, De Hosson JTh M. Acta Mater 1997;45:3587.
[118] Kooi BJ, De Hosson JTh M. Acta Mater 2000;48:3687.
[119] Ernst F, Pirouz P, Heuer AH. Philos Mag 1991;63A:259.
[120] Ichimori T, Katoh T, Ichinose H, Ito K, Ishida Y. In: Ishida Y, Morita M, Suga T, Ichinose H, Ohashi O, Echigoya J, editors. Interface science and materials interconnection. Toyama: The Japan Institute of Metals; 1996. p. 359.
[121] Furuhara T, Sugita N, Maki T. In: Ishida Y, Morita M, Suga T, Ichinose H, Ohashi O, Echigoya J, editors. Interface science and materials interconnection. Toyama: The Japan Institute of Metals; 1996. p. 363.
[122] Sundararaman M, Mukhopadhyay P, Banerjee S. Metall Trans 1988;19A:453.
[123] Rao G, Howe JM, Wynblatt P. Scripta Metall Mater 1994;30:731.
[124] Dahmen U. Ultramicroscopy 1989;30:102.
[125] Chen JK, Purdy GR, Weatherly GC, Kroupa A. Metall Mater Trans 1998;29A:2049.
[126] Bourret A, Lasalmonie A, Naka S. Scripta Metall 1986;20:861.
[127] Prasad KS, Gokhale AA, Mukhopadhyay AK, Banerjee D, Goel DB. Acta Mater 1999;47:2581.
[128] Tang K, Wang C-A, Huang Y, Wu L. Mater Lett 2002;57:106.
[129] Howe JM, Aaronson HI, Gronsky R. Acta Metall 1985;33:649.
[130] Howe JM, Dahmen U, Gronsky R. Philos Mag 1987;56A:31.
[131] Muddle BC, Polmear IJ. Acta Metall 1989;37:777.
[132] Dai JY, Wang YG, Li DX, Ye HQ. Philos Mag 1994;70A:905.
[133] Xiao SQ, Dahmen U, Maloy SA, Heuer AH. Mater Sci Forum 1996;207–209:117.
[134] Celotto S. Acta Mater 2000;48:1775.
[135] Radmilovic V, Kilaas R, Dahmen U, Shiflet GJ. Acta Mater 1999;47:3987.
[136] Hugo GR, Muddle BC. Acta Metall Mater 1990;38:351.
[137] Yu R, He LL, Guo JT, Ye HQ, Lupinc V. Acta Mater 2000;48:3701.
[138] Nie JF, Muddle BC. Acta Mater 2000;48:1691.
[139] Wang RM, Han YF, Li CZ, Zhang SW, Ping DH, Yan MG. J Mater Sci 1998;33:5069.
[140] Weatherly GC, Perovic A, Mukhopadhyay NK, Lloyd DJ, Perovic DD. Metall Mater Trans 2001;32A:213.
[141] Garg A, Noebe RD, Darolia R. Acta Mater 1996;44:2809.
[142] Dravid VP, Lyman CE, Notis MR. Ultramicroscopy 1989;29:60.
[143] Das S, Howe JM, Perepezko JH. Metall Mater Trans 1996;27A:1623.
[144] Shtansky DV, Nakai K, Ohmori Y. Acta Mater 1999;47:1105.
[145] Sinclair CW. Phd thesis. McMaster University, Canada; 2001.
[146] Kumar KS, Liu CT. Acta Mater 1997;45:3671.
[147] Chen JK, Farkas D, Reynolds Jr WT. Acta Mater 1997;45:4415.
[148] Brown LM, private communication.
[149] Lee HJ, Aaronson HI. Acta Metall 1988;36:787.
[150] Furuhara T, Ogawa T, Maki T. Scripta Metall 1996;34:381.
[151] Guo H, Enomoto M. Acta Mater 2002;50:929.
[152] Shek CH, Dong C, Lai JKL, Wong KW. Metall Mater Trans 2000;31A:15.
[153] Hall MG, Rigsbee JM, Aaronson HI. Acta Metall 1986;34:1419.
[154] Dahmen U. Scripta Metall 1981;15:77.
[155] Qiu D, Shen YX, Zhang W-Z. Acta Mater [to be submitted].
[156] Kelly PM, Zhang M-X. Mater Forum 1999;23:41.
[157] Purdy GR. In: Cahn RW, Haasen P, Kramer EJ, editor. Materials science and technology. Phase transformations in materials, vol. 5; 1991. p. 305.
[158] Rigsbee JM, Aaronson HI. Acta Metall 1978;27:365.
[159] Mou Y. Metall Mater Trans 1994;25A:1905.
[160] Dahmen U. Scripta Metall 1987;21:1029.
[161] Howe JM, Smith DA. Acta Metall Mater 1992;40:2343.
[162] Shen YX, Qiu D, Zhang W-Z. Unpublished research.
[163] Hall MG, Furuhara T, Aaronson HI, Hirth JP. Acta Mater 2001;49:3487.

[164] Howe JM, Reynolds Jr WT, Vasudevan VK. Metall Mater Trans 2002;33A:2391.
[165] Miyano N, Ameyama K, Weatherly GC. Metall Mater Trans 2002;33A:1547.
[166] Miyano N, Fujiwara H, Ameyama K, Weatherly GC. Mater Sci Eng 2002;A333:85.
[167] Furuhara T, Oishi K, Maki T. Metall Mater Trans 2002;33A:2327.
[168] Wang YG, Zhang Z, Yan GH, De Hosson JTHM. J Maters Sci 2002;37:2511.
[169] Fecht HJ, Gleiter H. Acta Metall 1985;33:557.
[170] van der Merwe. Philos Mag 1982;45:127.
[171] Loubradou M, Penisson JM, Bonnet R. Ultramicroscopy 1993;51:270.
[172] Zhang WZ. Acta Metall Sin 2002;38:785.
[173] Zhang M, Zhang WZ, Ye F. Scripta Mater Trans [accepted].

**W.-Z. Zhang** is a Professor in the Department of Materials Science and Engineering at Tsinghua University, Beijing, China. She received the M.E. degree in 1983 from University of Science and Technology, Beijing, and Ph.D. degree in 1992 from McMaster University, Canada, both in Materials Engineering. She has engaged in experimental and theoretical research on the problems related to precipitation crystallography for about 17 years.

**G.C. Weatherly** was a Professor in the Department of Materials Science and Engineering at McMaster University, Hamilton, Canada, before he died in April 2003. A graduate of Cambridge University, he spent 23 years at the University of Toronto before moving to McMaster University eleven years ago. He has published over 200 in the field of analytical electron microscopy, interfacial structure analysis, and phase transformation studies.